State of Oregon
Department of
Environmental
Quality

OREGON DEPARTMENT OF ENVIRONMENTAL QUALITY
December 2008

Molalla-Pudding Subbasin TMDL
Technical Appendices

<u>Table of Contents: Technical Appendices</u>:

For more information:
http://www.deq.state.or.us/wq/TMDLs/willamette.htm#mp
Karen Font Williams, Basin Coordinator
Oregon Department of Environmental Quality
2020 SW 4th Ave. Suite 400
Portland, Oregon 97201
Phone 503-229-6254 • Fax 503-229-6957

Appendix A
Technical Basis for Temperature TMDL Analysis

List of Figures

List ofTables

MODELING PURPOSE, APPLICATIONS AND LIMITATIONS

The scale of this analysis is the Molalla-Pudding subbasin (Hydrologic Unit Code 17090009). While the stream temperature TMDL considers all surface waters within these subbasins, this analysis largely focuses on the two largest streams within the subbasin, the Molalla and Pudding Rivers. The Molalla and Pudding Rivers each received a unique temperature analysis.

Parameters that affect stream temperature can be grouped as near stream vegetation land cover, channel morphology, and hydrology. These parameters affect stream heat transfer processes and stream mass transfer processes and may be interrelated (Figure A- 1). The analytical techniques in this temperature TMDL include all parameters that affect stream temperature, given sufficient data and methodologies to allow accurate quantification.

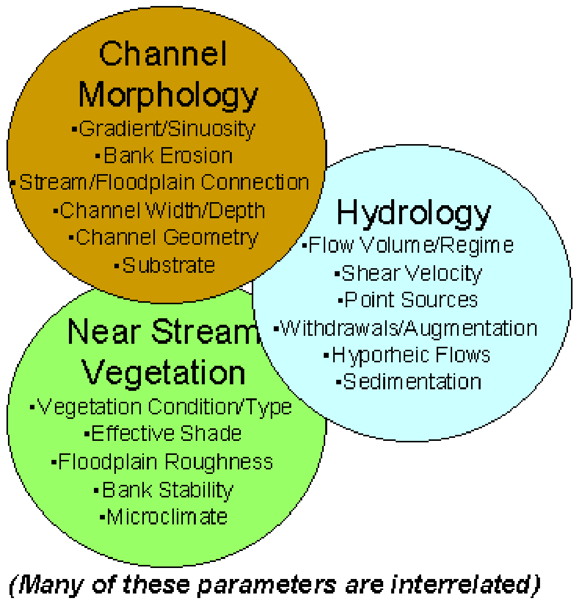

Figure A- 1: Factors that affect stream temperature dynamics.

The purpose of this analysis is to better understand spatial and temporal stream temperature dynamics. The analysis consists of four components: near stream land cover vegetation assessment, analysis of hydrology, effective shade modeling, and stream temperature modeling. Each analytical component has specific purposes, as follows:

Near Stream Land Cover Analysis

Purpose

- Quantify existing near stream land cover types and physical attributes.
- Develop a methodology to estimate potential natural conditions.
- Establish threshold near stream land cover type and physical attributes for the stream network. below which land cover conditions are considered to deviate from a potential natural condition.

Applications

- Estimate current near stream land cover type and physical attributes.
- Estimate potential natural condition near stream land cover types and attributes.
- Identify site-specific deviations of current near stream land cover conditions from threshold potential conditions.

Limitations

- Methodology is based on ground level and geographic information system (GIS) data such as vegetation surveys and digitized polygons developed using aerial photographs. Each data source has accuracy limitations.
- Associations used for land cover classifications are assigned median values to describe physical attributes. In some cases, this methodology significantly underestimates landscape variability.

Hydrology Analysis

Purpose

- Map and quantify surface and subsurface inflows and withdrawals.
- Develop a mass balance for the stream network by quantifying existing instream flow volumes
- Quantify average velocity and average stream depth as a function of flow volume, stream gradient, channel width and channel roughness.
- Develop a potential natural flow regime that estimates flow volumes when withdrawals and associated return flows are eliminated.

Applications

- Estimate current flow volumes, velocities and stream depths.
- Estimate potential natural condition flow volumes, velocities and depths.
- Identify site specific deviations of current flow conditions from estimated natural flow conditions..

Limitations

- Many small mass transfer processes are not accounted for.
- Ground level flow data is often limited, which limits the accuracy of derived flow balances.
- Water withdrawals are not directly quantified
- Water withdrawals are assumed to occur only at OWRD mapped points of diversion.
- Return flows are oversimplified.
- It is not possible to determine the amount of return flows derived from ground water withdrawals relative to those derived from instream withdrawals.
- Return flows may deliver water that is diverted from another watershed.
- Analyses do not quantify potential subsurface inflows/returns or behavior within substrate.
- Inter-annual variations are not simulated since analyses focused on a single season.

Effective Shade Analysis

Purpose

- Simulate current effective shade levels over stream network.
- Simulate potential natural condition effective shade levels based on channel width and land cover types and physical attributes over stream network.
- Establish threshold effective shade values for the stream network, below which current conditions are considered to deviate from a potential natural condition.
- Develop curves that provide shade targets for use where site-specific targets are not available..

Valid Applications

- Estimate current effective shade levels for the stream network.
- Estimate potential natural condition effective shade levels for the stream network.
- Identify site-specific deviations of current effective shade conditions from threshold potential conditions.

Limitations

- Limitations for input parameters apply (i.e., hydrology, near stream land cover type and physical attributes).
- The period of simulation is valid for effective shade values that occur in July and early August.
- Uncertainty associated with channel widths measurable from aerial photographs may reduce accuracy of the effective shade simulations.

Stream Temperature Analysis

Modeling Purpose

- Analyze stream temperatures for current and critical conditions.
- Determine the sensitivity of stream temperature to changes in land cover, flow, and point source heat loads.
- Analyze potential natural condition stream temperatures for potential land cover types, channel morphology, and flow conditions.
- Establish threshold stream temperature values for the stream, above which current conditions are considered to deviate from a potential condition.
- Determine if stream temperature regimes are significantly different for conditions which minimize anthropogenic heat loads.
- Provide a reasonable assurance that beneficial uses are protected in the potential natural condition to the extent possible given the natural constraints for channel morphology, land cover type, and physical attributes.
- Provide a robust methodology for stream temperature analysis.

Valid Applications

- Estimate critical condition stream temperatures.
- Estimate potential critical condition stream temperatures.
- Identify site-specific deviations of current stream temperatures from potential conditions.
- Analyze the sensitivity of single or multiple parameters on stream temperature regimes.
- Identify stream temperature distributions during critical conditions.

Limitations

- Limitations on accuracy of input parameters apply (i.e., channel morphology, near stream land cover type and physical attributes, and hydrology).
- Accuracy of the methodology is limited to how well calculated values match observations (quantified using standard model validation statistics).
- Stream temperature results are limited to streams for which models are developed. Considerable uncertainty is associated with extrapolating information derived from modeled streams to streams that have not been modeled.
- Near stream, microclimatic impacts are considered only for wind speed and not for air temperature or humidity.
- The period of simulation is valid for stream temperature values that occur in July and August.
- Inter-annual variations are considered but not modeled.

While the limitations described above outline potential areas of weakness in the methodology used in the stream temperature analysis, DEQ has undertaken a comprehensive approach. All important stream parameters that can be accurately quantified are included in the analysis. In the context of understanding of stream temperature dynamics, these areas of limitations should be the focus for future study.

DATA USED IN ANALYSIS

Ground Level Data

Available ground level data sources are described in this section. Specifically, this stream temperature analysis relied on the following data types: continuous temperature data, flow volume (gage data and instream measurements), channel morphology surveys, and effective shade measurements.

CONTINUOUS TEMPERATURE DATA

Continuous temperature data are used in this analysis to:

- Calibrate stream emissivity for thermal infrared radiometry (TIR) measurements (described below),
- Develop calibrated models which match observed stream temperatures for all hours of the day.
- Calculate temperature statistics and assess the temporal component of stream temperature,
- Perform temporal temperature simulations.

DEQ placed probes which measure temperature on a continuous basis (thermisters) at multiple locations along the mainstem Molalla and Pudding Rivers and their major tributaries from late May through mid October, 2004 (Table 1). DEQ adhered to quality assurance/quality control procedures specified in the DEQ Method of Operations Manual (DEQ, March 2004, http://www.deq.state.or.us/lab/techrpts/technicaldocs.htm).

Temperature monitors were lost from three locations (North Fork Molalla and Milk Creek at mouth, and Molalla at Feyrer Park), and compromised by being exposed to air at one location in the Molalla and four locations in the Pudding (Table A- 1). Data compromised by a thermister being exposed to air during times of low stream flow were not used. While continuous temperature was not available for all locations, DEQ was able to use the instantaneous temperatures measured with TIR as an estimate during the modeling period.

Table A- 1: Continuous temperature monitoring locations in the Molalla-Pudding Subbasin.

STATION_KEY	DESCRIPTION	PROBE	Approximate River Mile	
10362	Pudding River at Arndt Road (Barlow)	9406	4.0	
10917	Pudding River at Hwy 99E (Aurora)	9408	8.0	data file starts on 8/3/2004
11528	Pudding River at Bernard Road (Whiskey Hill)	9387	17.0	probably exposed to air 7/27 - 8/22/2004
10640	Pudding River at Hwy 211 (Woodburn)	9386	22.0	probably exposed to air 8/14 - 8/22/2004
10641	Pudding River at Hwy 214 (downstream of cannery outfall)	9385	27.0	probably exposed to air 8/14 - 8/22/2004
11530	Pudding River at Monitor-Mckee Road	9384	31.0	
11536	Pudding River at Nusom Road	9379	45.5	probably exposed to air 6 - 9/2004
31877	Pudding River at Saratoga Road	9382	41.0	exposed to air
31878	Pudding River below Drift Creek	9377	51.0	
32056	Pudding River at Sunnyview Road	9375	54.0	
32055	Pudding River at State Street	9373	58.0	
31876	Mill Creek Ehlen Road	9389	0.3	
32060	Mill Creek upstream of Hubbard STP (Pudding River)	9440	5.8	
10646	Silver Creek at Brush Creek Road	9378	1.0	
32057	Drift Creek at Hibbard Road (Pudding River)	9376	0.5	
32054	Drift Creek at Victor Point Road	9371	6.0	
32053	Drift Creek, West Fork, at Hwy 214 (Silver Falls Hwy)	9370	10.0	
10636	Molalla River at mouth	9405	0.1	
32059	Molalla River at 22nd Avenue	9412	1.0	data file starts on 7/23/2004
10637	Molalla River at Knights Bridge Road (Canby)	9409	1.5	
32058	Molalla River at Canby-Marquam Hwy (Goods Bridge)	9391	6.0	data file starts on 7/23/2004
32061	Molalla River upstream of Milk Creek	9402	8.0	

Table A-1 Continued

STATION_KEY	DESCRIPTION	PROBE	Approximate River Mile	
32062	Molalla River north of Oak Grove Road	9403	11.0	
10881	Molalla River at Hwy 213 Bridge (Mulino)	9398	15.0	data file starts on 7/30/2004
10638	Molalla River at Hwy 211 Bridge (Molalla)	9363	19.0	probably exposed to air 7/21 - 8/16/2004
31871	Molalla River above North Fork LD	9360	26.5	
32051	Molalla River upstream of Pine Creek	9356	33.0	
32049	Molalla River upstream of Horse Creek	9354	38.0	
32046	Molalla River at River Mile 44	9351	44.0	
32052	Gribble Creek at Mark Road	9364	1.0	
32048	Table Rock Fork Molalla River at River Mile 1	9353	0.1	
32050	Pine Creek at mouth (Molalla River)	9355	0.1	
32047	Copper Creek at mouth (Molalla River)	9352	0.1	
11824	Silverton STP, final effluent	9437	6.8	
19950	Hubbard STP, effluent	9441	5.3	
20339	Woodburn STP, effluent	9438	21.5	

STREAM AND HABITAT SURVEYS

During summer 2004, Oregon DEQ collected ground-level habitat data in the Molalla-Pudding subbasin. Stream survey data focuses on near stream land cover classification and measurements, channel morphology measurements, and stream shade measurements.

Flow volume data was collected at stream survey sites and from existing flow gages during the critical stream temperature period in summer of 2004 in the Molalla River watershed. These instream measurements were used to develop flow mass balances for the streams that were modeled for temperature. Flow gages and stream flow measurement sites are listed in Table A- 2.

One flow gauge is currently active on the Molalla River, at Canby (USGS Station 14200000), at approximately river mile 9. The flow record at this gauge extends discontinuously back to 1928. A second gauge at approximately river mile 31 (river kilometer 50), at Wilhoit (USGS 14198500), was active from 1935 until 1993. By plotting the flow from these two gauges during periods when flow measurements were available at both, DEQ derived a mathematical relationship between the flows so that missing periods at the Canby flow gauge could be filled in with calculated measurements. Using that relationship and a combined data set extending from 1928 to 1993, DEQ calculated the average low flow at Canby, or that flow exceeded 90% of the time, to be 27 cubic feet per second (cfs). This low flow, also called the 7Q10 flow, is calculated by taking a rolling 7 day average of all the flows in the record and then finding the 90th percentile of all the flows arranged highest to lowest.

DEQ measured stream discharge one time at several locations on the Molalla River and its major tributaries between July 20 and 22, 2004. At that time, DEQ also recorded stream channel measurements and riparian characteristics at several locations.

Table A- 2: Stream flow measured (cfs) on July 20, 22, or 23, 2004.

Site Location	River Mile	Flow (cfs)	Comment
Molalla R. at mouth	0.1	not measured	
Molalla R. at 22nd Ave.	1	not measured	
Molalla R. at Knight's Bridge Rd.	1.5	not measured	
Molalla R. at Canby-Marquam Hwy.	6	not measured	
Molalla R. upstream of Milk Cr.	8	not measured	
Molalla R. at Kraxburger Rd.	11	not measured	
Molalla R. at HWY 213	15.2	88.6	
Molalla R. at Hwy. 211	19		
Molalla R. at Feyrer Park	22.1	50.2	Lost temperature monitor

Table A-2 continued.

Site Location	River Mile	Flow (cfs)	Comment
Molalla R. upstream N. Fork Molalla	28	67.1	
Molalla R. upstream Pine Cr.	33.8	59.7	
Molalla R. above Horse Cr.	40.3	46.2	
Molalla R. at Locked Gate	46.8	9.6	
North Fork Molalla R. at mouth	0.1	44.6	Lost temperature monitor
Milk Cr. at Mulino Rd.	2.0		Lost temperature monitor
Pudding R. at Arndt Rd.	4.0	69	Flow from USGS gauge at Aurora
Gribble Cr. at Mark Road	1.0	not measured	
Table Rock Fork at river mile 1	1.0	26.9	
Pine Cr. at mouth	0.1	not measured	
Copper Cr. at mouth	0.1	1.2	

GIS and Remotely Sensed Data

This report relies extensively on GIS and remotely sensed data. Some of the GIS data used to develop this report are listed in Table A- 3 along with the application for which it was used.

Table A- 3: GIS and remotely sensed data used in the Molalla-Pudding Subbasin temperature TMDL

Spatial Data	Application
10-Meter Digital Elevation Models (DEM)	• Measure Valley Morphology • Measure Topographic Shade Angles
Aerial Imagery – Digital Orthophoto Quads and Rectified Aerial Photos	• Map Near Stream Land Cover • Map Channel Morphology • Map Roads, Development, Structures
Water Rights Information System (WRIS) and Points of Diversion (POD) Data	• Map locations and estimate quantities of water withdrawals
TIR Temperature Data	• Measure Surface Temperatures • Develop Longitudinal Temperature Profiles • Identify Subsurface Hydrology, Groundwater Inflow, Springs

The Digital Elevation Model (DEM) data files are representations of cartographic information in a raster form. DEMs consist of a sampled array of elevations for a number of ground positions at regularly spaced intervals. The U.S. Geological Survey, as part of the National Mapping Program, produces these digital cartographic/geographic data files. DEM grid data are rounded to the nearest meter for ten-meter pixels. DEMs are used to determine stream elevation, stream gradient, valley gradient, valley shape/landform and topographic shade angles.

Aerial imagery is used in this analysis to:

- Map stream features such as stream position, channel edges and wetted channel edges,
- Map near-stream land cover,
- Map instream structures such as dams, weirs, unmapped diversions/withdrawals, etc.

A digital orthophoto quad (DOQ) is a digital image of an aerial photograph in which displacements caused by the camera angle and terrain have been removed. In addition, DOQs are projected in map coordinates combining the image characteristics of a photograph with the geometric qualities of a map. The standard digital orthophoto is black-and-white with one-meter pixels covering a USGS quarter quadrangle.

DEQ used 1:5,000 scale aerial photographs from years 1994, 1995, 2000 and 2001 for the Molalla River model to map the right and left banks of the channel and distinguished areas of vegetation and other features within 300 feet of the stream bank. The GIS program measures channel width between the digitized right and left banks and assigns topographic and vegetation characteristics at 30 m (98.4) foot intervals along the stream.

WRIS and POD Data – Water Withdrawal Mapping

WRIS and POD Data are used in this analysis to:

- Map stream instream diversions/withdrawals,
- Associate an estimated flow rate to each diversion/withdrawal.

The Oregon Water Resources Department (OWRD) maintains the Water Rights Information System (WRIS). WRIS is a database used to monitor information related to water rights. A separate database tracks points of diversions (POD). These two databases were linked by ODEQ to map the locations of diversions, rates of water use and types of water use in the Molalla-Pudding subbasin. POD locations reflect information downloaded from WRD website in September 2006. Consumptive use was estimated using these data and incorporated in developing mass balance flow profiles for some modeled streams.

Thermal Infrared (TIR) Temperature Data

Thermal infrared (TIR) temperature data measured with forward looking infrared (FLIR) radiometers carried by aircraft are used in this analysis to:

- Develop continuous spatial temperature data sets,
- Calculate longitudinal heating profile/gradients,
- Visually observe complex distributions of stream temperatures at a large landscape scale,
- Map/Identify significant thermal features,
- Develop flow mass balances,
- Validate simulated stream temperatures.

TIR imagery measures the temperature of the outermost portions of the bodies/objects in the image (i.e., ground, riparian vegetation, stream). The bodies of interest are opaque to longer wavelengths and there is little, if any, penetration of the bodies.

TIR data are remotely sensed from a sensor mounted on a helicopter that collects digital data directly from the sensor to an on-board computer at a rate that insures the imagery maintains a continuous image overlap of at least 40%. The TIR detects emitted radiation at wavelengths from 8-12 microns (long-wave) and records the level of emitted radiation as a digital image across the full 12-bit dynamic range of the sensor. Each image pixel contains a measured value that is directly converted to a temperature. Each thermal image has a spatial resolution of less than one-half meter/pixel. Visible video sensor captures the same field-of-view as the TIR sensor. GPS time is encoded on the recorded video as a means to correlate visible video images with the TIR images during post-processing.

Data collection is timed to capture maximum daily stream temperatures, which typically occur between 14:00 and 18:00 hours. The helicopter is flown longitudinally over the center of the stream channel with the sensors in a vertical (or near vertical) position. In general, the flight altitude is selected so that the stream channel occupies approximately 20-40% of the image frame. A minimum altitude of approximately 300 meters (984 ft) is used both for maneuverability and for safety reasons. If the stream splits into two channels that cannot be covered in the sensor's field of view, then the survey is conducted over the larger of the two channels.

In-stream temperature data loggers (Onset Stowaways or VEMCOs) are distributed in each subbasin prior to the survey to verify the accuracy of the radiant temperatures measured by the TIR. TIR data can be viewed as GIS point coverages or TIR imagery.

Direct observation of spatial temperature patterns and thermal gradients is a powerful application of TIR derived stream temperature data. Thermally significant areas can be identified in a longitudinal stream temperature profile and related directly to specific sources (i.e., water withdrawal, tributary confluence, land cover patterns, etc.). Areas with stream water mixing with subsurface flows (i.e., hyporheic and inflows) are apparent, and often dramatic, in TIR data. Thermal changes captured with TIR data can be quantified as a specific change in stream temperature or a stream temperature gradient that results in a temperature change over a specified distance.

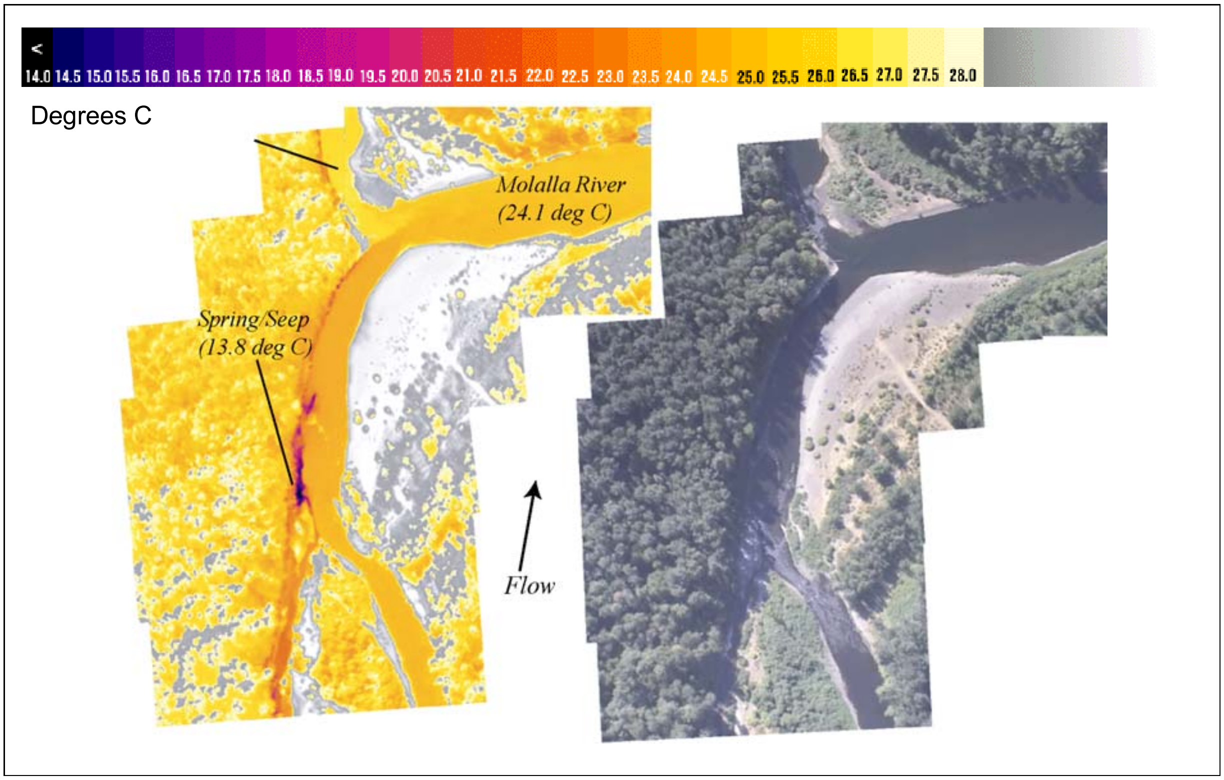

Figure A- 2: TIR/color video image pair showing the location of a spring or seep near the confluence of the Molalla and Pudding Rivers, July 26, 2004.

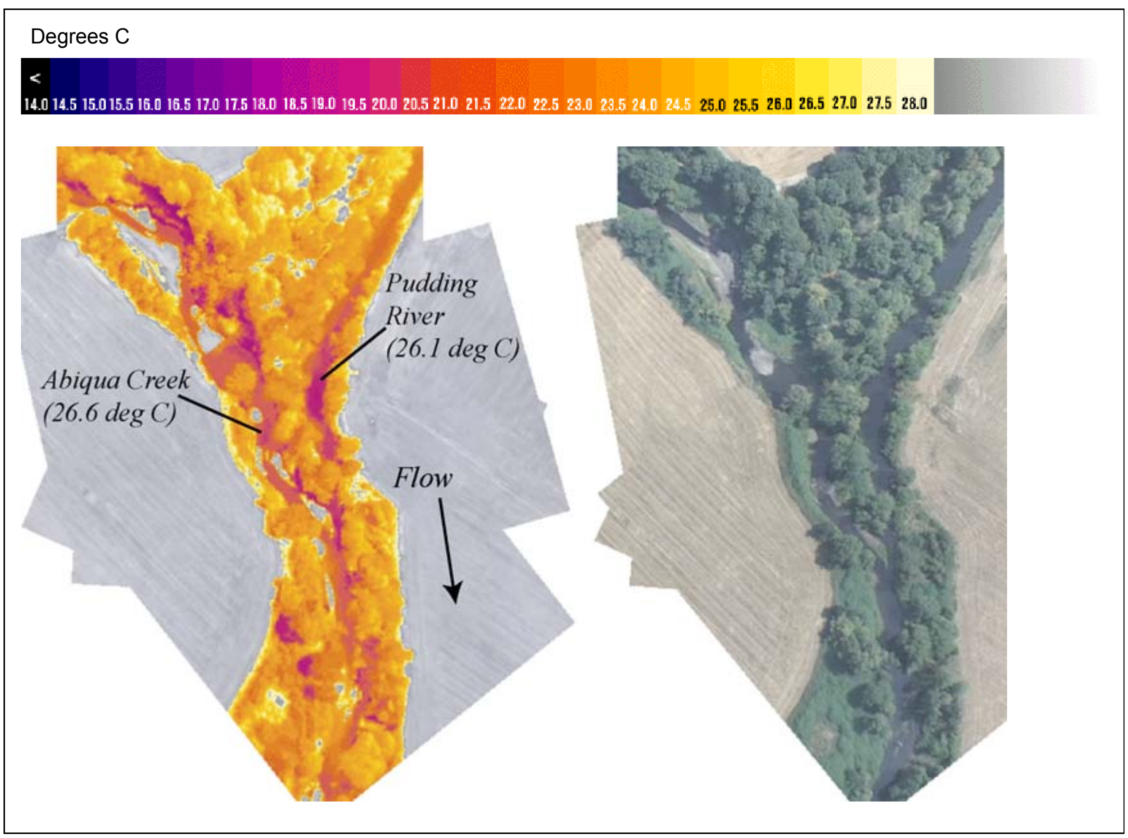

Figure A- 3: TIR/color video image pair showing Pudding River and Abiqua Creek temperatures on August 11, 2004.

Derived Data and Sampled Parameters

Spatial data input to the model comes from sampling numeric GIS data sets for landscape parameters via the analysis tool TTools (Boyd and Kasper, 2002). Sampling density is user-defined and generally matches GIS data resolution and accuracy. The sampled parameters used in the stream temperature analysis are:

- Stream Position and Aspect
- Stream Elevation and Gradient (stream bed, valley – transverse and longitudinal)
- Maximum Topographic Shade Angles (East, South, West)
- Channel Width
- TIR Temperature Data Associations
- Near Stream Land Cover

CHANNEL WIDTH ASSESSMENT

Channel width is an important component in stream heat transfer and mass transfer processes. Effective shade, stream surface area, wetted perimeter, stream depth and stream hydraulics are all highly sensitive to channel width. Accurate measurement of channel width across the stream network, coupled with other derived data, allows a comprehensive analytical methodology for assessing channel morphology. The steps for conducting channel width assessment are listed below.

Step 1. **Bankfull Channel Boundaries are digitized from DOQs at 1:5,000 or less (**Figure A- 4**).** The digitized bankfull channel boundaries are defined for purposes of the TMDL, as the width between shade-producing near-stream vegetation. Where near-stream vegetation is absent, the bankfull channel boundary is defined as the downcut stream banks or where the near-stream zone is unsuitable for vegetation growth due to external factors (i.e., roads, railways, buildings, etc.).

Step 2. **Sample Channel at each stream data node using TTools**. The sampling algorithm measures the channel width in the transverse direction relative to the stream aspect.

Step 3. **Compare GIS sampled channel widths and ground level measurements**. Establish statistical limitations for near stream disturbance zone width values when sampled from aerial photograph (DOQ) analysis.

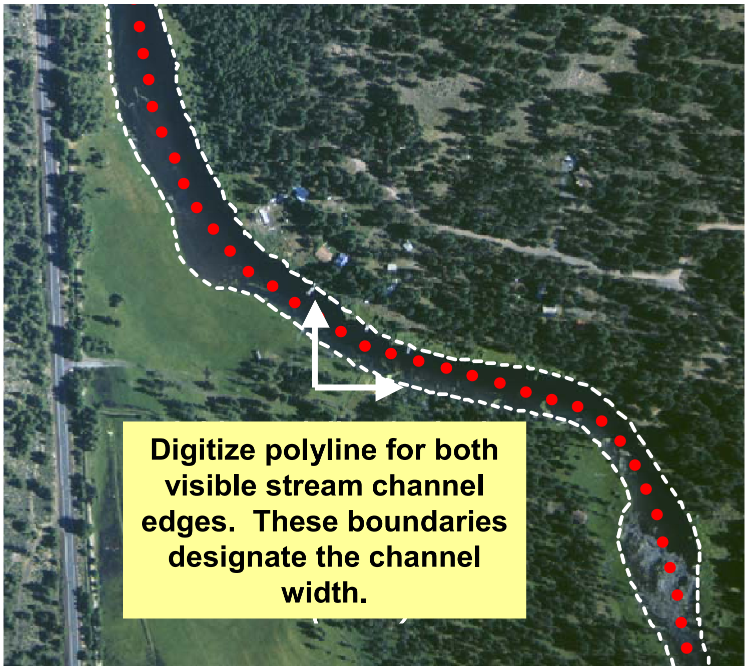

Figure A- 4: Example of digitized channel width from 1:5000 digital ortho quad aerial photograph.

NEAR STREAM LAND COVER

Oregon DEQ has mapped near stream land cover using Digital Orthophoto Quads (DOQs) at a 1:5,000 scale, ODFW's Willamette Valley landuse/landcover GIS database (ODWF, 1998), and PNWERC's Willamette River Basin Landuse and Landcover ca. 1990 GIS dataset (PNWERC/ISE, 1999). Land cover features were mapped 300 feet in the transverse direction from each stream bank. Land cover data are developed by ODEQ in successive steps.

Step 1. Land cover polygons and stream polylines are digitized from DOQs and integrated with ODFW and PNWERC datasets. All digitized polygons are drawn to capture visually like land cover features. All ODEQ digitized line work is verified at 1:5,000 or less.

Step 2. Basic land cover types are developed and assigned to individual polygons. The land cover types used in this effort are aggregate land cover groups, such as: conifers, hardwoods, shrubs, etc., and as defined by ODFW's Willamette Valley database (ODFW, 1998) and PNWERC's Willamette River Basin Landuse and Landcover ca 1990 dataset (PNWERC/ISE, 1999). Table 1A-3 lists landcover classifications and attributes used to describe current condition near stream landcover.

Step 3. Automated sampling (via TTools version 3.3, Boyd and Kasper, 2002) is conducted on classified land cover spatial data set every 100 ft. (33 m) along the stream (i.e., in the longitudinal direction). The near stream land cover is sampled every 49.5 ft. (15 m) in seven directions (S, NNW, NNE, E, W, SSE, SSW) starting at the channel center, out to 60 meters.

Step 4. Ground level land cover data are statistically summarized and sorted by land cover type.

Figure A- 5 summarizes the steps followed for near stream land cover classification. Table A- 4 lists the current land cover classification codes and descriptions as well as height and density attributes used in the modeling.

Example of Polygon Mapping of Near Stream Land Cover

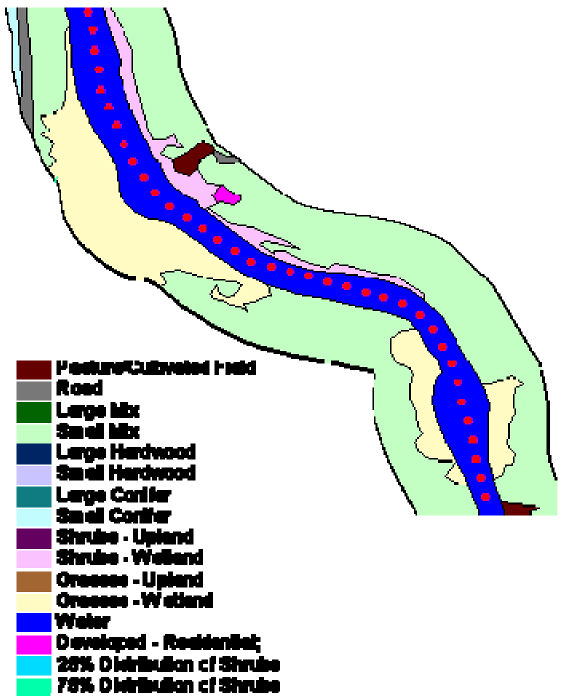

Example of Classification of the Land Cover Polygons Associating a Land Cover Type to Each of the Polygons (At this point a land cover type numeric code is associated with each polygon.)

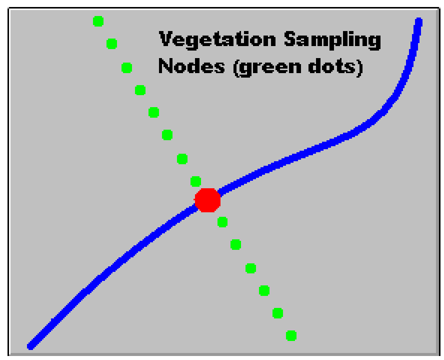

TTools longitudinal sampling pattern for near stream land cover (sampling interval is user defined). Sampling occurs for every stream data node at 4 user-defined intervals from the stream centerline, in seven directions. A database of land cover type is created for each stream data node

Figure A- 5: Examples of classifying near stream land cover.

Table A- 4: Current condition land cover classifications and attributes.

ODFW Landcover Code	PNWERC Landcover Code	ODEQ Landcover Code	Landcover Type	Height (ft)	Density
9	32 , 33	**3011**	Water	0	0%
N/A	N/A	**304**	Barren - Rock	0	0%
N/A	N/A	**308**	Barren - Clearcut	0	0%
N/A	N/A	**400**	Barren - Road	0	0%
N/A	N/A	**401**	Barren - Forest Road	0	0%
N/A	N/A	**402**	Barren - Railroad	0	0%
N/A	N/A	**403**	Barren - Ag. Road	0	0%
N/A	N/A	**3011**	River Bottom - Floodplain	0	0%
N/A	N/A	**3248**	Developed - Residential	20	100%
3	N/A	**3249**	Urban Industrial	30	100%
N/A	N/A	**3249**	Developed - Industrial	30	100%
N/A	N/A	**3252**	Dam	0	0%
N/A	N/A	**3254**	WWTP	0	0%
2.1	N/A	**21**	Annual Row Crops	0	0%
2.2	N/A	**22**	Annual Grass	3	75%
2.3	N/A	**23**	Perennial Grass	3	75%
2.4	N/A	**24**	Orchards, Vineyards, Berries, Christmas Trees, Nursery Stock	10	75%
2.4	N/A	**28**	Orchards, Vineyards, Berries, Christmas Trees, Nursery Stock	40	75%
2.5	N/A	**25**	Unmanaged Pasture	0	0%
2.6	N/A	**26**	Parks and Cemeteries	0	0%
3	N/A	**3248**	Urban Residential	20	100%
20	N/A	**202**	Black Hawthorn, Hedgerows, Brushy Fields	19	25%
20	N/A	**204**	Black Hawthorn, Hedgerows, Brushy Fields	26	25%
20	N/A	**206**	Black Hawthorn, Hedgerows, Brushy Fields	19	75%
20	N/A	**208**	Black Hawthorn, Hedgerows, Brushy Fields	26	75%
21	N/A	**212**	Cottonwood	75	25%
21	N/A	**214**	Cottonwood	105	25%
21	N/A	**216**	Cottonwood	75	75%
21	N/A	**218**	Cottonwood	105	75%
22	N/A	**222**	Willow	28	25%
22	N/A	**224**	Willow	43	25%
22	N/A	**226**	Willow	28	75%
22	N/A	**228**	Willow	43	75%
30	N/A	**30**	Reed Canary Grass	6	75%
30	N/A	**35**	Reed Canary Grass	6	25%
31	N/A	**31**	Cattail, Bulrush	5	75%
31	N/A	**315**	Cattail, Bulrush	5	25%
463	N/A	**4632**	Ash, Cottonwood - Bottomland Pasture Mosaic	33	25%
463	N/A	**4634**	Ash, Cottonwood - Bottomland Pasture Mosaic	93	25%
463	N/A	**4636**	Ash, Cottonwood - Bottomland Pasture Mosaic	33	75%
463	N/A	**4638**	Ash, Cottonwood - Bottomland Pasture Mosaic	93	75%
476	N/A	**4762**	Oak, Douglas Fir - >50% Oak	53	25%
476	N/A	**4764**	Oak, Douglas Fir - >50% Oak	93	25%
476	N/A	**4766**	Oak, Douglas Fir - >50% Oak	53	75%
476	N/A	**4768**	Oak, Douglas Fir - >50% Oak	93	75%
505	N/A	**5052**	Douglas Fir, Oak - < 50% Oak	53	25%
505	N/A	**5054**	Douglas Fir, Oak - < 50% Oak	91	25%
505	N/A	**5056**	Douglas Fir, Oak - < 50% Oak	53	75%
505	N/A	**5058**	Douglas Fir, Oak - < 50% Oak	91	75%
506	N/A	**5062**	Oak, Madrone, Douglas Fir	50	25%
506	N/A	**5064**	Oak, Madrone, Douglas Fir	87	25%
506	N/A	**5066**	Oak, Madrone, Douglas Fir	50	75%
506	N/A	**5068**	Oak, Madrone, Douglas Fir	87	75%
510	N/A	**5102**	Maple, Alder, Fir	65	25%
510	N/A	**5104**	Maple, Alder, Fir	93	25%
510	N/A	**5106**	Maple, Alder, Fir	65	75%
510	N/A	**5108**	Maple, Alder, Fir	93	75%
512	N/A	**5122**	Douglas Fir or any Conifer	102	25%
512	N/A	**5124**	Douglas Fir or any Conifer	160	25%
512	N/A	**5126**	Douglas Fir or any Conifer	102	75%
512	N/A	**5128**	Douglas Fir or any Conifer	160	75%
999	N/A	**999**	Gravel and Sand	0	0%
1000	N/A	**1002**	Unclassified Forest	56	25%
1000	N/A	**1004**	Unclassified Forest	89	25%
1000	N/A	**1006**	Unclassified Forest	56	75%
1000	N/A	**1008**	Unclassified Forest	89	75%

Table A-4 continued.

ODFW Landcover Code	PNWERC Landcover Code	ODEQ Landcover Code	Landcover Type	Height (ft)	Density
N/A	1	**3248**	Residential 0-4 DU/ac	20	100%
N/A	6	**3249**	Commercial	30	100%
N/A	7	**3249**	Comm/Industrial	30	100%
N/A	8	**3249**	Industrial	30	100%
N/A	11	**11**	Urban non-vegetated unknown	0	0%
N/A	12	**12**	Civic/open space	0	0%
N/A	16	**16**	Rural structures	20	100%
N/A	18	**402**	Railroad	0	0%
N/A	19	**400**	Primary roads	0	0%
N/A	20	**400**	Secondary roads	0	0%
N/A	21	**400**	Light duty roads	0	0%
N/A	24	**88**	Rural non-vegetated unknown	0	0%
N/A	29	**301**	Channel non-vegetated	0	0%
N/A	32	**301**	Stream orders 5-7	0	0%
N/A	33	**301**	Water	0	0%
N/A	49	**492**	Urban tree overstory	19	25%
N/A	49	**494**	Urban tree overstory	26	25%
N/A	49	**496**	Urban tree overstory	19	75%
N/A	49	**498**	Urban tree overstory	26	75%
N/A	51	**51**	Forest open	0	0%
N/A	52	**52**	Forest Semi-closed mixed	56	25%
N/A	52	**525**	Forest Semi-closed mixed	90	25%
N/A	53	**53**	Forest Closed hardwood	38	75%
N/A	53	**535**	Forest Closed hardwood	67	75%
N/A	54	**54**	Forest Closed mixed	56	75%
N/A	54	**545**	Forest Closed mixed	90	75%
N/A	55	**55**	Forest Semi-closed conifer	101	25%
N/A	55	**555**	Forest Semi-closed conifer	162	25%
N/A	56	**56**	Conifers 0-20 yrs (20)	50	25%
N/A	56	**565**	Conifers 0-20 yrs (20)	50	75%
N/A	57	**57**	FCC 21-40 yrs (30)	86	25%
N/A	57	**575**	FCC 21-40 yrs (30)	86	75%
N/A	58	**58**	FCC 41-60 yrs (50)	129	25%
N/A	58	**585**	FCC 41-60 yrs (50)	129	75%
N/A	59	**59**	FCC 61-80 yrs (70)	156	25%
N/A	59	**595**	FCC 61-80 yrs (70)	156	75%
N/A	60	**60**	FCC 81-200 yrs (140)	205	25%
N/A	60	**605**	FCC 81-200 yrs (140)	205	75%
N/A	61	**61**	FCC >200 yrs * (140)	205	25%
N/A	61	**615**	FCC >200 yrs * (140)	205	75%
N/A	62	**62**	Forest Semi-closed hardwood	38	25%
N/A	62	**625**	Forest Semi-closed hardwood	67	25%
N/A	68	**21**	Irrigated annual rotation	0	0%
N/A	71	**22**	Grains	3	75%
N/A	72	**24**	Nursery	10	75%
N/A	72	**28**	Nursery	40	75%
N/A	73	**24**	Caneberries & Vineyards	10	75%
N/A	73	**28**	Caneberries & Vineyards	40	75%
N/A	75	**24**	Hops	10	75%
N/A	79	**21**	Row crop	0	0%
N/A	82	**21**	Field crop	0	0%
N/A	83	**22**	Hay	3	75%
N/A	84	**21**	Late field crop	0	0%
N/A	85	**85**	Pasture	0	0%
N/A	86	**23**	Natural grassland	3	75%
N/A	87	**87**	Natural shrub	15	25%
N/A	87	**875**	Natural shrub	15	75%
N/A	88	**88**	Bare/fallow	0	0%
N/A	89	**301**	Flooded/marsh	0	0%
N/A	90	**21**	Irrigated field crop	0	0%
N/A	91	**91**	Turfgrass/park	0	0%
N/A	92	**24**	Orchard	10	75%
N/A	92	**28**	Orchard	40	75%
N/A	93	**932**	Christmas trees	10	75%
N/A	93	**934**	Christmas trees	40	75%
N/A	N/A	**156**	Oak - Bottomland	40	25%
N/A	N/A	**158**	Oak - Bottomland	40	75%
N/A	N/A	**152**	Oak - Bottomland	20	25%
N/A	N/A	**154**	Oak - Bottomland	20	75%

EFFECTIVE SHADE

Stream surface shade is an important parameter that controls the stream heating derived from solar radiation. Solar radiation has the potential to be the largest heat transfer mechanism in a stream system. Effective shade is the percent of solar radiation that is blocked from the stream surface (Figure A- 6).

In the Northern Hemisphere, the earth tilts on its axis toward the sun during summertime months allowing longer day length and higher solar altitude, both of which are functions of solar declination (i.e., a measure of the earth's tilt toward the sun). Geographic position (i.e., latitude and longitude) fixes the stream to a position on the globe, while aspect provides the stream/riparian orientation. Near stream land cover height, width and density describe the physical barriers between the stream and sun that can attenuate and scatter incoming solar radiation or solar flux (i.e., produce shade). The solar position has a vertical component (i.e., solar altitude) and a horizontal component (i.e., solar azimuth) (Figure A- 7) are both functions of time/date (i.e., solar declination) and the earth's rotation (i.e., hour angle measured as 15^{o} per hour). While the interaction of these shade variables may seem complex, the mathematics that describe them is relatively straightforward geometry. Using solar tables or mathematical simulations, the *potential daily solar load* can be quantified. The *measured solar load* at the stream surface can easily be measured with a Solar Pathfinder© or estimated using mathematical shade simulation computer programs (Boyd, 1996 and Park, 1993).

Factors that influence stream surface effective shade are incorporated into the simulation methodology, and include the following:

Season/Time: Date/Time
Stream Morphology: Aspect, Channel Width, Incision
Geographic Position: Latitude, Longitude, Topography
Land Cover: Near Stream Land Cover Height, Width, Density
Solar Position: Solar Altitude, Solar Azimuth

The temperature model Heat Source (Boyd and Kasper, 2004) and a subset model of Heat Source called Shade-a-lator were used to model solar flux, potential daily solar load, measured solar load at the stream surface, and effective shade.

Figure A- 6: Effective shade defined.

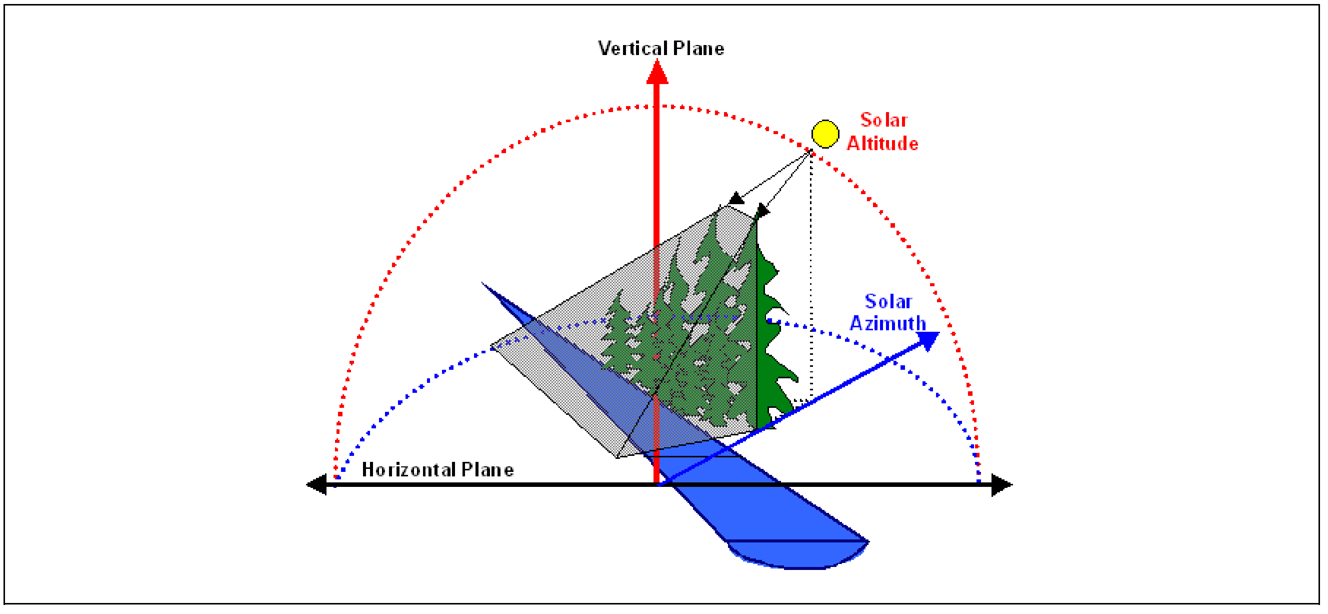

Figure A- 7: Solar Altitude and Solar Azimuth

The effective shade analysis was conducted with data input sampling and a computation rate every 100 longitudinal feet (33 m) along the stream. The effective shade model is calibrated to analyze and predict effective shade for narrow periods of time as a function of Julian Day. The output data are reliable for mid July through mid September.

Once effective shade models are calibrated, potential near stream land cover scenarios are simulated (as detailed in Appendix C – Potential Near Stream Land Cover in the Willamette Basin for TMDLs). System potential vegetation conditions are simulated with a monte carlo method that randomly distributes the percentage of natural disturbance. Natural disturbance is modeled as a decrease in effective shading.

MODEL CALIBRATIONS

The stream temperature model Heat Source (Boyd and Kasper, 2004) was used to develop calibrated models of the Molalla and Pudding Rivers. Heat Source version 7 was used to model the Molalla River and Heat Source version 8 was used to model the Pudding River. For detailed information regarding Heat Source and the methodologies used, refer to Appendix B -Heat Source Analytical Framework or "*Analytical Methods for Dynamic Open Channel Heat and Mass Transfer: Methodology for Heat Source Model Version 7.0*" (Boyd, Kasper, 2003). Active channel width and vegetative shade inputs for the modeling were derived via GIS analysis and the analysis tool TTools (Boyd and Kasper, 2002).

Two different DEQ modelers performed the Molalla River and Pudding River modeling. While the modelers used the same general methodology in developing and calibrating the models, there are some differences in analysis and presentation between the two models.

Error Statistics

Several statistics were used to estimate the ability of the models to accurately predict stream temperatures. The statistics quantify how well model calculated stream temperatures match observed stream temperatures. Statistics used are mean error (ME), mean absolute error (MAE), root mean square (RMS) error, and the square of the Pearson correlation coefficient (R^2), as follows:

Mean Error (ME) – A mean error of zero indicates a perfect fit. A positive value indicates on average the model predicted values are less than the observed data. A negative value indicates on average the model predicted values are greater than the observed data. The mean error statistic may give a false ideal value of zero (or near zero) if the average of the positive deviations between predictions and observations is about equal to the average of the negative deviations in a data set. Because of this, the mean absolute error statistic should be used in conjunction with mean error to measure model performance.

$$ME = \frac{\sum (y-x)}{n}$$

Mean Absolute Error (MAE) - A mean absolute error of zero indicates a perfect fit. The magnitude of the mean absolute error indicates the average deviation between model predicted values and observed data. The mean absolute error cannot give a false zero.

$$MAE = \frac{\sum |(y-x)|}{n}$$

Root Mean Square Error (RMS) – A root mean square error of zero indicates a perfect fit. Root mean square error is a measure of the magnitude of the difference between model predicted values and observed data.

$$RMS = \sqrt{\frac{\sum (y-x)^2}{n}}$$

R Squared – An r squared of one indicates a perfect fit. R squared measures how well a regression line fits observed data.

$$R^2 = \frac{n\left(\sum xy\right) - \left(\sum x\right)\left(\sum y\right)}{\sqrt{\left[n\sum x^2 - \left(\sum x\right)^2\right]\left[n\sum y^2 - \left(\sum y\right)^2\right]}}$$

y = A single predicted or modeled data value
x = A single corresponding field or observed data value
n = Total number of data points or observations

Molalla River Model Calibration

The temperature model was calibrated to the TIR data collected on July 26, 2004 as well as the continuous temperature data collected at several locations throughout the modeled period (July 20 – August 2, 2004). Simulations were performed for a total of 44 stream miles (76 km).

TIR COMPARISON

The first simulation step is to calibrate the model to current condition stream temperatures. DEQ adjusted input variables such as channel width-to-depth ratio, Manning's roughness coefficient (*n*) (which affects stream velocity), amount of groundwater/surface water interaction, and wind speed (which affects evaporation) in order to simulate the temperatures measured with the TIR. Modeling results comparing simulated current condition for the Molalla River to the TIR data are presented in Figure A- 8. Comparison of the TIR data with the Molalla River model simulation meets the target of errors less than 1.0ºC (Table A- 5).

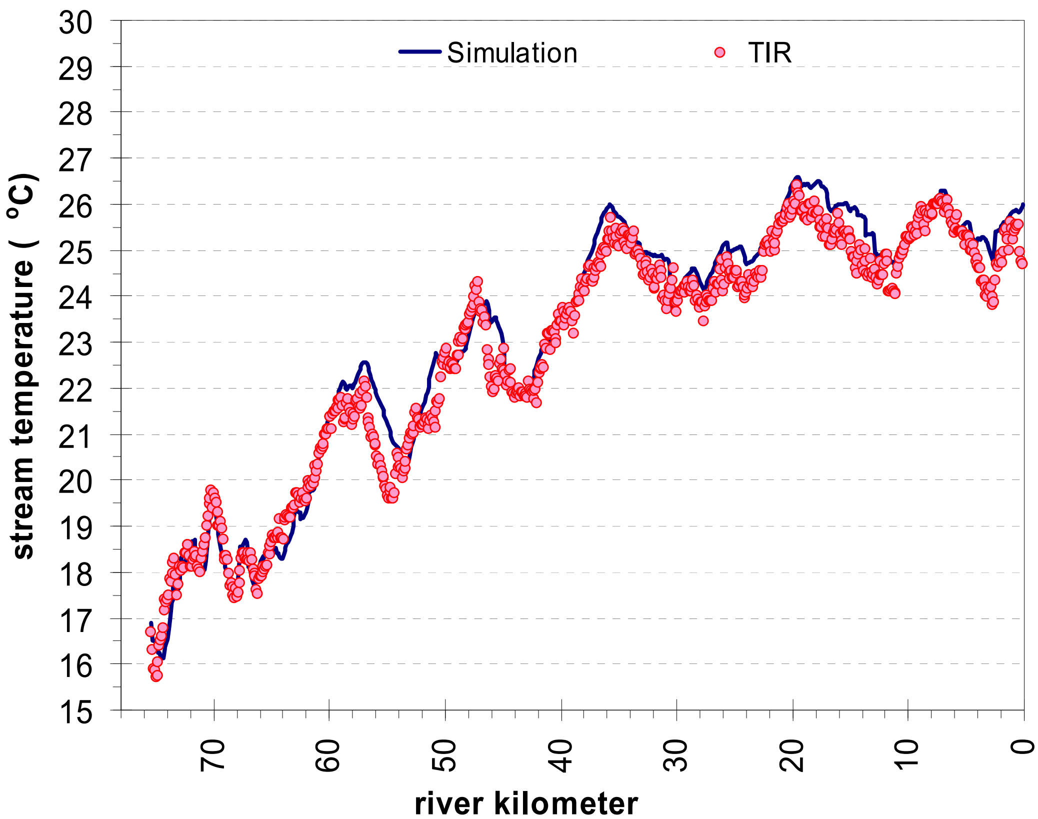

Figure A- 8: Thermal Infrared Radiometry measured temperature compared with model simulated temperature. Periodic temperature decreases may indicate the influence of cooler tributaries, springs, seeps, and groundwater interaction.

Table A- 5: Error statistics for Molalla River model versus TIR data.

	Entire River (°C)
Mean Error	0.32
Mean Absolute Error	0.44
RMS Error	0.56

CONTINUOUS TEMPERATURE MONITORING LOCATIONS

For the purposes of this analytical effort, validation refers to the statistical comparison of measured field data and the Heat Source model simulated current condition. Standard error statistics are calculated for instream measured continuous temperature data sets. Since TIR temperature data sets are robust spatially, there is a possibility that the simulation could be calibrated to the specific time when TIR data was obtained, yet perform poorly for other periods of the day. The model's simulation of continuous temperature for stations upstream of river mile 6 generally meets the standard error target of <1.0 ºC, but the agreement between model simulated temperatures and continuously measured temperatures decreases somewhat for stations between river mile 6 and the mouth.

Statistics for the Molalla River model calibration and validation are presented in Table A- 6. Graphical comparisons of modeled temperature and measured temperature at the continuously monitored locations are presented in Figure A- 9 through Figure A- 19. The figures show that the greatest discrepancy between simulated and measured temperatures, especially at stations 10 and 11, occurs in the first week of the model period when measured stream temperatures are higher than simulated stream temperatures. Air temperatures during this first week (July 20 – 26) were higher than the second week of the model period (July 27 – August 2). In particular, maximum measured air temperatures on July 23, 24, and 25 were near or exceeding 38ºC (100 ºF). Possibly, the model is not as sensitive to spikes in air temperature as is the stream itself: the wide stream conditions in the lower river miles may respond more rapidly to increases in air temperature than does the simulation.

Table A- 6: Error statistics for Molalla River model.
SE = standard error, RMS = root mean square error, ME = mean error, MAE = mean absolute error. R^2 is the regression coefficient or a statistic that describes the degree of difference between the modeled and measured temperatures. The thermister failed at node 5 and the data is not included in this table.

Temperature measurement location	River Km	River Mile	SE	R^2	RMS	ME	MAE
1	75.4	46.8	0.03	1.00	0.03	0.00	0.02
2	64.8	40.3	0.53	0.83	0.99	-0.79	0.83
3	54.5	33.8	1.02	0.48	**1.24**	-0.68	0.99
4	45.0	28.0	**1.07**	0.72	**1.15**	-0.41	0.93
6	24.4	15.2	**1.08**	0.69	**1.94**	**-1.58**	**1.59**
7	20.5	12.7	1.00	0.81	**1.59**	**-1.24**	**1.34**
8	13.7	8.5	0.61	0.88	**1.55**	**-1.42**	**1.43**
9	10.4	6.5	0.91	0.73	**1.35**	-0.99	**1.04**
10	4.8	3.0	**1.59**	0.42	**2.19**	**-1.51**	**1.79**
11	3.2	2.0	**1.23**	0.45	**2.15**	**-1.74**	**1.77**
12	0.3	0.2	0.50	0.88	0.96	-0.72	0.77
July 26 TIR			0.41	0.98	0.56	0.32	0.44

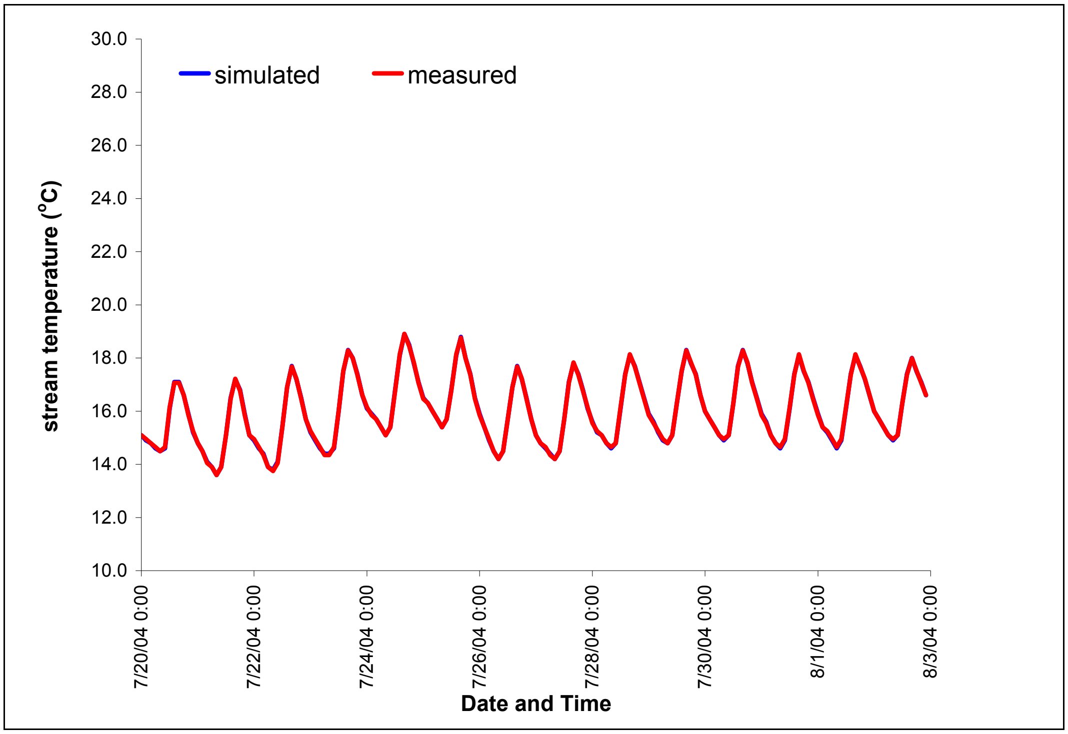

Figure A- 9: Continuous temperature measured and simulated at Molalla River at Locked Gate, river kilometer 75.4 (46.8 river miles).

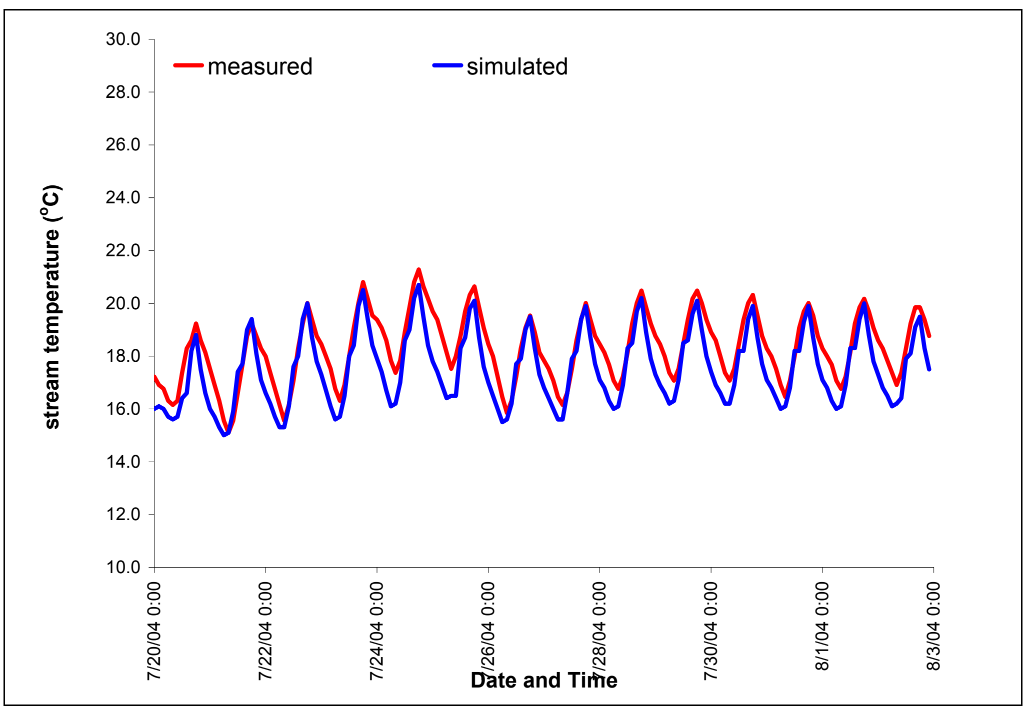

Figure A- 10: Continuous temperature measured and simulated at Molalla River upstream of Horse Creek, river kilometer 64.8 (40.3 river miles).

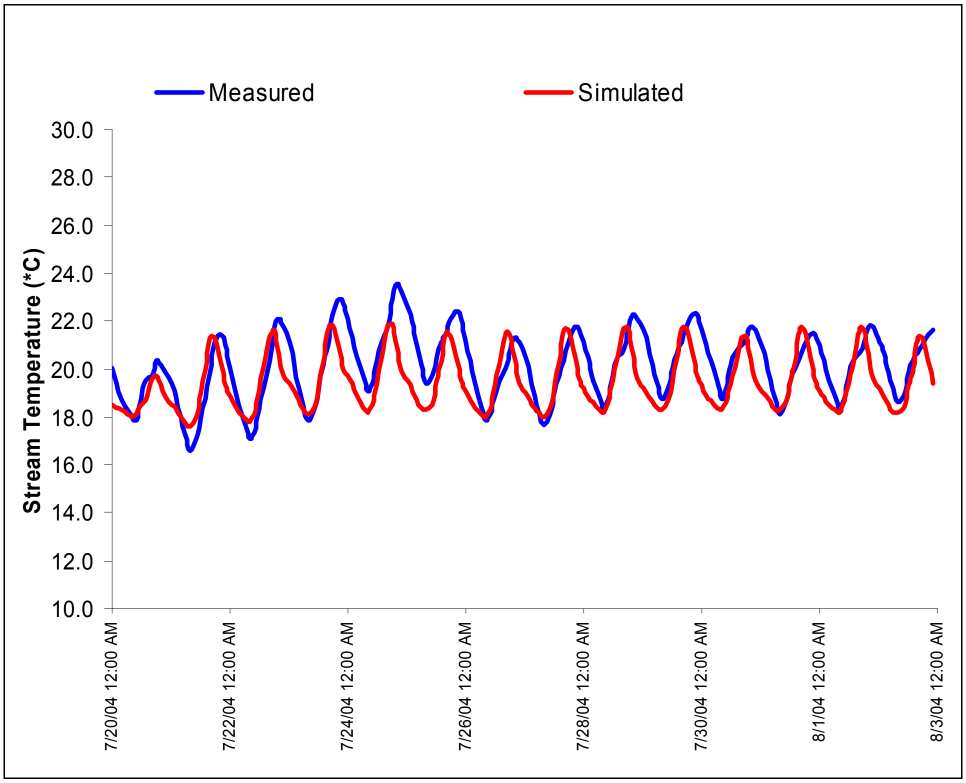

Figure A- 11: Continuous temperature measured and simulated at Molalla River upstream of Pine Creek, river kilometer 54.4 (33.8 river miles).

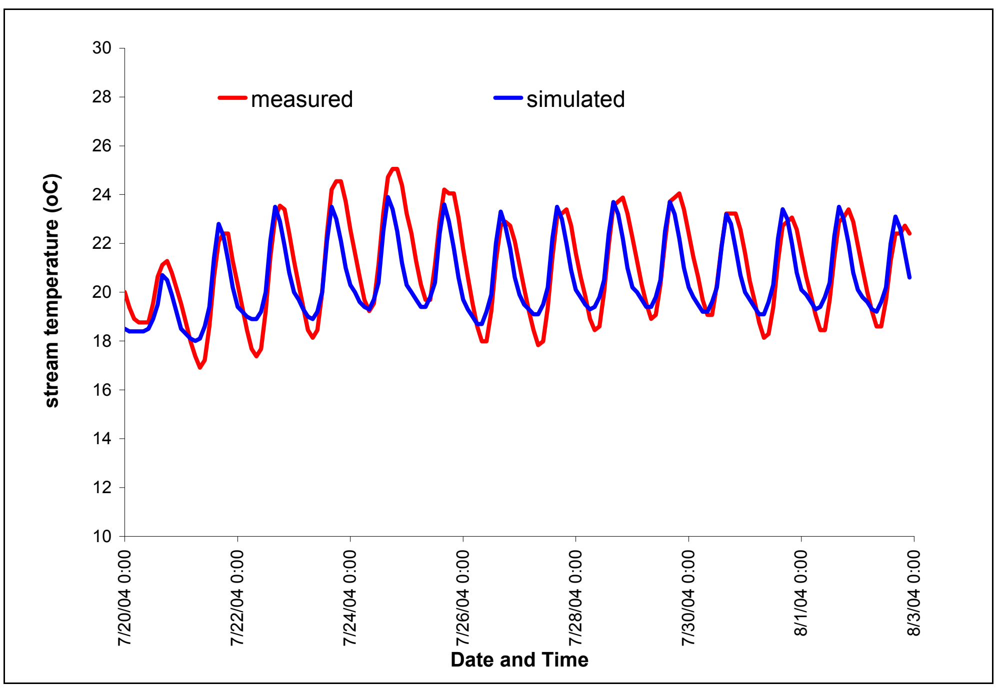

Figure A- 12: Continuous temperature measured and simulated at Molalla River upstream of North Fork Molalla River, river kilometer 45 (28 river miles).

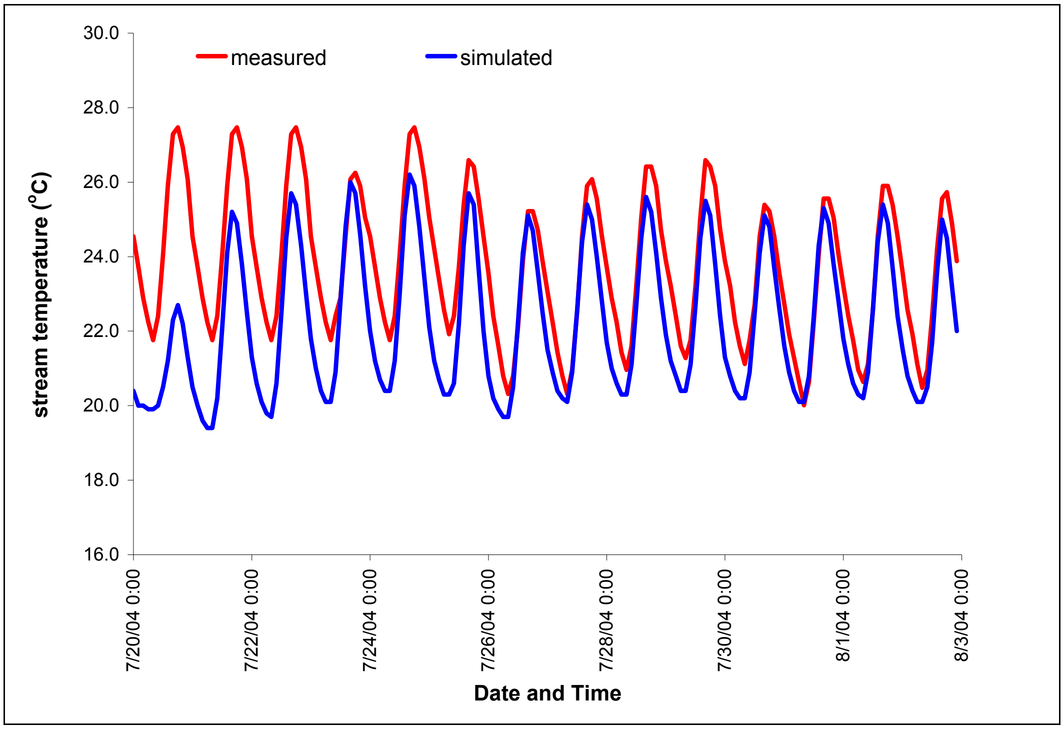

Figure A- 13: Continuous temperature measured and simulated at Molalla River at Highway 213, river kilometer 24.4 (15.2 river miles).

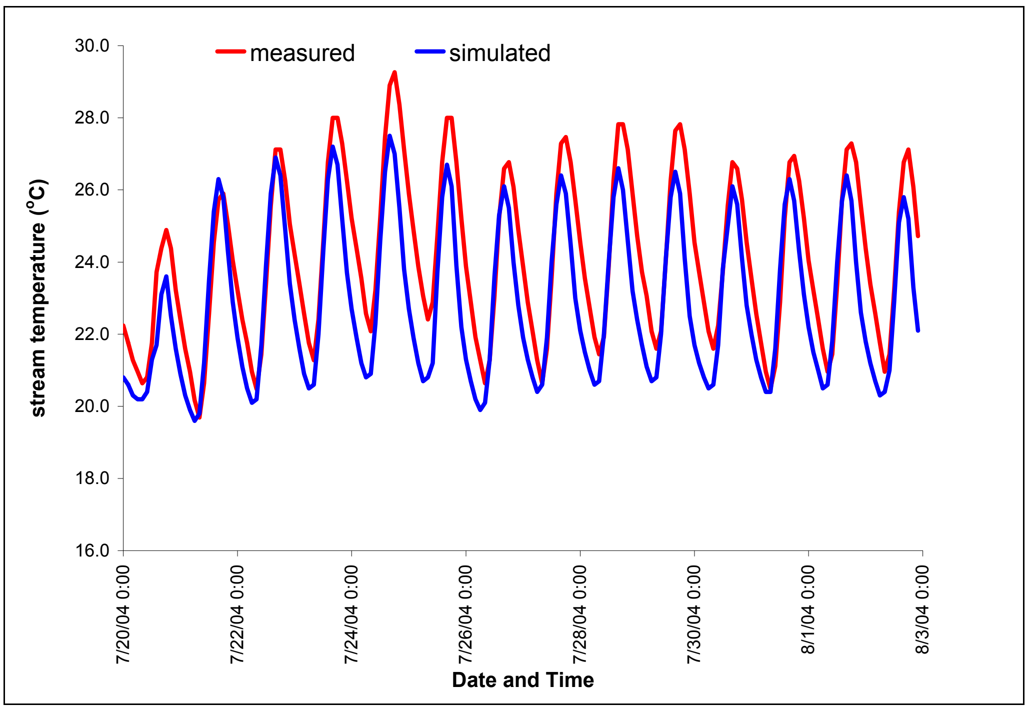

Figure A- 14: Continuous temperature measured and simulated at Molalla River at Kraxberger Rd., river kilometer 20.5 (12.7 river miles).

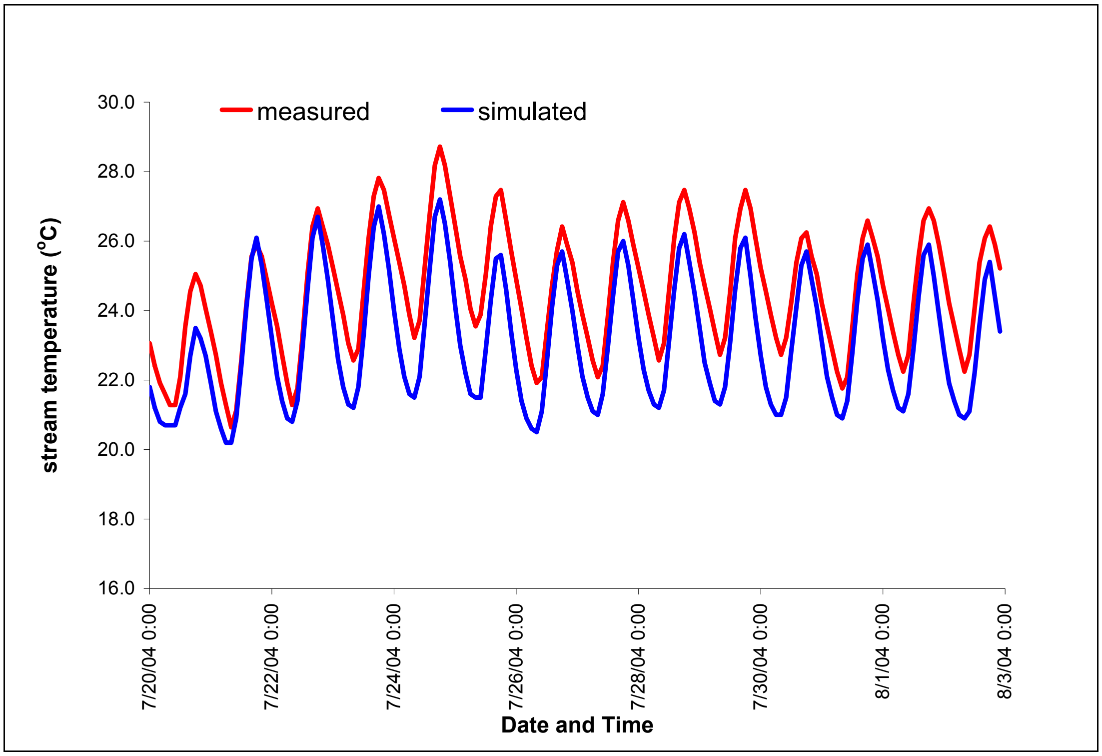

Figure A- 15: Continuous temperature measured and simulated at Molalla River upstream of Milk Creek, river kilometer 13.6 (8.5 river miles).

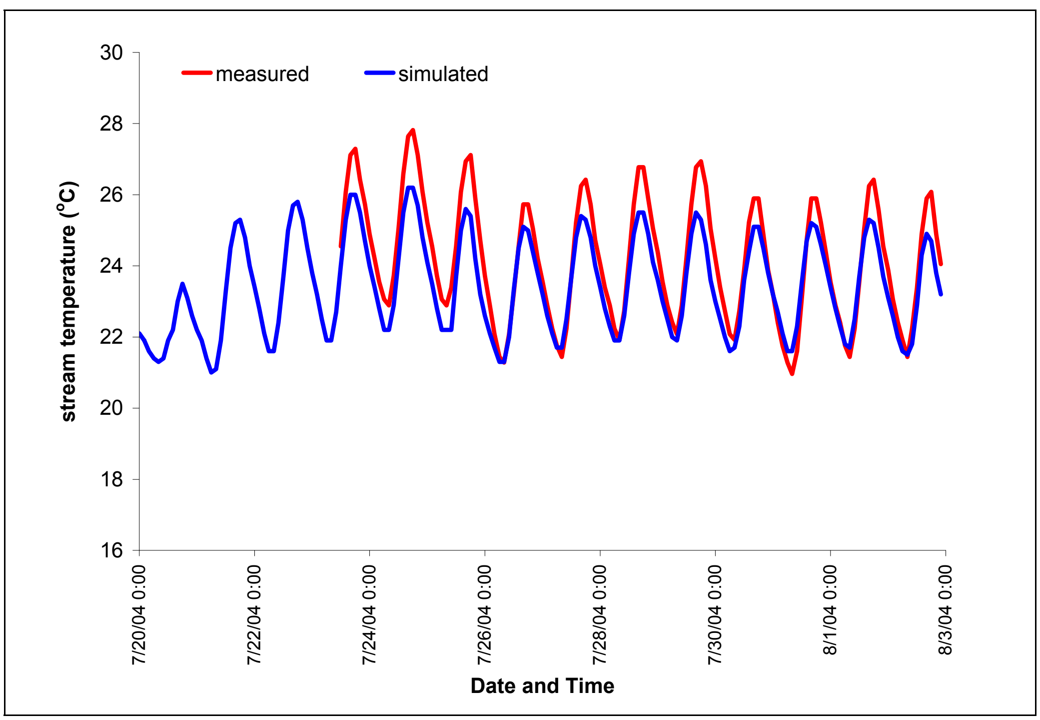

Figure A- 16: Continuous temperature measured and simulated at Molalla River at Goods Bridge, river kilometer 10.4 (6.5 river miles).

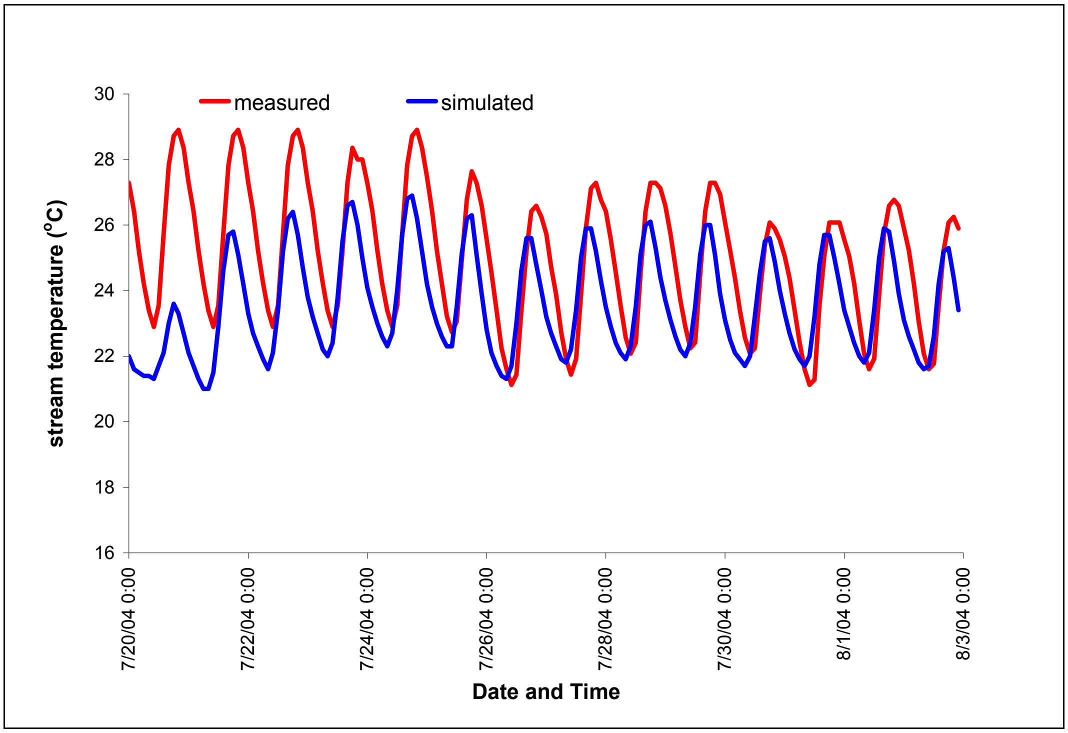

Figure A- 17: Continuous temperature measured and simulated at Molalla River at Knights Bridge Rd., river kilometer 4.8 (3 river miles).

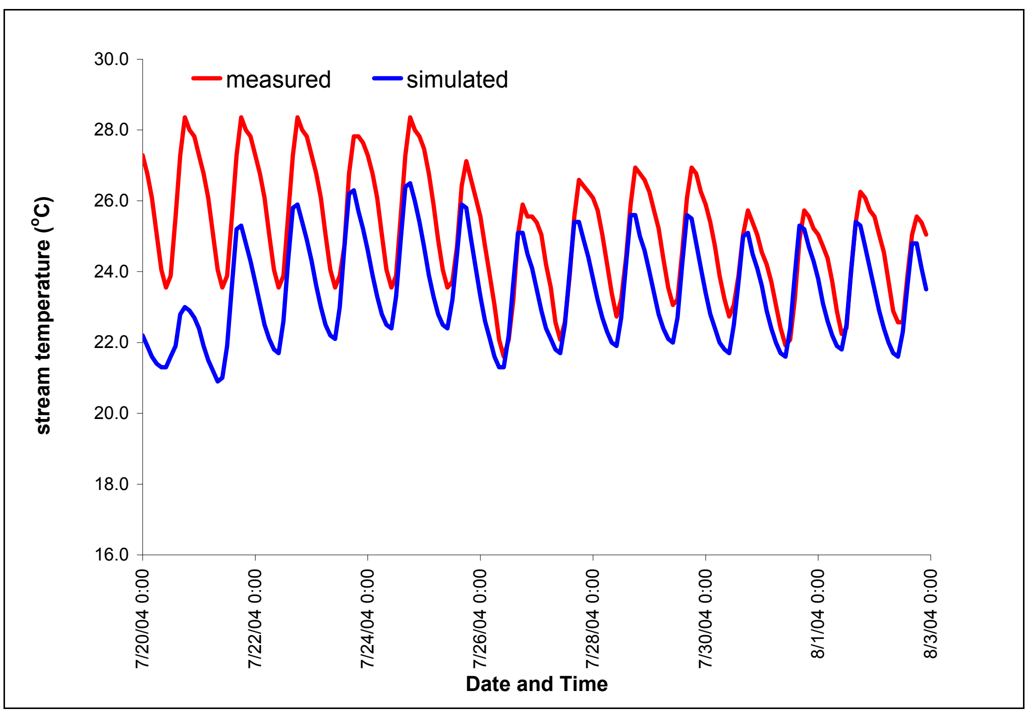

Figure A- 18: Continuous temperature measured and simulated at Molalla River at 22nd, river kilometer 3.2 (2 river miles).

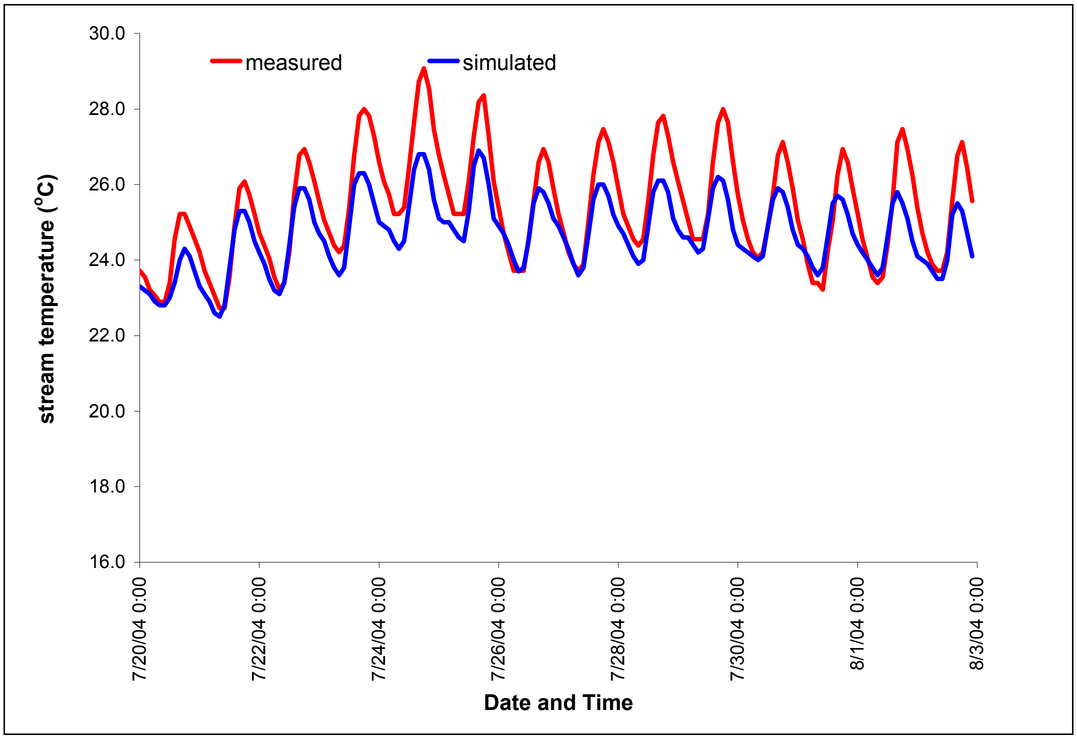

Figure A- 19: Continuous temperature measured and simulated at Molalla River at mouth, river kilometer 0.3 (0.2 river miles).

STREAM DISCHARGE AND CHANNEL MEASUREMENT COMPARISONS

Where measured discharge was not available for model input (e.g. springs and smaller tributary streams), DEQ used a mass balance approach to estimate discharge to the mainstem Molalla River. Provided that at least one instream flow rate is known the other flow rates can be calculated using the following relationship:

$$T_{mix} = \frac{(Q_{up} \cdot T_{up}) + (Q_{in} \cdot T_{in})}{(Q_{mix})} = \frac{(Q_{up} \cdot T_{up}) + (Q_{in} \cdot T_{in})}{(Q_{up} + Q_{in})}$$

where,

Q_{up}: Stream flow rate upstream from mass transfer process
Q_{in}: Inflow volume or flow rate
Q_{mix}: Resulting volume or flow rate from mass transfer process ($Q_{up} + Q_{in}$)
T_{up}: Stream temperature directly upstream from mass transfer process
T_{in}: Temperature of inflow
T_{mix}: Resulting stream temperature from mass transfer process assuming complete mix

The Molalla River modeled longitudinal stream discharge based on measured flows, OWRD points of diversion data, and mass balance estimates is presented with measured discharge points in Figure A- 20.

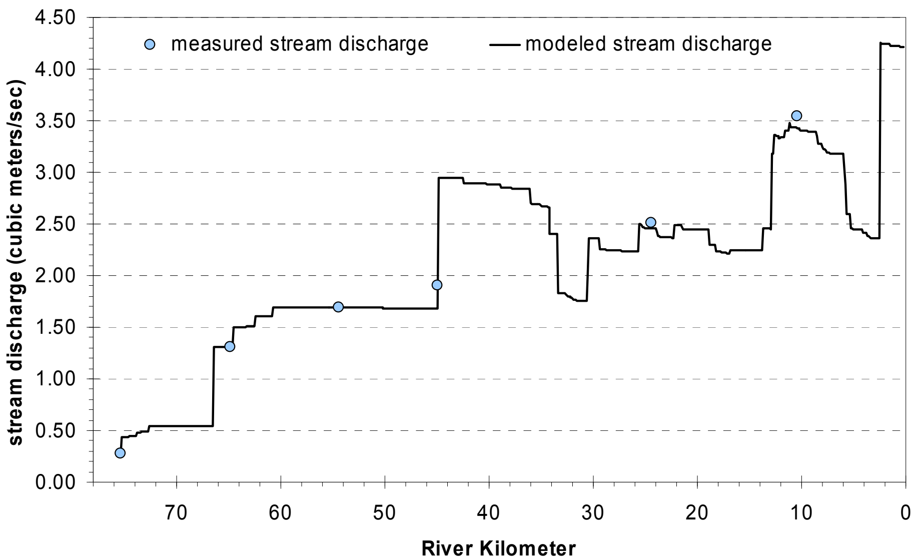

Figure A- 20: Modeled and measured stream discharge on the Molalla River.
Stream discharge measurements were collected on July 20 and 22, 2004. The model simulates stream discharge on July 26.

DEQ verified model output by comparing model simulated characteristics with measurements of wetted depth, wetted width, and bankfull width. The average stream depth at a site is the average of each of the depth measurements (usually 10 to 20, depending on the width of the channel) recorded during the cross sectional stream discharge measurements. The average depth measurements for the Molalla River compared with the modeled depths are shown in Figure A- 21. The measured depths are shown with bars that represent the range of depth measurements across the channel at that site.

Results comparing channel widths derived from GIS and modeling to those measured in the field are presented in Figure A- 22. The wetted width measurements agree with the simulated measurements reasonably well.

DEQ verified those remote measurements of bankfull width with four field measurements (Figure A- 23). The agreement is reasonable and the discrepancy between remotely measured and field measured bankfull width near the headwaters is likely because the more dense vegetation obscures the stream banks in the aerial photographs. The discrepancy may also result from the GIS measurement and the field measurement occurring at slightly different locations on the stream.

Figure A- 24 illustrates a comparison of the GIS-measured bankfull width with the simulated wetted width. The wetted width is a model-calculated characteristic based on the channel shape and the amount of stream flow. One would expect the wetted width to be less than the bankfull width, but follow a similarly varying pattern. Figure A- 24 indicates this is generally the case and that the model's calculations of wetted width are realistic.

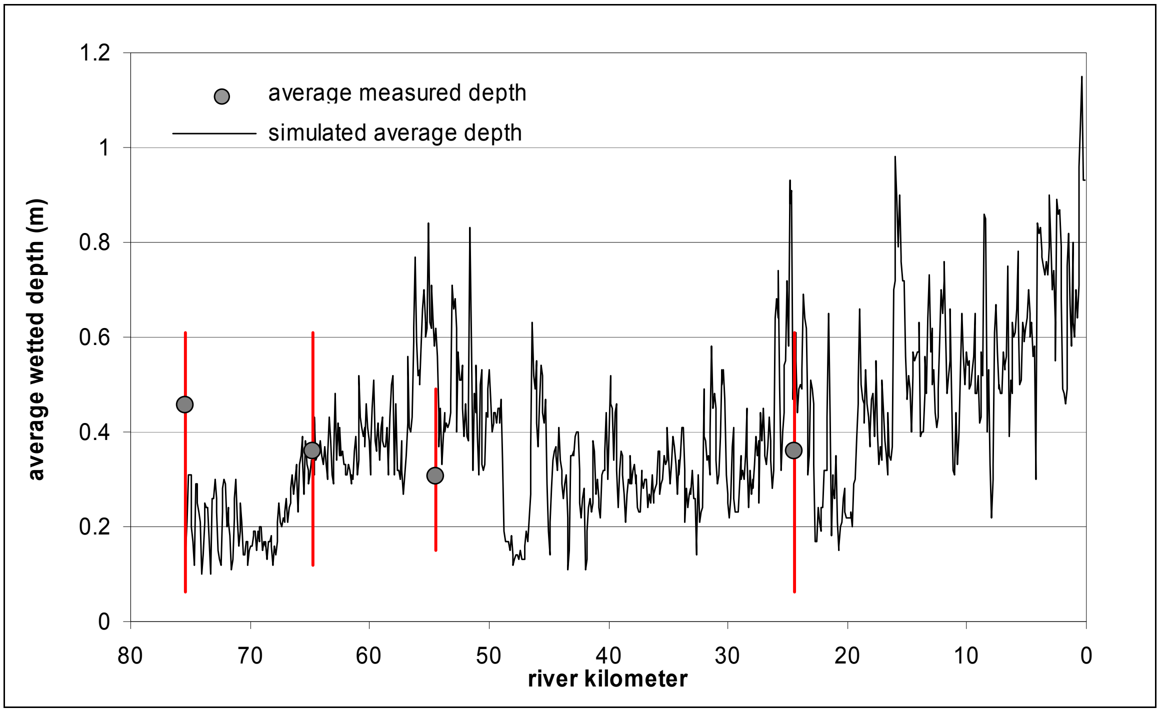

Figure A- 21: Simulated Molalla River wetted depth and average depth measurements.

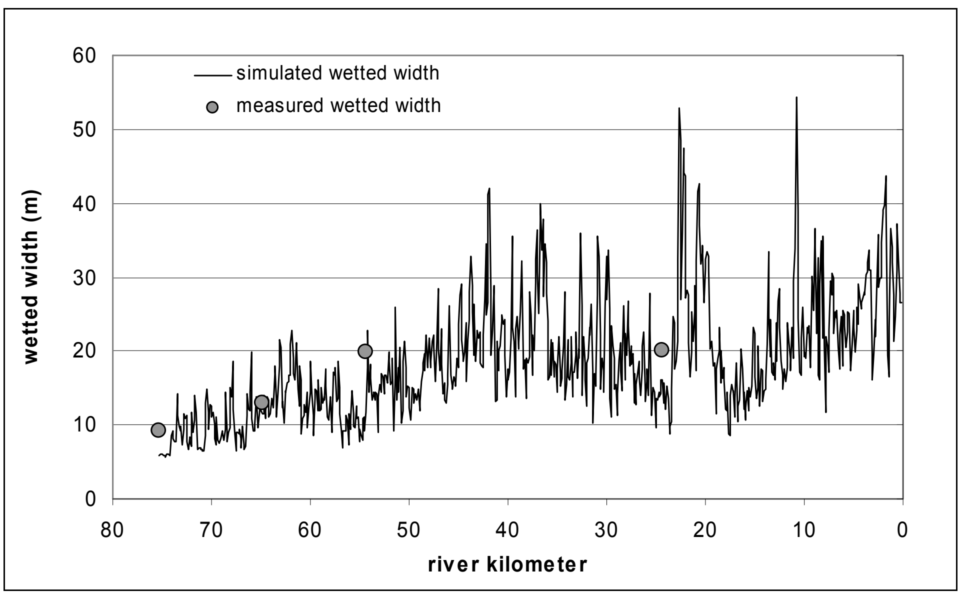

Figure A- 22: Simulated Molalla River wetted width and wetted width measurements.

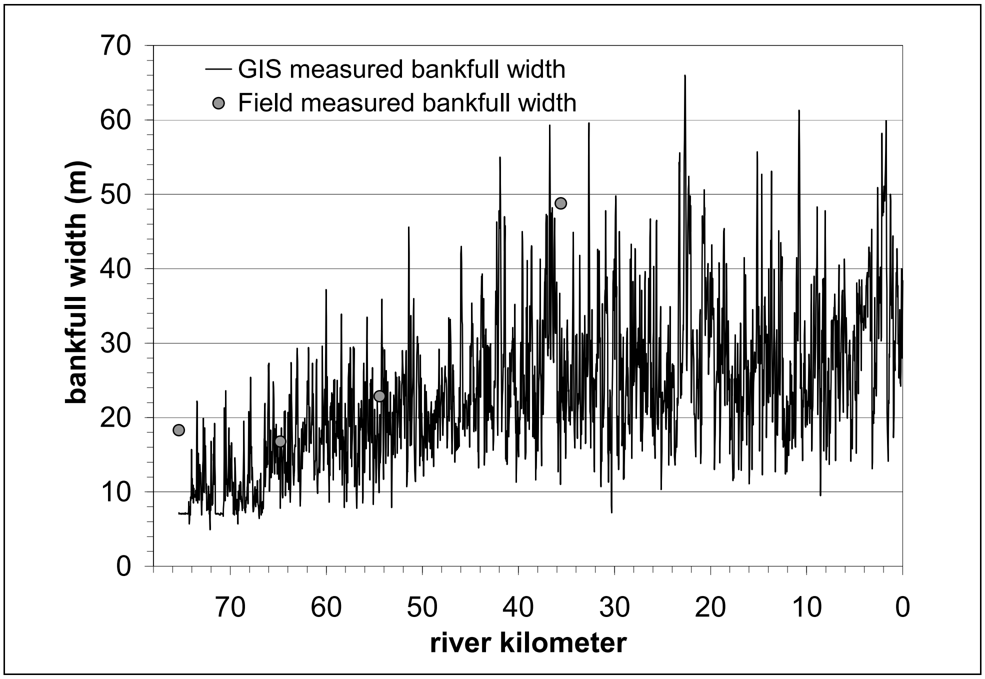

Figure A- 23: Remotely measured bankfull width and field measured bankfull width.

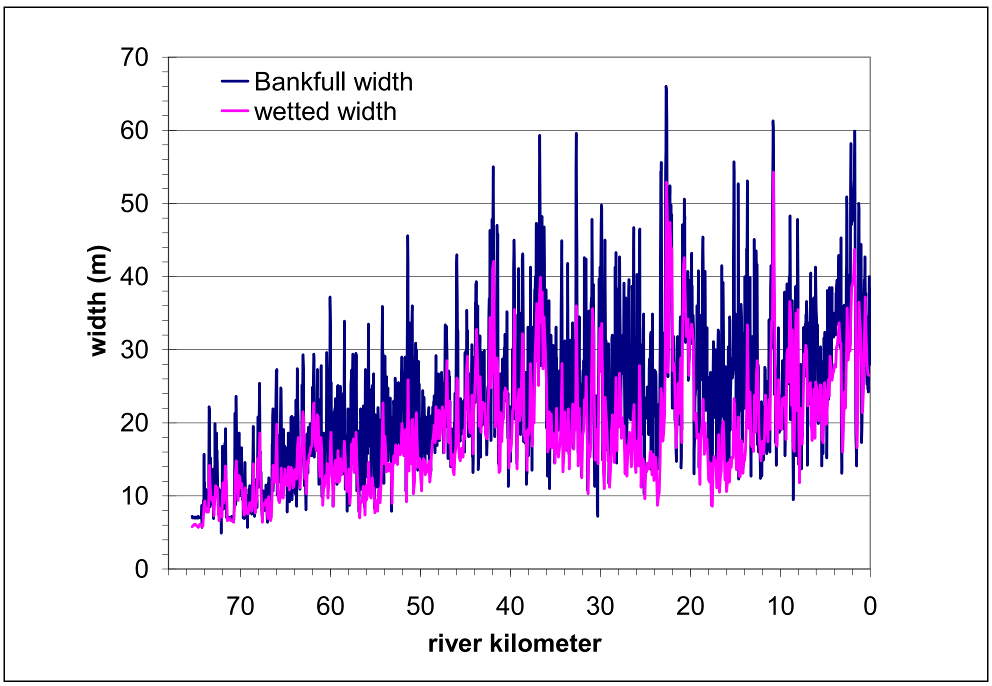

Figure A- 24: Comparison of bankfull width and simulated wetted width of the Molalla River

Pudding River model calibration

The Pudding River model was calibrated for a 14 day period from August 1 to August 14, 2004. This time period includes the August 11 and 12 dates of thermal infrared (TIR) temperature data collection and corresponds to a period of low flow (Figure A- 25). During the 14 day calibration period, flows ranged from 14 to 50 cfs at the Pudding River USGS gage at Woodburn (RKm 38.0, RM 23.4) and 13 to 92 cfs at the gage at Aurora (RKm12.5, RM 8.1). These correspond to flow rates between the first and 20th percentiles. After August 14, flow rates decreased to significantly less than the 7Q10 low flow rate of 15 cfs at Woodburn gage and 25 cfs at the Aurora gage. Since flows were less than 7Q10 and since several Pudding River thermisters failed during this very low flow period, model simulations were not continued beyond August 14.

For the period modeled, most days were sunny, as indicated by solar radiation data at Aurora[1] (Figure A-25). In order to account for the reduction in solar radiation on cloudy days, cloud cover data from Aurora was input to the model.

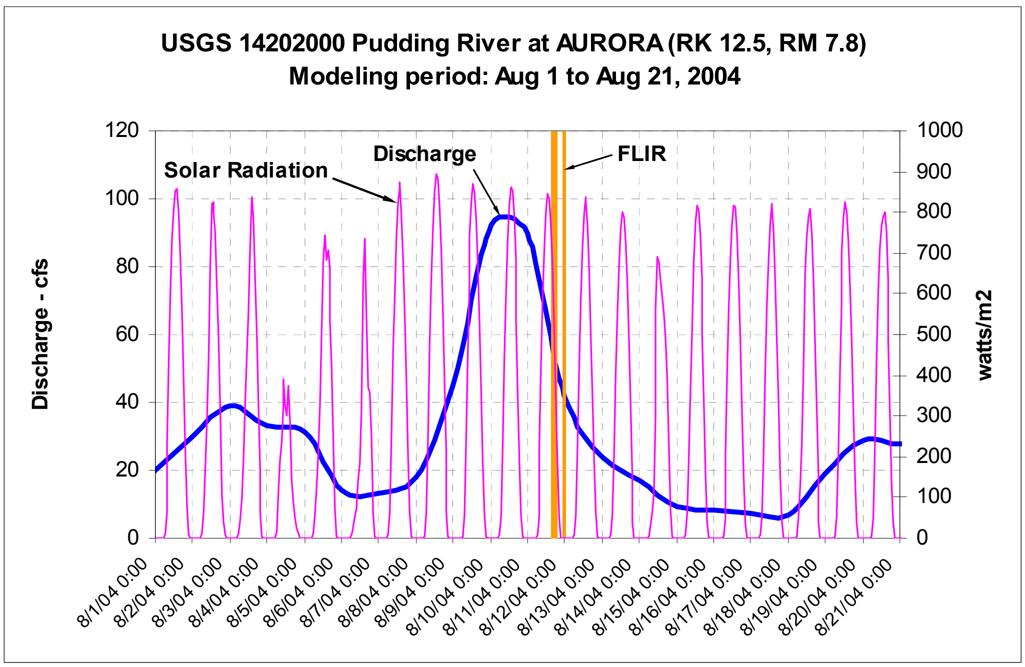

Figure A- 25. Pudding River discharge and solar radiation at USGS Gage at Aurora

The river was modeled from just upstream of the confluence of Drift Creek at river kilometer 84.5 (RM 51.0) to the mouth of the Pudding River, where it enters the Molalla River. Upstream from Drift Creek, Pudding River flow rates were too low during the calibration period to allow accurate modeling.

TRIBUTARY INFLOW ESTIMATES

To provide a uniform method for estimating Pudding River tributary inflow rates, tributary inflows were based on the discharge from a reference watershed, Little Abiqua Creek. Discharge from this watershed was measured by the Little Abiqua Creek at Scotts Mills USGS gage (14200400, active from 1993 through 2004). Because little or no water is diverted from Little Abiqua Creek, it was useful for estimating natural stream flows for the subbasin. Flow statistics for the stream are shown in Table A- 7. As shown, the Annual 7Q10 flow rate for the stream is 1.7 cfs, which equals 50% of the median August flow rate.

[1] U.S. Bureau of Reclamation, Hydromet/AgriMet station ARAO.

Since natural stream flow rates were available for this gage, natural flows for all tributaries to the Pudding River were referenced to this site.

Table A- 7. Flow statistics for Little Abiqua Creek (cfs).

Time period	1st percentile	10th percentile	Median	Annual 7Q10	August Median
1993-2004	1.9	3.0	18.0	1.7	3.4

Oregon Water Resources Department (OWRD) water availability reports (Detailed Report on the Water Availability Calculation) were used to obtain median (i.e. exceedance level: 50) August natural stream flow rates for Drift Creek, Silver Creek, Abiqua Creek, Butte Creek and Mill Creek as well as for the Pudding River at several locations (Table A- 8) (OWRD, 2002). As shown, the median August natural stream flow rate per unit drainage area for the Pudding River is 0.173 cfs/mi^2, based on the natural flow rate at the Pudding River mouth divided by the watershed drainage area. For tributaries, the natural flow per unit area ranges from 0.082 to 0.265 cfs/mi^2. For flow contributed by tributaries other than Drift, Silver, Abiqua, Butte and Mill Creeks, the natural flow per unit area is 0.155 cfs/mi^2.

Table A- 8: Median August stream discharge per unit area for Pudding River and tributaries based on OWRD estimates.

	DA (sq.mi.)	Flow (cfs)	Median Flow / Area (cfs/sq.mi.)
Pudding River at Mouth	525	91	0.173
Pudding River above Mill Creek (Aurora gage)	480	89.6	0.187
Pudding River above Howell Prairie (Mt. Angel gage)	206	34.6	0.168
Drift Creek	17.9	2.37	0.132
Silver Creek	53.2	14.1	0.265
Abiqua Creek	78.1	15.1	0.193
Butte Creek	69.7	14.7	0.211
Mill Creek	37	3.03	0.082
Pudding River at mouth minus tributaries (Drift, Silver, Abiqua, Butte and Mill)	269.1	41.7	0.155

This information was used along with stream flow rates measured in August 2007 to derive natural flow and consumptive use estimates to calibrate the Heat Source model for flow. The goal was to match the measured flow at the Woodburn and Aurora gages during the period modeled.

Much of the available natural tributary flows are consumptively used, with most of the consumptive use during the summer by irrigation. Figure A- 26 shows points of diversion for the Pudding River and tributaries.

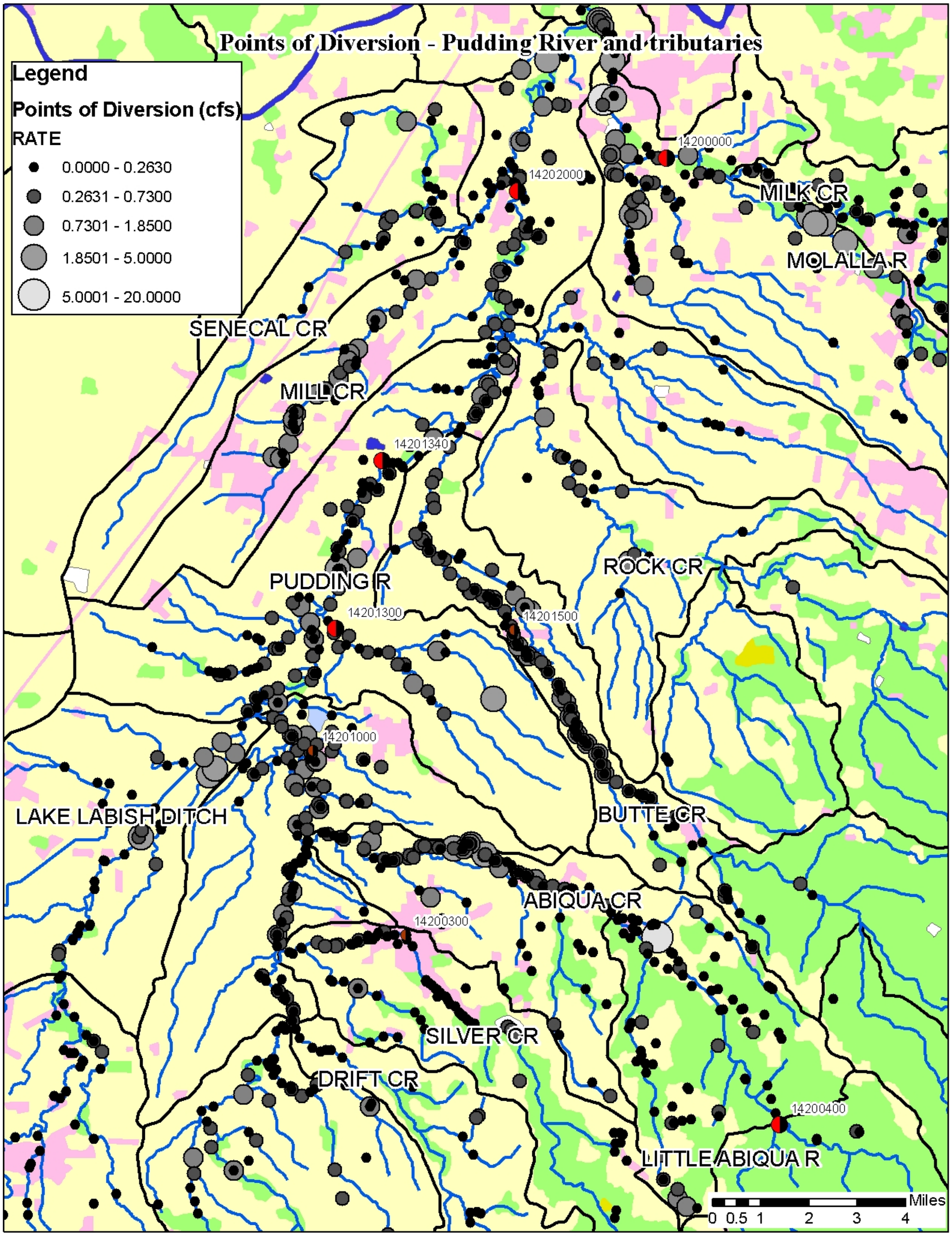

Figure A- 26: Points of diversion from Pudding River and tributaries.

An example for Silver Creek of how the natural stream flow rate for a tributary was calculated is shown by Equation A1. As shown, the Silver Creek natural stream flow rate, without consumptive use via diversions, equals 4.15 times the gauged Little Abiqua Creek flow rate, times an adjustment factor of 123% derived during the model calibration process. Therefore, the estimated Silver Creek natural flow rate for a given day equaled 5.1 times the gauged Little Abiqua Creek flow rate for the day. The amount of flow consumed for each day was calculated by using Equation A1.

The typical percent natural flow consumed, $F_{\%Consumed,\ Normal}$ in Equation A2, is an estimate of the percent of natural flow consumed during typical August conditions (warm, sunny days with no precipitation). It is a constant for each tributary. The percent of typical consumptive use (CU) on a given day, $F_{\%ofNormal}$, is value that was varied day by day in order to match observed flows. For most days, the percent of typical CU consumed ranged from 90% to 110%. On one day, August 7, which was the only day with significant precipitation, this value reduced to 20% to allow sufficient water to remain in the system to match the large increase in flow observed at Woodburn. This is appropriate because during a rainfall event, less water is diverted for irrigation and because more of any water that is diverted is not consumed by evaporation and transpiration and, therefore, is returned to the stream.

$$Q_{R,Natural} = F_{Cali}\left(\frac{Q_{R,AugMedian}}{Q_{R,LittleAbiquaCr,AugMedian}}\right)Q_{R,LittleAbiquaCr} \quad \text{(Equation A1)}$$

where:

$Q_{R,Natural}$ = Natural flow rate for given date, cfs

F_{Cali} = Calibration adjusment factor = 123%

$Q_{R,AugMedian}$ = Median August natural stream flow rate via OWRD = 14.1 cfs for Silver Creek

$Q_{R,LittleAbiquaCr,AugMedian}$ = Median August Little Abiqua flow rate via gage = 3.4 cfs

$$\frac{Q_{R,AugMedian}}{Q_{R,LittleAbiquaCr,AugMedian}} = 14.1/3.4 = 4.15$$

$Q_{R,LittleAbiquaCr}$ = Little Abiqua Creek flow rate for given date via gage, cfs

$$CU = F_{\%ofNormal} \times F_{\%Consumed,Normal} \times Q_{R,Natural,\min} \quad \text{(Equation A2)}$$

where:

CU = Quantity of stream flow consumed, cfs

$F_{\%ofNormal}$ = Percent of typical CU consumed on a given day

$F_{\%Consumed,Normal}$ = Typical percent of natural flow consumed = 51.5% for Silver Creek

$Q_{R,Natural,\min}$ = 10th percentile low August natural flow = 12.3 cfs for Drift Creek

For Silver Creek, OWRD water availability reports indicate that the median August consumptive use is 6.31 cfs. Therefore, OWRD estimates that 51.5% of the estimated 14.1 cfs median August natural flow stream is consumed.

The flow input to the model for each tributary is the natural stream flow minus the consumptive use, as shown in Equation A3, with the inflows shifted by 1-day to account for time-of-travel through Silver Creek. In some cases calculated CU exceeded $Q_{R,Natural}$, in which case $Q_{R,Tributary}$ was set to zero. Resultant

Silver Creek inflows to the Pudding River model are shown in Table A- 9. The values were input as hourly values, with hourly values derived via linear interpolation from daily values.

$$Q_{R,Tributary} = Q_{R,Natural} - CU \quad \text{(Equation A3)}$$

where

$$Q_{R,Tributary} = \text{Tributary inflow to Pudding R, cfs}$$

Table A- 9: Tributary inflows - Silver Creek Example

Date	Tributary Consumptive use adjustment factor	Little Abiqua Creek flow rate	Natural Flow	Estimated Consump-tive Use	Net Flow	Net Flow Shifted 1-day
	$F_{\%ofNormal}$	$Q_{R,LittleAbiquaCr}$ (cfs)	$Q_{R,Natural}$ (cfs)	CU (cfs)	$Q_{R,Tributary}$ (cfs)	$Q_{R,Tributary}$ (cfs)
8/1/2004	70.0%	3.3	16.86	4.42	12.44	12.44
8/2/2004	100.0%	3.3	16.86	6.31	10.55	12.44
8/3/2004	110.0%	3.2	16.35	6.95	9.40	10.55
8/4/2004	110.0%	3.1	15.84	6.95	8.89	9.40
8/5/2004	100.0%	3.2	16.35	6.31	10.03	8.89
8/6/2004	80.0%	3.6	18.39	5.05	13.34	10.03
8/7/2004	20.0%	4.2	21.46	1.26	20.20	13.34
8/8/2004	110.0%	4.5	22.99	6.95	16.04	20.20
8/9/2004	100.0%	3.4	17.37	6.31	11.06	16.04
8/10/2004	90.0%	3	15.33	5.68	9.64	11.06
8/11/2004	100.0%	2.8	14.31	6.31	7.99	9.64
8/12/2004	100.0%	2.7	13.79	6.31	7.48	7.99
8/13/2004	100.0%	2.7	13.79	6.31	7.48	7.48
8/14/2004	100.0%	2.6	13.28	6.31	6.97	7.48

For tributaries other than those for which natural stream flow and consumptive use estimates were explicitly provided by OWRD, natural flow was based on a natural flow per unit area of 0.155 cfs/m^2 (Table A- 8, last row). To derive this value, natural flows of Drift, Silver, Abiqua, Butte and Mill Creeks were subtracted from the natural flow of the Pudding River at mouth. The resultant flow was then divided by the Pudding River drainage area not associated with the five tributaries to derive the 0.155 cfs/m^2 value. This value was used for the headwater area upstream from Drift Creek; several significant tributaries for which natural flows were not estimated by OWRD including Howell Prairie Creek, Little Pudding River, Zollner Creek, and Rock Creek; and a number of small drainage areas located close to the Pudding River that are not associated with named tributaries.

While estimation of natural flow rates was relatively straightforward, estimation of the percent of the natural flow that was consumptively used was more complicated, particularly because very little flow data was collected during the August 2004 calibration period. Two sets of data were used to help guide derivation of the consumptive use values for each tributary: the USGS flow data at the two gages and supplemental river and tributary flow data measured by DEQ during a similar low flow period in 2007. The consumptive use terms in Equation A2, $F_{\%Consumed,\ Normal}$ and $F_{\%ofNormal}$, were then derived through an iterative model calibration process.

ESTIMATES OF DIRECT DIVERSIONS FROM PUDDING RIVER

Water is diverted not only from tributaries, but also directly from the Pudding River. Since the amount of water allocated to diversions exceeds the available natural water supply, at times during the irrigation season nearly all of the water in the Pudding River may be consumed for irrigation and other uses. Figure A- 26 shows a map of authorized diversions, with the size of each diversion indicated by the size of the circle. Only a portion of the amount of water authorized to be diverted is actually consumed. In the model, the amount diverted by each diversion was set to a constant percent, and then the amount diverted was varied using the same $F_{\%ofNormal}$ used in Equation A2. Above the Woodburn gage, the typical amount diverted was set to 20%, with this amount reduced by $F_{\%ofNormal}$. For example, on the day that it rained, the diversion when $F_{\%ofNormal}$ equaled 20%, the direct diversions from the Pudding River equaled 20% x 20% of the authorized diversions, or 4%. Note that this does not mean than only 4% of the total amount authorized to be diverted was diverted. It means that only 4% of the total amount authorized to be diverted was consumed. For example, if half the water diverted was returned to the stream as an irrigation return flow, then the amount actually diverted may have been 8% of the total amount authorized.

FLOW CALIBRATION ON USGS PUDDING RIVER STREAM FLOW GAGES

Comparisons of model calculated flow rates at Woodburn to values measured by the USGS gage are shown in Figure A- 27. As shown, the flow calibration at this gage is quite good. The flow calibration at the Aurora gage is not nearly as good as at the Woodburn gage (Figure A- 28). The model does a relatively poor job of replicating the large fluctuations in flow at this gage. As shown by Figure A- 27 and Figure A- 28, peak flows nearly double from Woodburn to Aurora. Two major tributaries enter between these sites, Butte Creek and Rock Creek, which implies that much of the large flow increase is due to these two tributaries. Unfortunately, neither of these tributaries is currently gauged, so flow rates cannot be accurately determined. The poor performance may also be partially due to longitudinal dispersion provided by the model. The longitudinal dispersion coefficient, which is not available to users for adjustment, may be larger than is appropriate for the Pudding River.

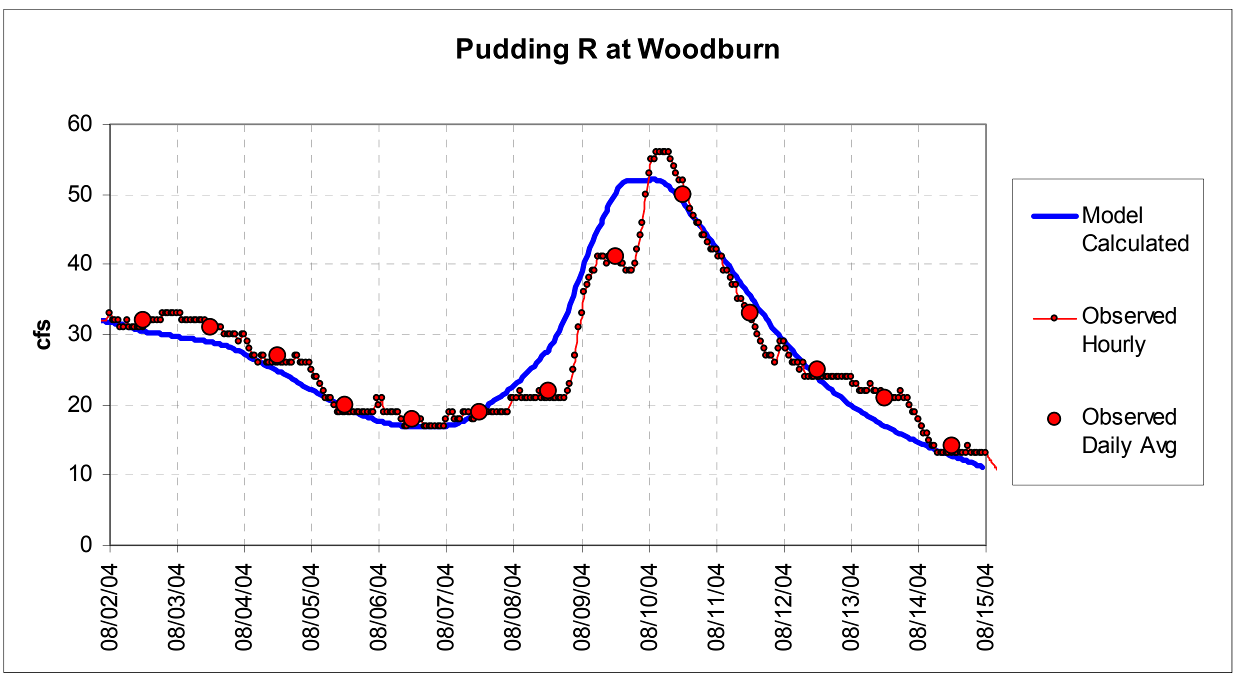

Figure A- 27. Model flow calibration, Pudding River near Woodburn, river km 37.5 (river mile 23.3).

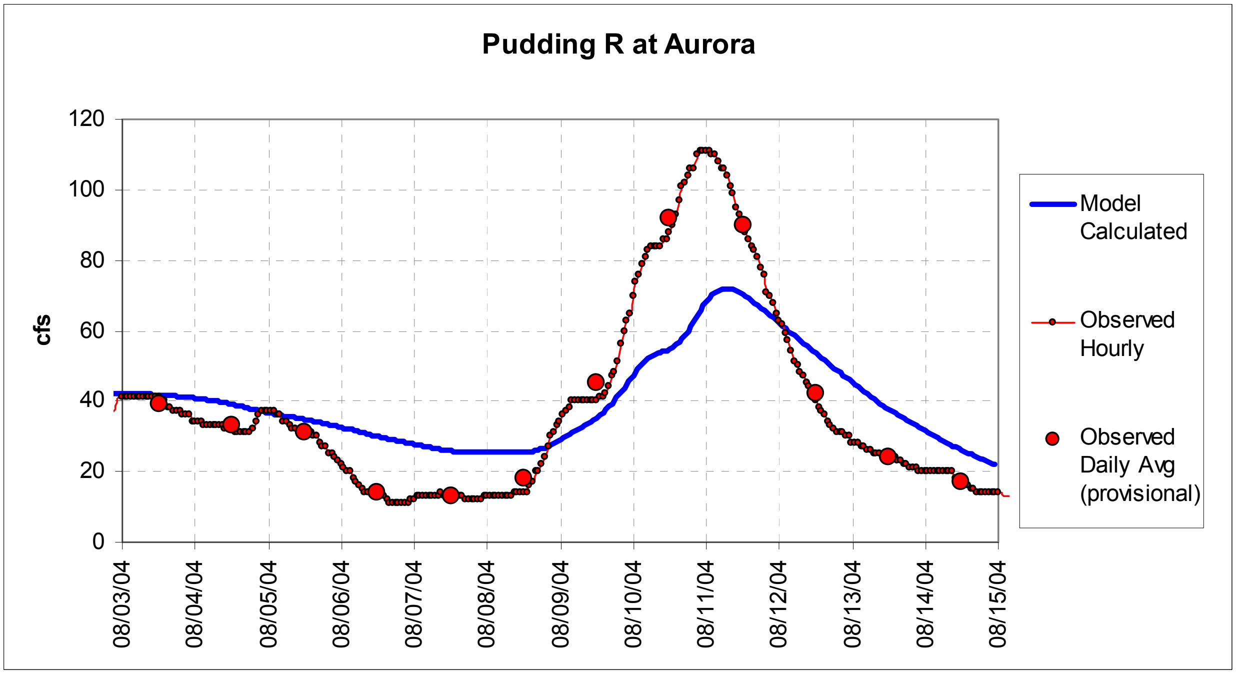

Figure A- 28: Model flow calibration, Pudding R at Aurora, river km 13 (river mile 8.1).

BATHYMETRY AND VELOCITY CALIBRATION

A QUAL2E model of the Pudding River was developed by ODEQ in the 1990's using data collected in the early 1990's (Brown and Barnwell, 1987). While the extensive dataset collected to calibrate the model could not be located, the QUAL2E model, which includes calibrated width, depth, and velocity relationships, was available. The model used relationships in which velocity, depth, and width are functions of flow, as follows:

$$\text{Velocity} = aQ^b$$
$$\text{Depth} = cQ^d$$
$$\text{Width} = eQ^e$$

Bottom widths, side angles, and Manning's roughness coefficient (*n*) were adjusted to produce surface widths which matched GIS measured widths and QUAL2E model depths, cross-sectional areas and velocities. Note that the coefficients and exponents for the QUAL2E velocity, depth and width equations were constant for each QUAL2E model reach, so the values for each QUAL2E reach are nearly constant, with variations within each reach only due to variations in flow. The ten QUAL2E reaches, reaches 1, 3, 5, 7, 9, 10, 11, 13, 14, 16 and 17, are identified in the following figures. Reaches 6, 8, 12, etc., are tributary reaches and hence do not appear in the following figures. Reaches 17 and 18 were not modeled by QUAL2E, only Heat Source.

Average flow rates for August 1 to 20, as calculated by the model, are similar to flow conditions for which the QUAL2E model was calibrated. Average flow rates for this 20-day period are shown on Figure A- 29. As shown, these flow rates are slightly greater than the 7Q10 rates of 15 cfs at the Woodburn gage and 25 cfs at the Aurora gage. Also shown on the plot are gage and instantaneous flow measurements from July 31 to August 3, 2007. As shown, these flows for these dates were similar to flows during the August, 2004 model calibration period.

Calculated widths, depths, cross-sectional areas and velocities (based on the 20-day average flow rates) compared to QUAL2E and GIS measured values are shown in Figure A- 29 to Figure A- 33. Note that the QUAL2E width, depth, and velocities are reach average values which apply for reaches that extend for large distances. Therefore, values for some Heat Source segments will be greater than QUAL2E values and for others will be less. The goal of the calibration was to reproduce the QUAL2E values on average. As shown by the plots, the Heat Source values generally reproduce the QUAL2E values quite well.

The goal of the hydraulics calibration was for reach average velocities, depths, and cross-sectional areas to be within +/- 10% of reach average values for the QUALE model and for reach average surface widths to not exceed reach average GIS measured channel widths by more than 10%. As shown in Table A- 10, the model meets these specifications.

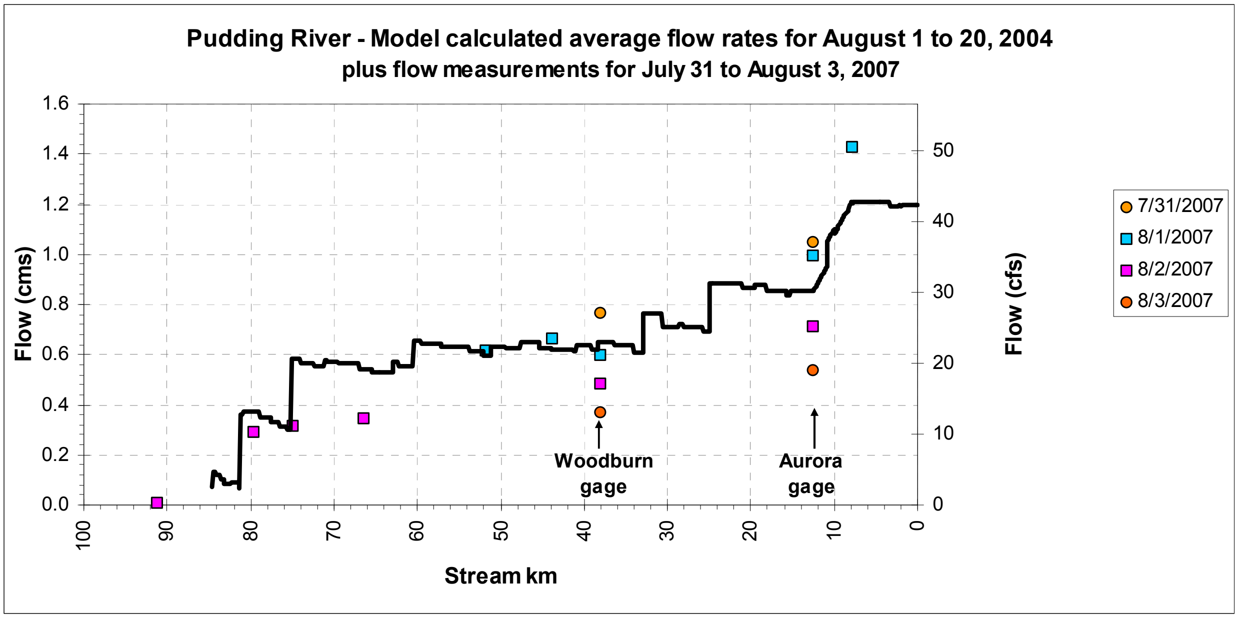

Figure A- 29. Flow rates used for hydraulics calibration and comparisons to Pudding River QUAL2E model

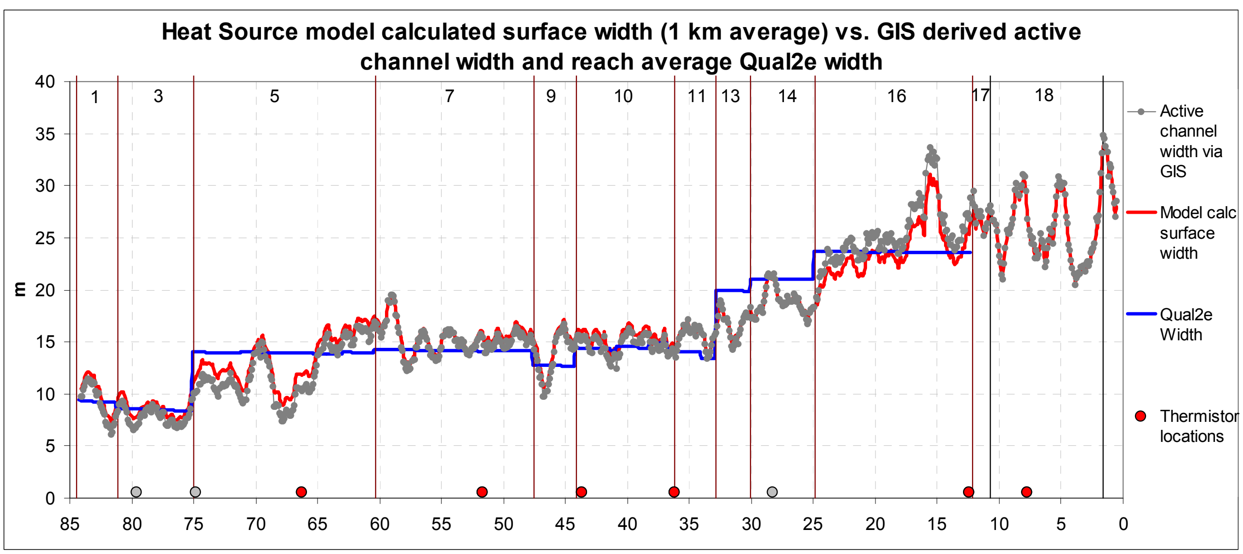

Figure A- 30. Pudding River model width calibration.

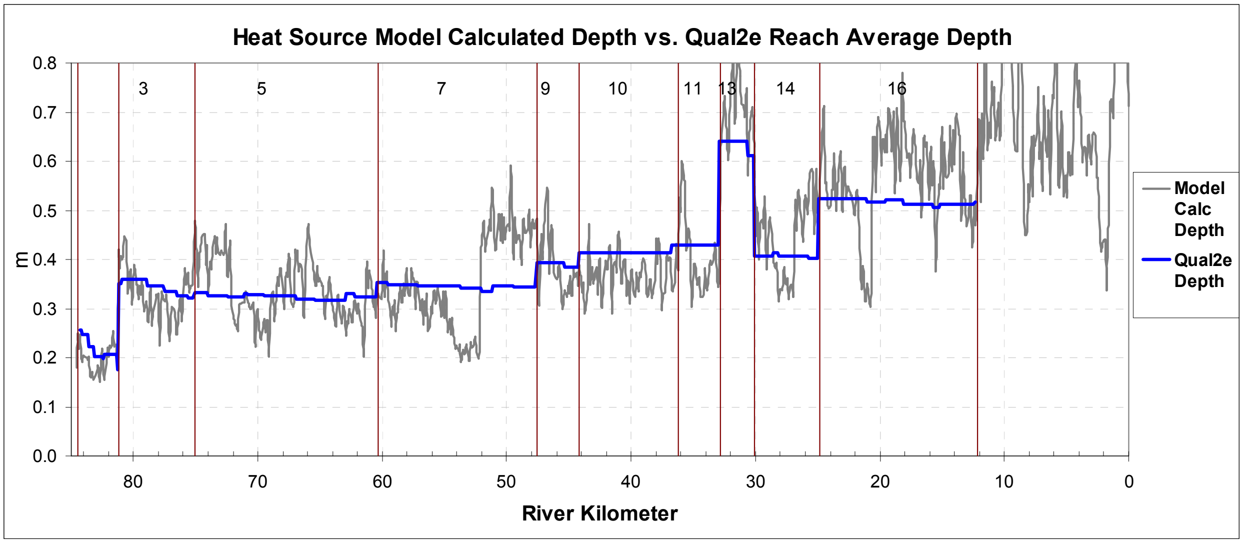

Figure A- 31. Pudding River model depth calibration.

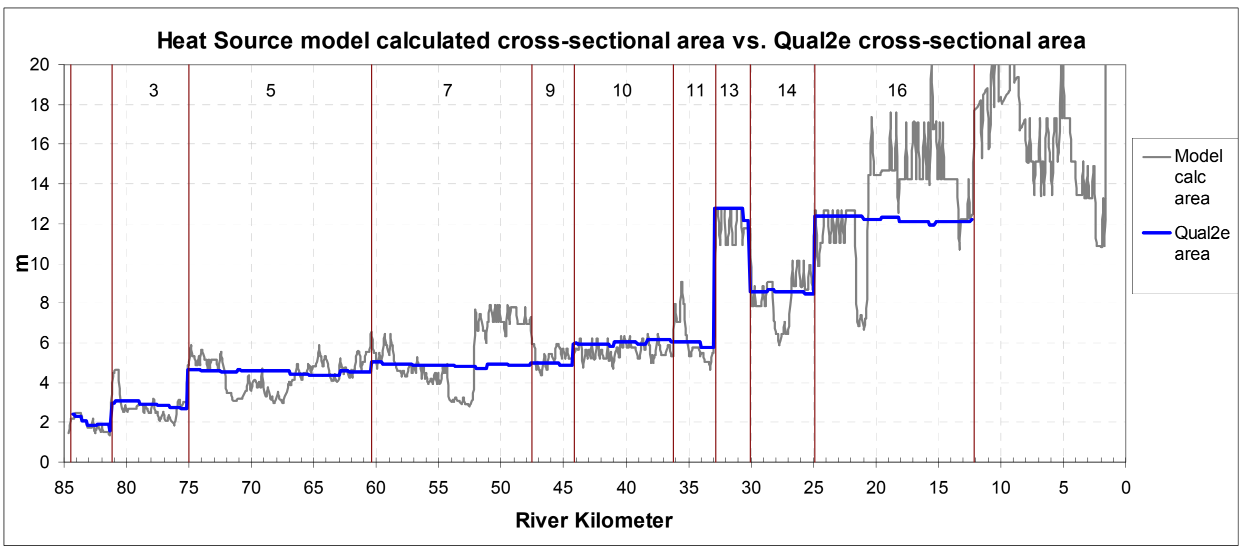

Figure A- 32. Pudding River model cross-sectional area calibration.

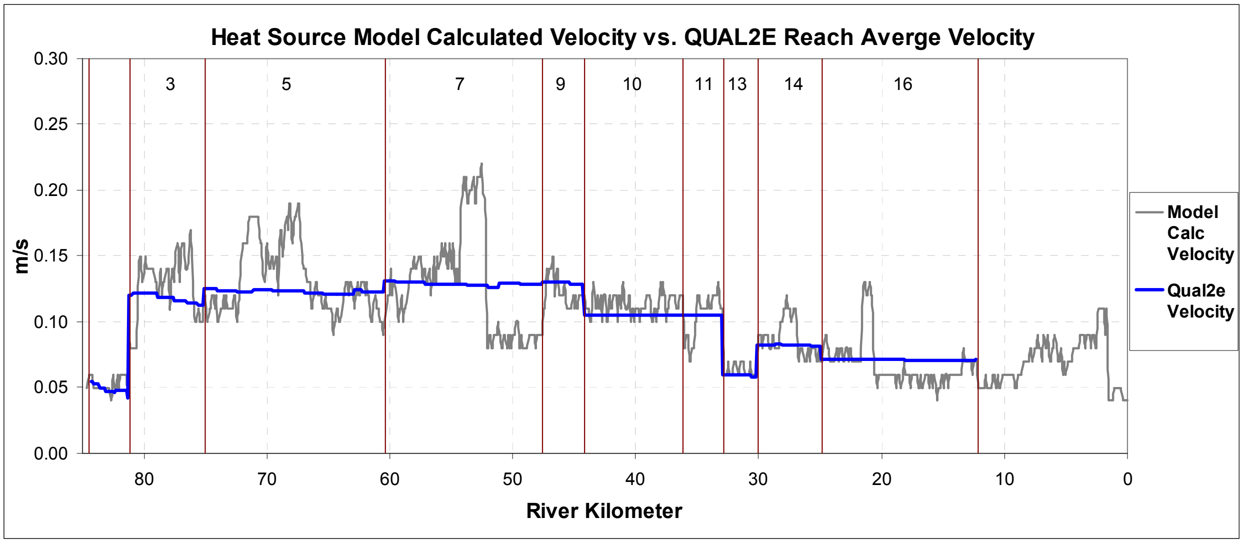

Figure A- 33. Pudding River model velocity calibration.

Table A- 10: Comparison of Heat Source velocity, depth, area and width to target values

Reach	Average Heat Source to QUAL2E Velocity	Average Heat Source to QUAL2E Depth	Average Heat Source to QUAL2E Width	Average Heat Source to QUAL2E Area	Ratio Model Calc Surface Width to Active Channel Width
0					1.08
1	108%	90%	106%	93%	1.09
3	108%	95%	101%	96%	1.09
5	107%	104%	96%	97%	1.09
7	99%	102%	109%	110%	1.03
9	94%	99%	113%	108%	1.05
10	107%	90%	106%	94%	1.05
11	100%	94%	111%	104%	1.01
13	109%	109%	87%	93%	1.01
14	106%	110%	89%	97%	1.00
16	96%	110%	101%	109%	0.94
17					0.98
18					0.99
19					0.99

TEMPERATURE CALIBRATION

The model was calibrated on both high resolution TIR temperature data and continuous thermister data. TIR data provides a snapshot of river temperature at a single point in time for all river locations while thermister data provides temperatures for all times but for only a few locations along the river. DEQ adjusted input variables such as channel side angle and width-to-depth ratios, channel roughness (which affects stream width, depth and velocity), groundwater/surface water interaction, and wind speed (which affects evaporation) in order to match both TIR and thermister data, while still meeting velocity, depth, cross-sectional area, and width specifications.

Thermal Infrared Imagery Data Comparison

A comparison of model calculated temperature to TIR measured temperatures for the Pudding River is shown in Figure A- 34**.** Error statistics are shown in Table A- 11. A reasonable target for model calibration is an RMS error of no more than 1.0°C and a mean error in the range +/- 1.0°C. These statistics are met for most of the river from the historic Mt. Angel Gage at river km 66.3 to the confluence of Mill Creek at river km 10.8, which are of most interest to point sources, particularly the Woodburn WWTP which enters at river km 38.3. However, for the entire river the RMS Error specification is slightly exceeded.

Table A- 11: Error statistics for Pudding River model output compared to TIR data

	Entire River (°C)	Mt. Angel Gage at RKm 66.3 to Mill Creek at RKm 10.8 (°C)
Mean Error	-0.7	-0.5
Mean Absolute Error	0.9	0.7
RMS Error	1.1	0.8

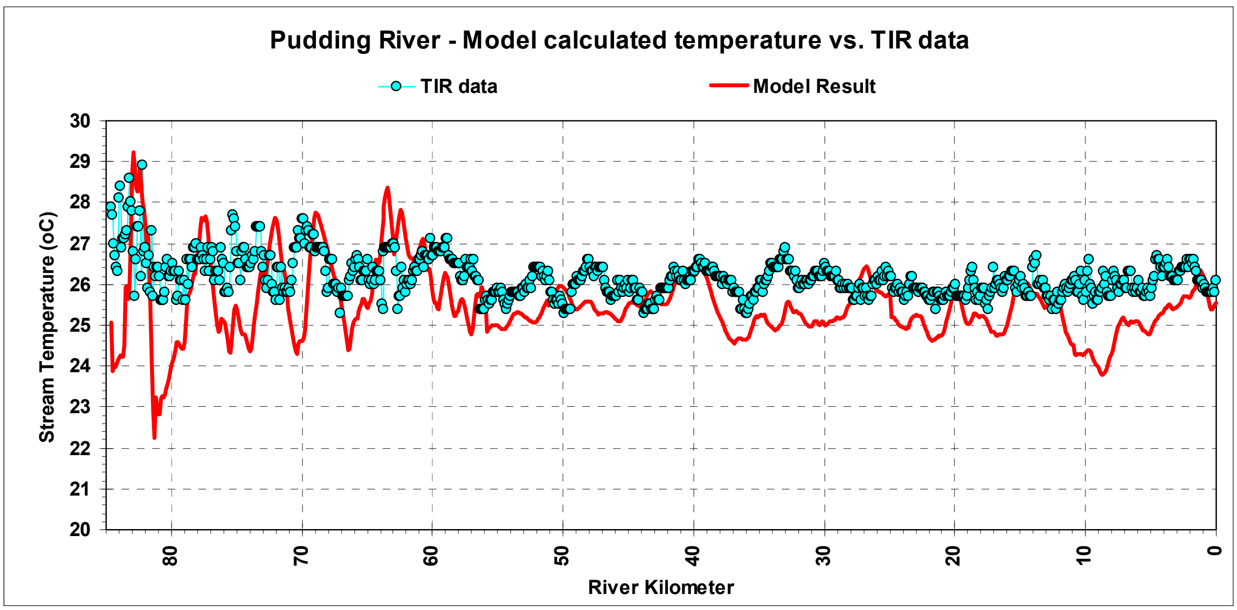

Figure A- 34: Pudding River model temperature calibration, TIR daily maximum temperatures for August 11 and 12.

Continuous Thermister Data Comparison

Comparisons of model calculated temperatures to continuous temperature data collected at thermister deployment locations where data was successfully retrieved is presented below. Mainstem Pudding River thermisters upon which the model was calibrated were deployed by ODEQ. Tributary temperatures for the calibration period were measured by thermisters deployed by the Marion Soil and Water Conservation District and ODEQ.

The Pudding River model closely matches DEQ continuous monitoring data at most locations. Error statistics for hourly values are presented in Table A- 12 and statistics for 7-day average daily maximum values are presented in Table A- 13. Comparisons of calculated hourly values to observed data are presented in Figure A- 35 to Figure A- 40. Note that no data is available for Node 7 since the thermister failed at this location during the time period modeled. Note also that the thermister for Node 3 (Saratoga

Road, LASAR No. 31877) occasionally generated some erratic temperatures (not shown on plot) and may not be reliable.

Root Mean Squared (RMS) error is commonly used to evaluate model performance. For example, for the recent Willamette River CE-QUAL-W2 modeling effort, an RMS of 1.0 was specified. Nodes 4 through 8 meet this specification, but Node 9 exceeds it, with an RMS error of 1.2.

Mean Error is a useful measure of model bias. If ME is positive, the model shows a positive bias (i.e., it over calculates temperature). If ME is negative, it shows a negative bias. Generally, ME values within the range +/- 1.0 are considered acceptable. ME for Nodes 4 to 9 meet this specification, although a slightly negative bias is exhibited.

For 7-day average daily maximum temperatures, all stations are within the desired ranges for the three statistics, except for Node 5, which slightly exceeds the desired values (RMSE = 1.1°C and an ME = -1.1°C) . Error statistics and visual observations of simulated compared to observed temperatures indicate that the model is sufficiently well calibrated to use to evaluate the sensitivity of river temperatures to various heat loads, including point source impacts.

Table A- 12: Pudding River Error statistics for model vs. hourly thermister data

Station	Location (RK)	Mean Error	Mean Absolute Error	RMS Error
Node 3: Saratoga Road DEQ Lasar No. 31877	66.3	1.8	2.1	2.5
Node 4: Monitor-McKee Rd DEQ Lasar No. 11530	51.7	-0.5	0.8	0.9
Node 5: Hwy 214 DEQ Lasar No. 10641	43.7	-0.5	0.8	0.9
Node 6: Hwy 211 (Woodburn) DEQ Lasar No. 10640	36.2	-0.6	0.7	0.8
Node 7: Bernard Rd DEQ Lasar No. 11528	28.3	No data	No data	No data
Node 8: Hwy 99E (Aurora) DEQ Lasar No. 10917	12.4	-0.1	0.8	1.0
Node 9: Arndt Road (Barlow) DEQ Lasar No. 10362	7.7	-0.7	1.0	1.2

Table A- 13: Pudding River Error statistics for model vs. 7DADM thermister data

Station	Location (RKm)	Mean Error	Mean Absolute Error	RMS Error
Node 3: Saratoga Road DEQ Lasar No. 31877	66.3	-0.1	0.5	0.5
Node 4: Monitor-McKee Rd DEQ Lasar No. 11530	51.7	-0.6	0.6	0.6
Node 5: Hwy 214 DEQ Lasar No. 10641	43.7	-0.1	0.2	0.2
Node 6: Hwy 211 (Woodburn) DEQ Lasar No. 10640	36.2	-1.1	1.1	1.1
Node 7: Bernard Rd DEQ Lasar No. 11528	28.3	No data	No data	No data
Node 8: Hwy 99E (Aurora) DEQ Lasar No. 10917	12.4	0.5	0.5	0.5
Node 9: Arndt Road (Barlow) DEQ Lasar No. 10362	7.7	0.1	0.1	0.1

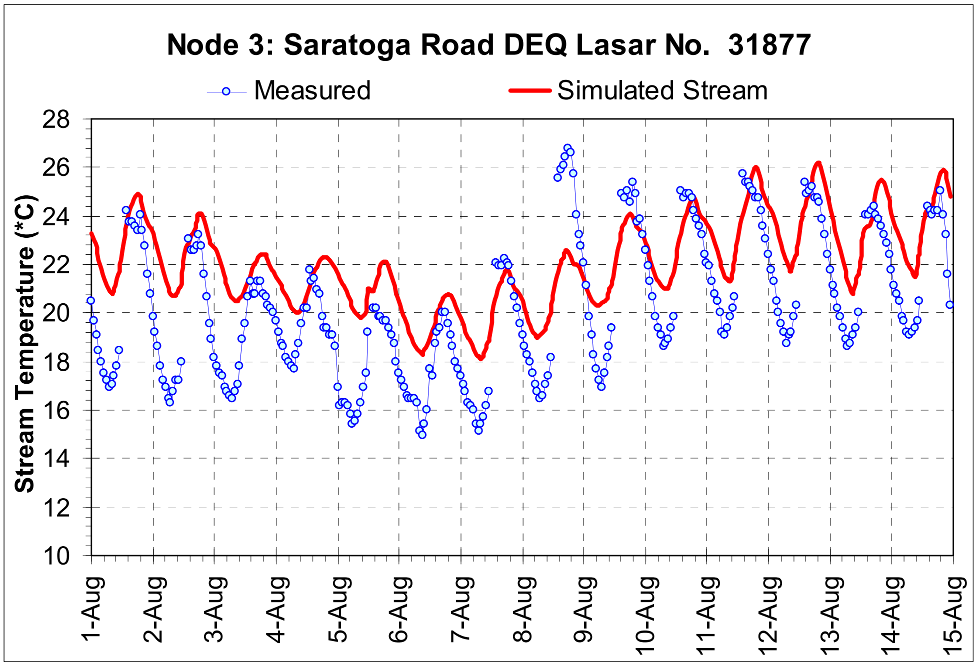

Figure A- 35: Model calculated vs. observed hourly temperatures – river km 66.3 (river mile 41.2).

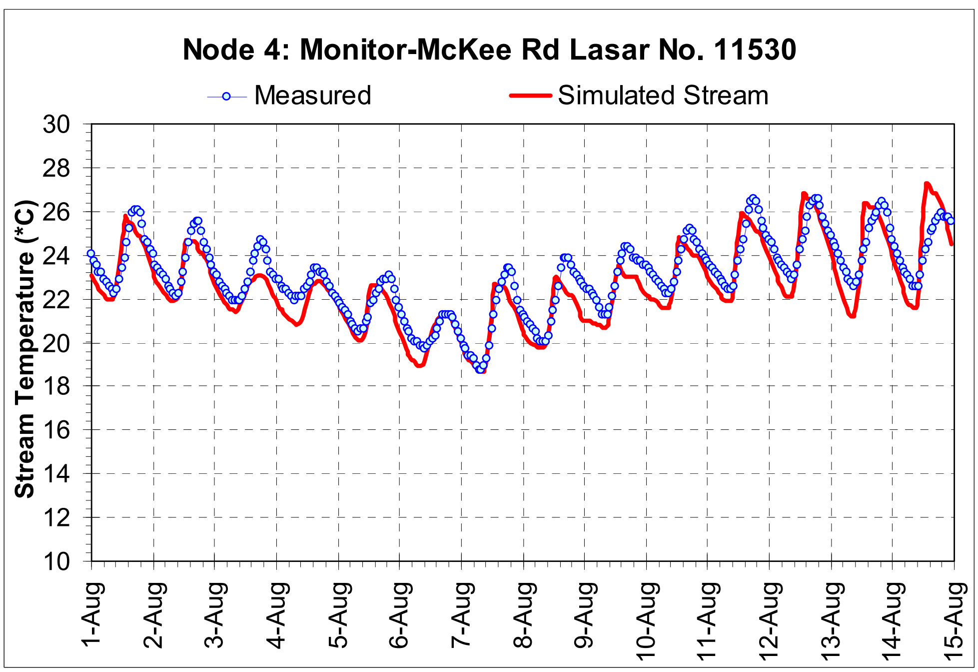

Figure A- 36: Model calculated vs. observed hourly temperatures – river km 51.7 (river mile 32.1).

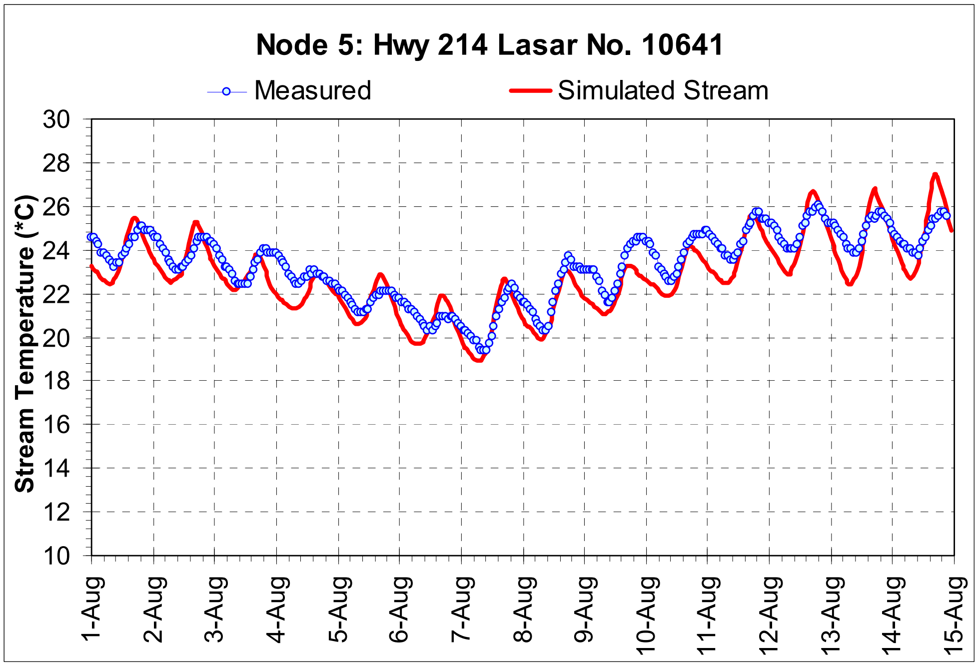

Figure A- 37: Model calculated vs. observed hourly temperatures – river km 43.7 (river mile 27.1)

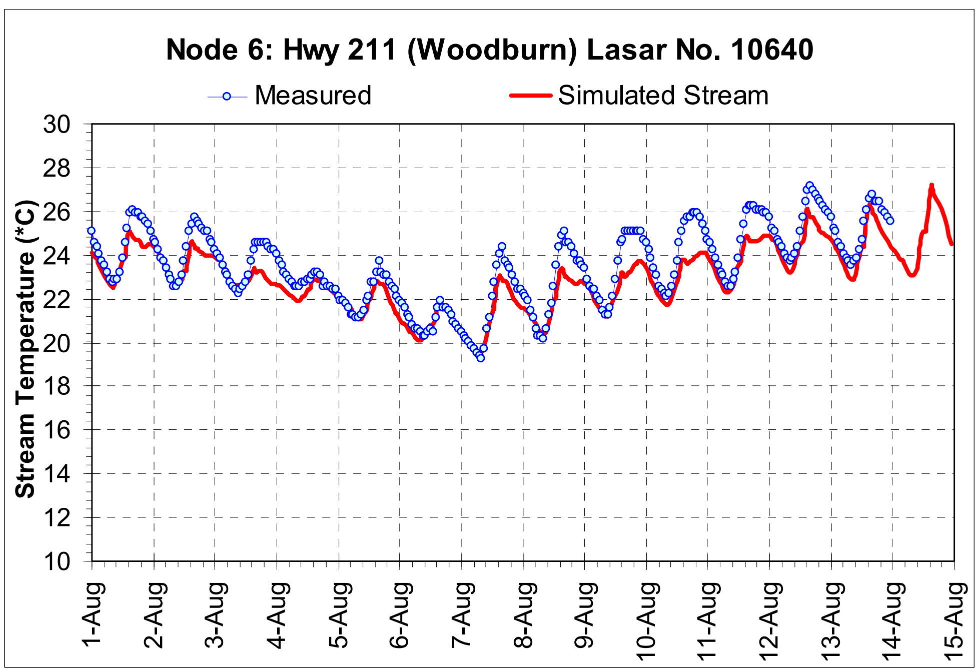

Figure A- 38: Model calculated vs. observed hourly temperatures – river km 36.2 (river mile 22.5).

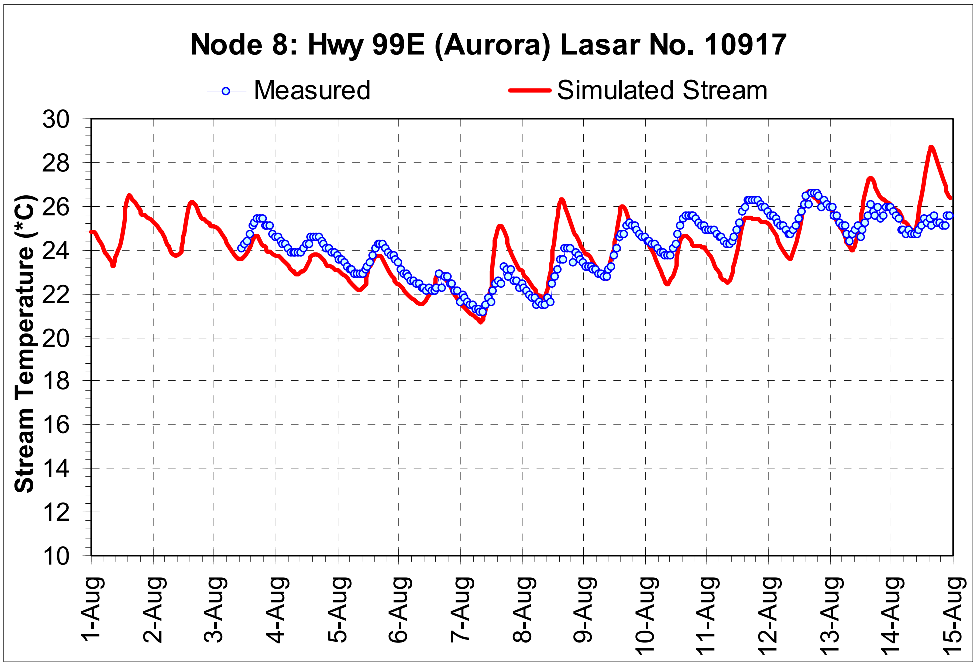

Figure A- 39: Model calculated vs. observed hourly temperatures – river km 12.4 (river mile 7.7).

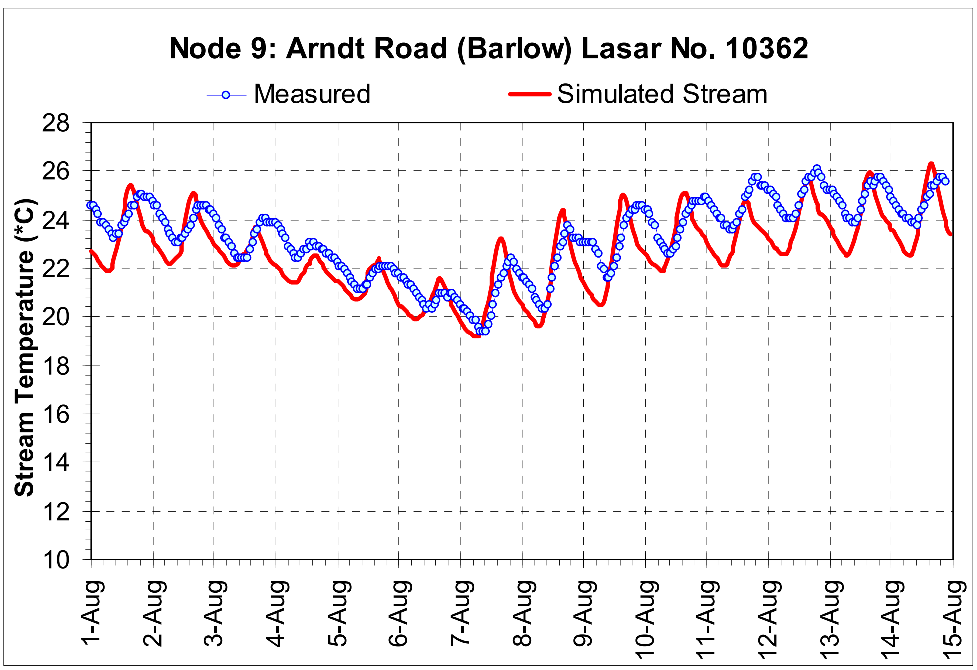

Figure A- 40: Model calculated vs. observed hourly temperatures – river km 7.7 (river mile 4.8).

SENSITIVITY ANALYSES

A series of modeling simulations were performed using the calibrated Molalla and Pudding River models in order to evaluate the sensitivity of stream temperatures to a variety of input parameters, including shade, flow, and heat loads from point sources.

Sensitivity Analysis - Molalla River

The calibrated Molalla River model was used to model the scenarios described in Table A- 14. The simulations model potential conditions for land cover, stream flow, and channel width. Combinations of these potential conditions were simulated to investigate the cumulative thermal effect of attaining certain potential conditions. Modeling results comparing simulated current conditions to that of potential conditions are presented in Figure A- 41 through Figure A- 45.

Figure A- 41 illustrates a small decrease in temperature, especially near the river mouth, that results from a system potential vegetation scenario of Upland Forest in the upper half of the Molalla River watershed and mixed forest/savannah/prairie in the lower half of the watershed. The scenarios simulating more natural stream flow conditions result in greater temperature decreases. Figure A- 42 illustrates two scenarios: reducing the surface water withdrawals (points of diversion or PODs) from the Molalla River to 50% of the current maximum allowed and eliminating surface water withdrawals entirely. The 0% POD withdrawal scenario is only an approximation of natural flow in the Molalla River because simulation only eliminates water withdrawals directly from the Molalla River, not groundwater or tributary withdrawals. Figure A- 42 indicates that a simulated flow increase in the Molalla River results in a lower temperature in the lower half of the watershed, where the majority and most significant water withdrawals occur. Modeling indicates that increased shading has approximately as much effect on stream temperature as increasing the flow in the lower river.

Table A- 14: Heat Source simulated scenarios for Molalla River model.

Current Calibrated Simulation	Current Conditions
Natural Thermal Potential	Potential Near Stream Land Cover (Vegetation) Conditions
Natural Thermal Potential /No PODS	Potential Near Stream Land Cover (Vegetation) Conditions No Water Withdrawals
Natural Thermal Potential /No PODs /reduced bankfull width	Potential Near Stream Land Cover (Vegetation) Conditions No Water Withdrawals Bankfull width reduced to regression of moving median of current bankfull width

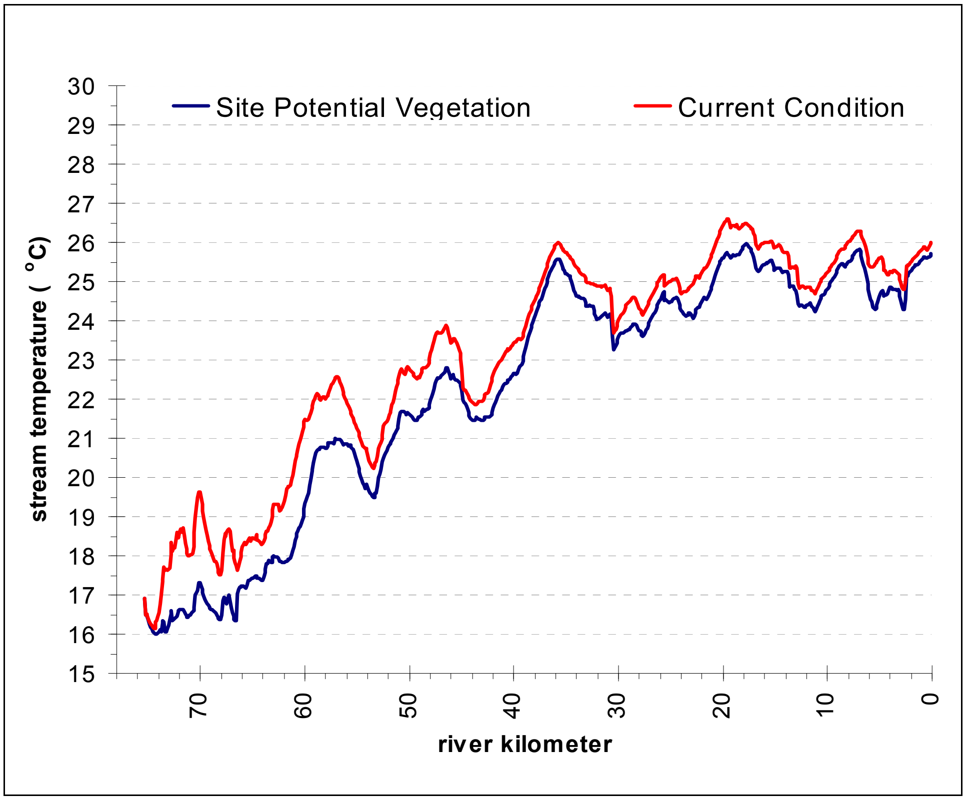

Figure A- 41: Simulated Molalla River temperature decrease resulting from system potential vegetation shading. Upland forest coverage is simulated in the upper half of the watershed and mixed forest/savannah/prairie in the lower half of the watershed.

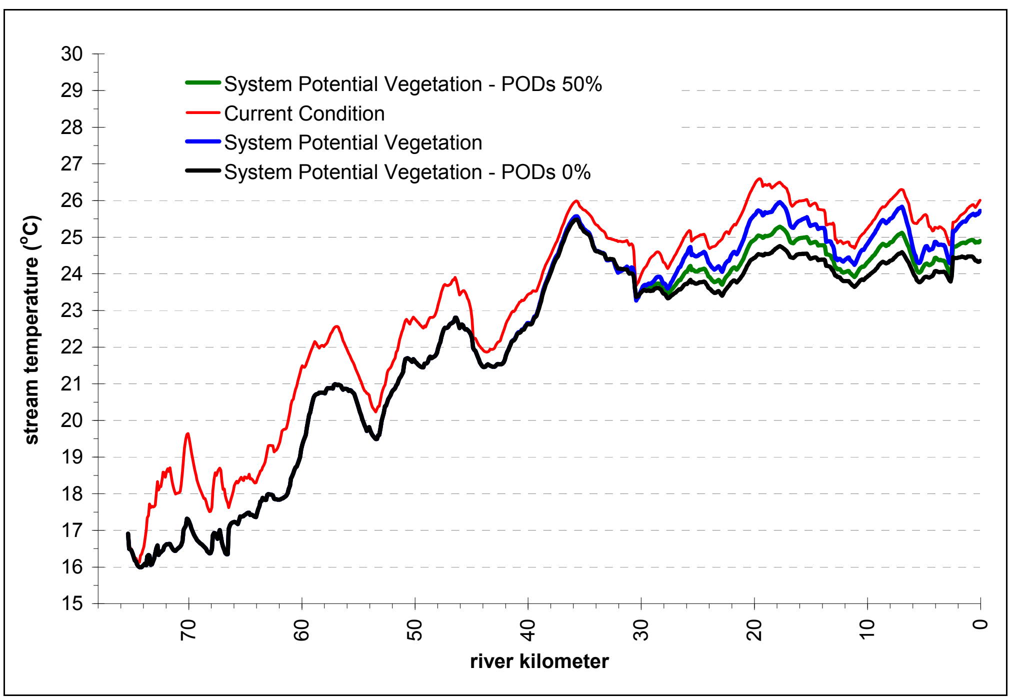

Figure A- 42: Simulated Molalla River temperature decrease from reducing surface water withdrawals. System potential vegetation modeled as upland forest in the upper half of the Molalla River watershed and mixed forest/savannah/prairie in the lower half.

Anthropogenic activities in the upper Molalla River watershed may be responsible for erosion and landslides of greater magnitude than would occur under natural conditions (BLM, 1994). Human activities that increase sediment loading to streams as well as activities that reduce riparian vegetation may result in stream channel widening (Rosgen 1996). Wider channels allow a greater stream surface area to be exposed to solar radiation and reduce ability of riparian vegetation to shade the stream's surface. For these reasons, DEQ simulated a scenario with a narrower Molalla River stream channel.

In order to simulate a potential natural channel width, DEQ followed the methodology used in the Tillamook TMDL (DEQ, 2001, Appendix A)[2]. DEQ calculated the moving median of each 1000-foot section of the stream from headwaters to mouth and then performed a regression of those points with river mile. The resulting linear equation was used to predict potential bankfull width (Figure A- 43). DEQ then ran the Heat Source model with either the measured bankfull width or the predicted potential bankfull width, whichever was less.

Simulating a narrowing of the Molalla River's bankfull width reduced the predicted temperatures a maximum of 0.9 ºC from the system potential vegetation scenario at approximately river kilometer 35 (approximately river mile 21). Figure A- 44 shows that the temperature effects from simulated channel narrowing were less pronounced upstream and downstream of river kilometer 35. The greatest temperature reductions were achieved in a simulation that combined site potential shading, natural stream flow, and a narrowed channel width (Figure A- 45).

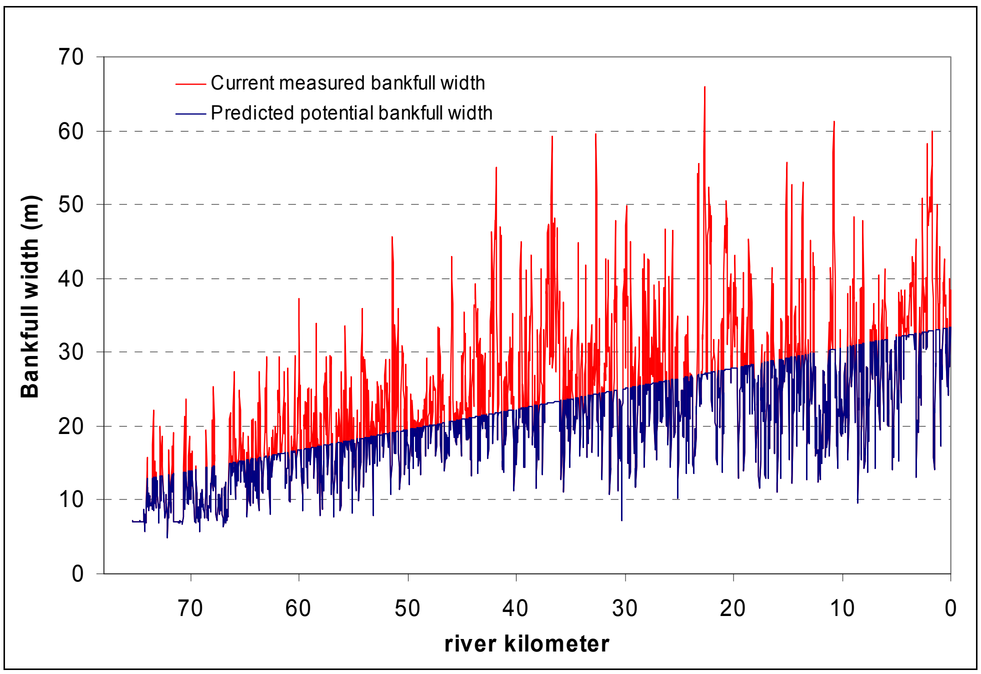

Figure A- 43: Current GIS measured bankfull width compared with predicted bankfull width.
A regression was performed of the moving median of bankfull width from headwaters to mouth. Modified bankfull width entered into the Heat Source model was the measured width, or the predicted width, the demarcating line in this figure, whichever was less.

[2] Appendix A of the Tillamook Bay TMDL can be found at:
http://www.deq.state.or.us/wq/TMDLs/docs/northcoastbasin/wilsontrasknestucca/appxs.pdf

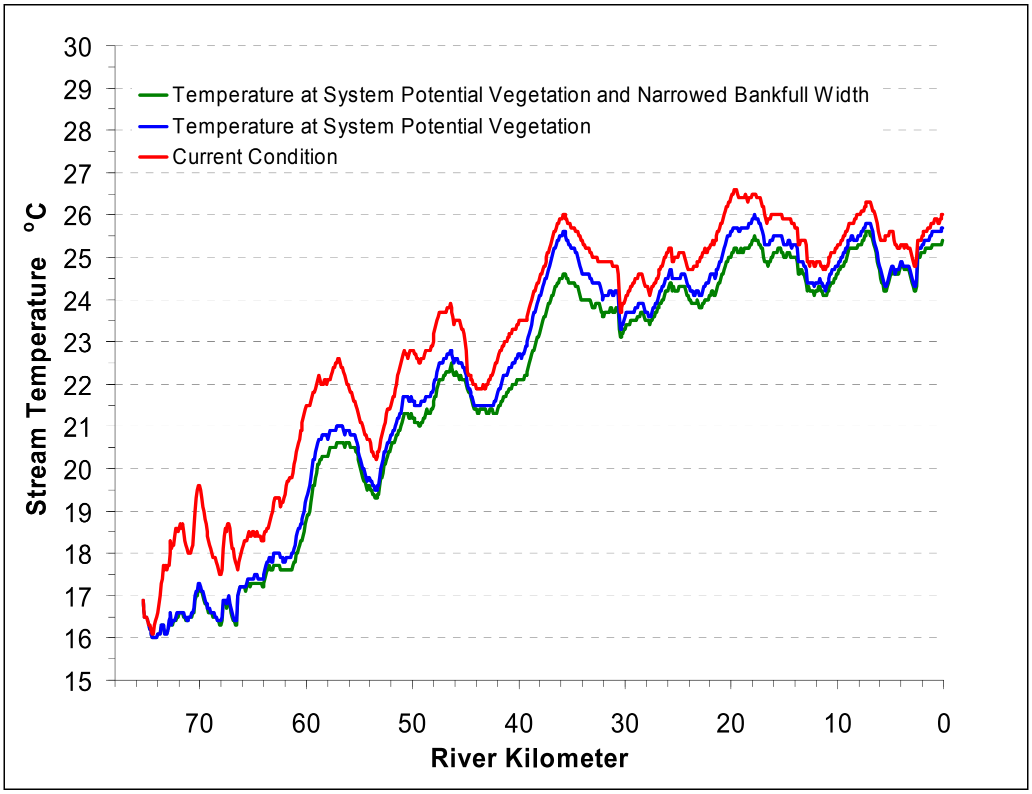

Figure A- 44: Predicted Molalla River stream temperatures resulting from a simulated narrowing of the Molalla River channel bankfull width.
The maximum predicted temperature reduction occurs approximately at river km 35 (approximately river mile 21).

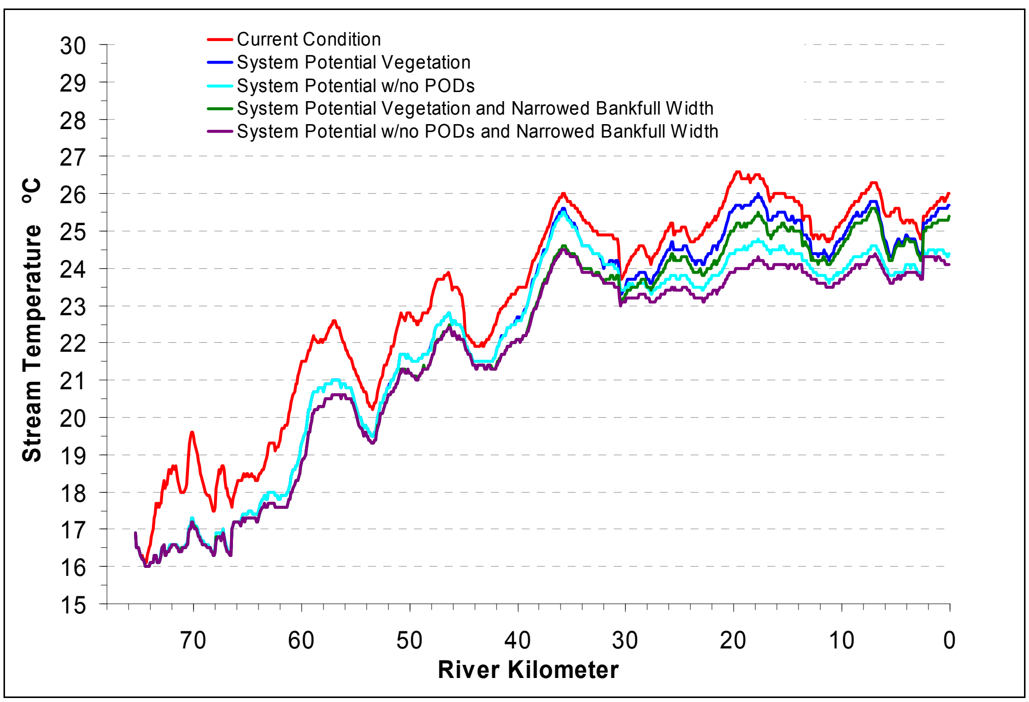

Figure A- 45: Predicted stream temperatures resulting from a simulated narrowing of the Molalla River channel bankfull width, system potential vegetation, and natural stream flows.

Figure A- 46 illustrates how the temperature distribution would change in the Molalla River under various scenarios of watershed restoration: attaining system potential vegetation, combining system potential vegetation with natural stream flow, and finally, each of those scenarios with a narrowed stream channel. The largest potential improvement would be reducing the percentage of stream miles that exceed 24ºC. Still, nearly 90% of stream miles would still exceed the applicable temperature criteria.

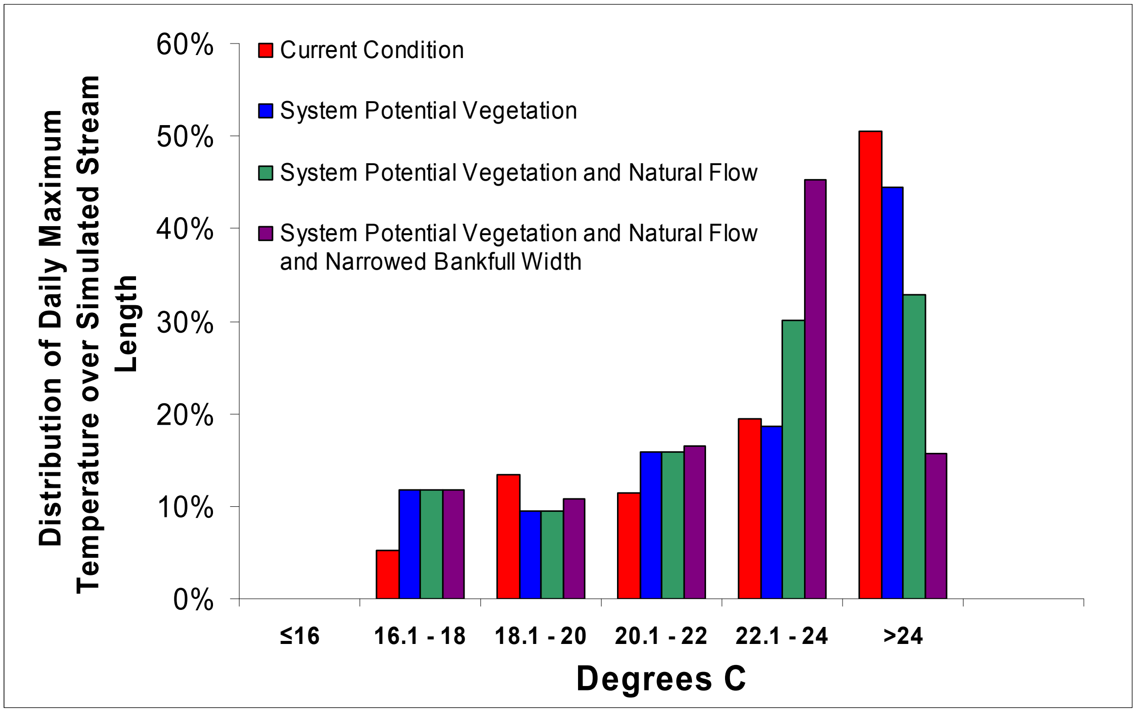

Figure A- 46: Molalla River distribution of maximum daily stream temperatures at current conditions, system potential vegetation, and system potential vegetation with natural flow. Natural flow was simulated by reducing all water withdrawals to zero.

Sensitivity Analysis - Pudding River

The calibrated Pudding River model was used to evaluate the sensitivity of Pudding River temperature to point sources, flow, and shade. The analyses focus on evaluating the combined impacts of improving flow and shade to natural conditions and determining natural thermal potential temperatures for the river.

CURRENT RIVER CONDITIONS: STREAM TEMPERATURE EFFECTS FROM POINT SOURCE HEAT LOADS

The only major NPDES permitted domestic wastewater treatment plant which discharges directly to the Pudding River during the summer is the City of Woodburn WWTP. Impacts of City of Woodburn WWTP effluent on river flow and temperature are shown in Figure A- 47 through Figure A- 53. Figure A- 47 shows the increase in 7-day average river flow due to the effluent for the August 1 to 14, 2004 period modeled. Figure A- 48 shows 7-day average daily maximum (7DADM) temperatures with and without the Woodburn effluent for the period modeled. The temperature increase resulting from the effluent, which is difference between 7DADM temperatures with and without the effluent, is currently less than 0.1^{o}C (Figure A- 49). The impacts on daily maximum temperature are generally small because daily maximum river temperatures currently are often as warm or warmer than daily maximum effluent temperatures (Figure A- 50).

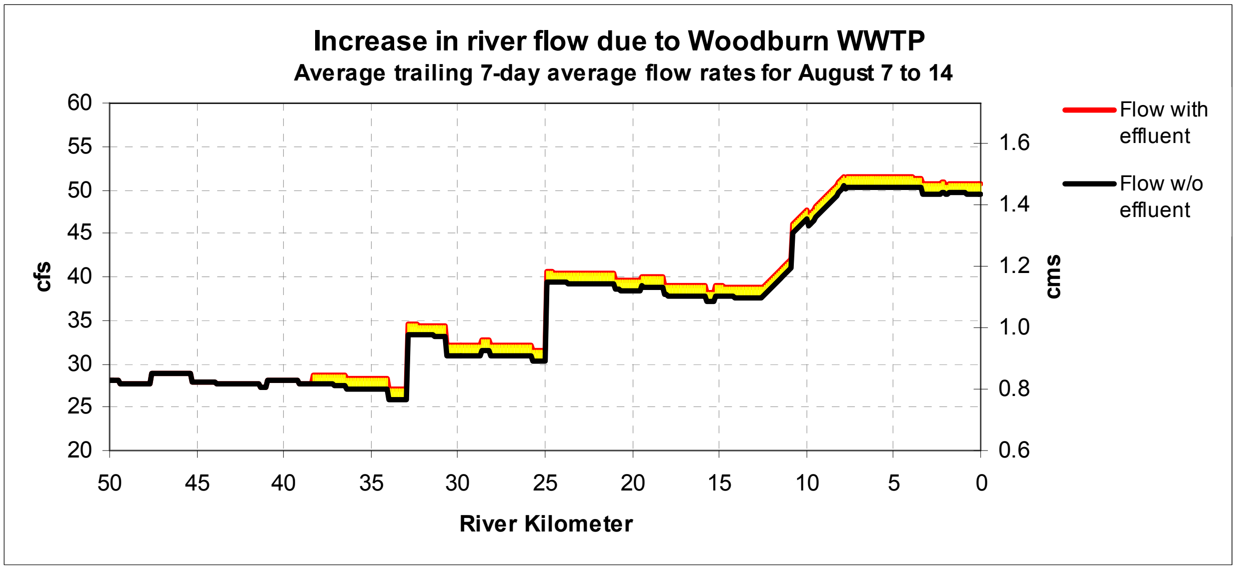

Figure A- 47: Increase in river flow due to Woodburn WWTP

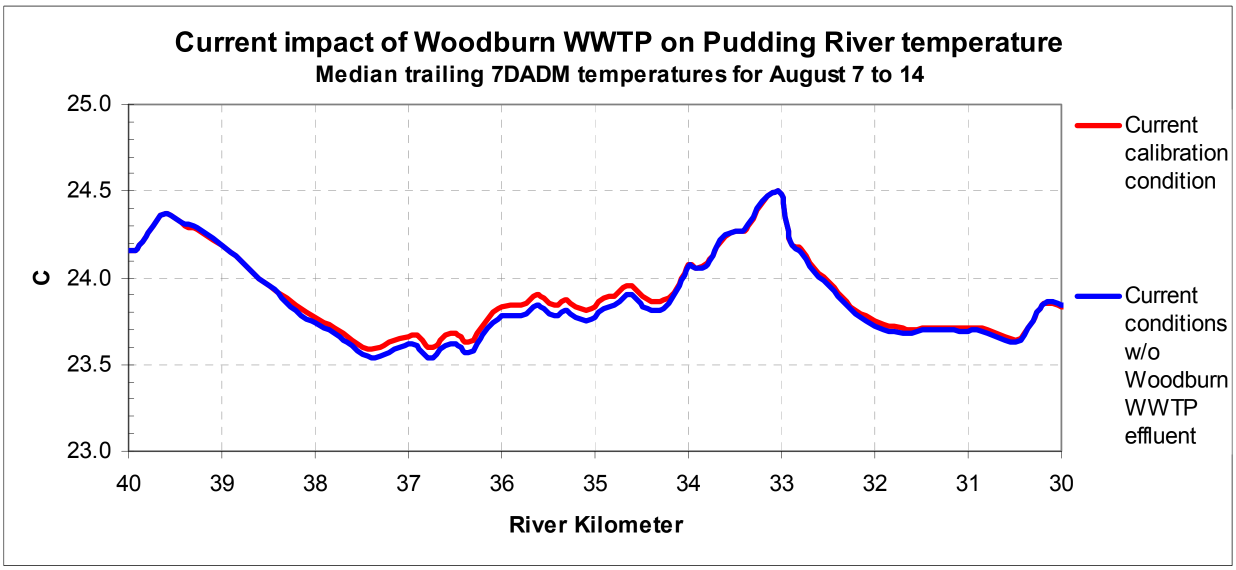

Figure A- 48: Increase in river temperature due to Woodburn WWTP.

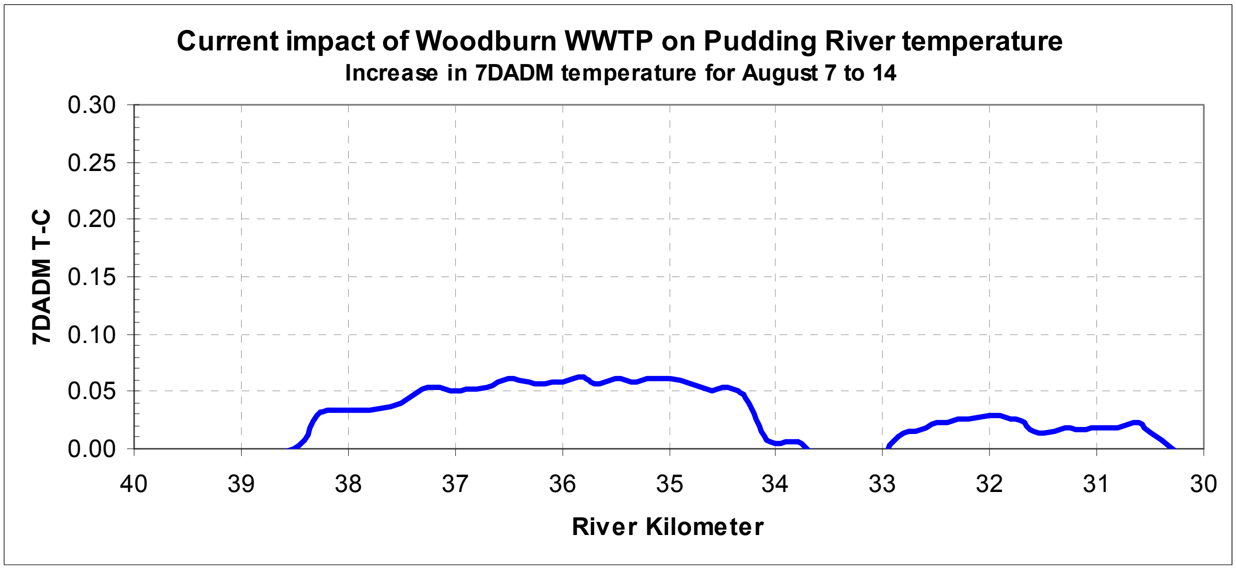

Figure A- 49: Current increase in daily maximum river temperature due to Woodburn WWTP.

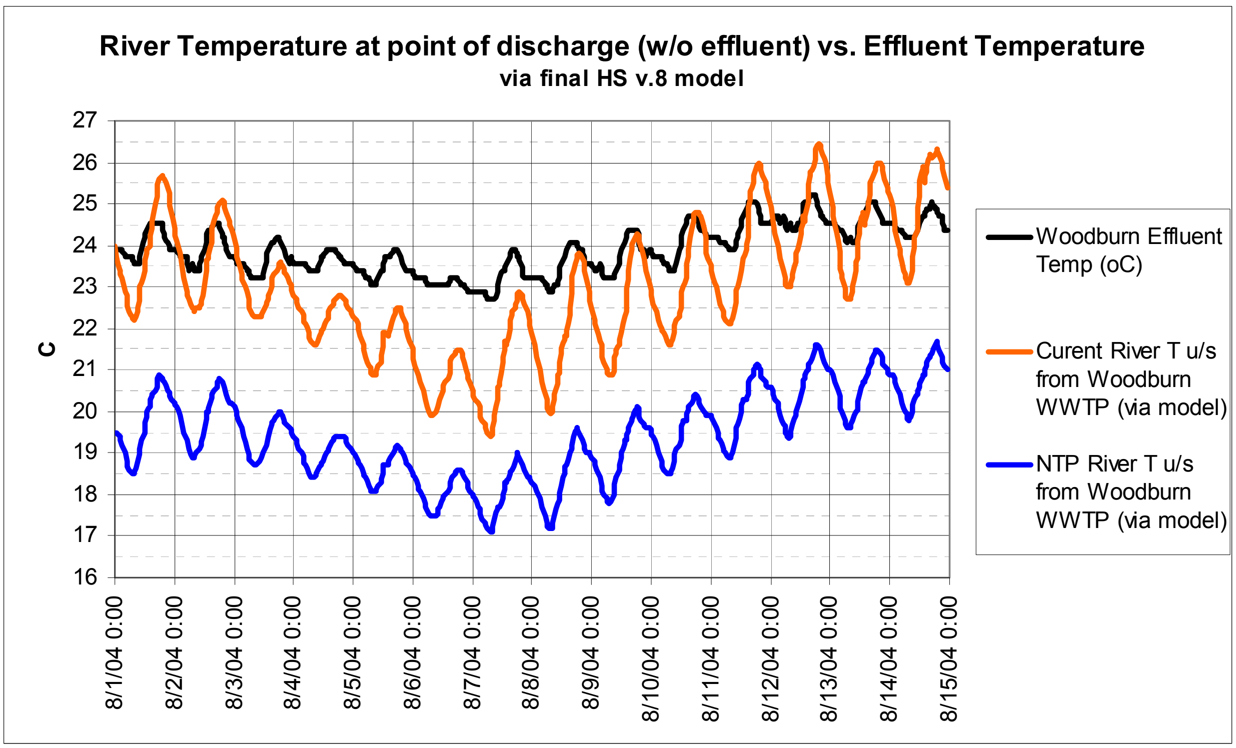

Figure A- 50: Woodburn effluent temperature relative to current and NTP river temperature.

While the effluent increases daily maximum temperatures near the discharge location, further downstream the presence of the effluent actually results in cooler daily maximum temperatures (Figure A-51). This is partly because the river is at times so warm that its temperature exceeds the temperature of the effluent and partly because the increased stream flow due to the effluent somewhat mitigates the temperature impacts, since river temperature is inversely related to the river flow rate. While effluent temperatures are often similar to daily maximum river temperatures, the effluent is always significantly warmer than the river in the early morning and daily average effluent temperatures are generally warmer than daily average river temperatures (Figure A- 50). Therefore, the effluent adds significantly more heat to the river in the early morning than in the late afternoon. This results in greater increases in daily average temperatures than in daily maximum temperatures (Figure A- 52 and Figure A- 53). Therefore, even though the presence of the effluent may reduce daily maximum temperatures downstream from RKm 30, it generally increases daily average temperatures and, therefore, reduces the capacity of the river to assimilate additional heat loads, such as anthropogenic solar radiation heat loads.

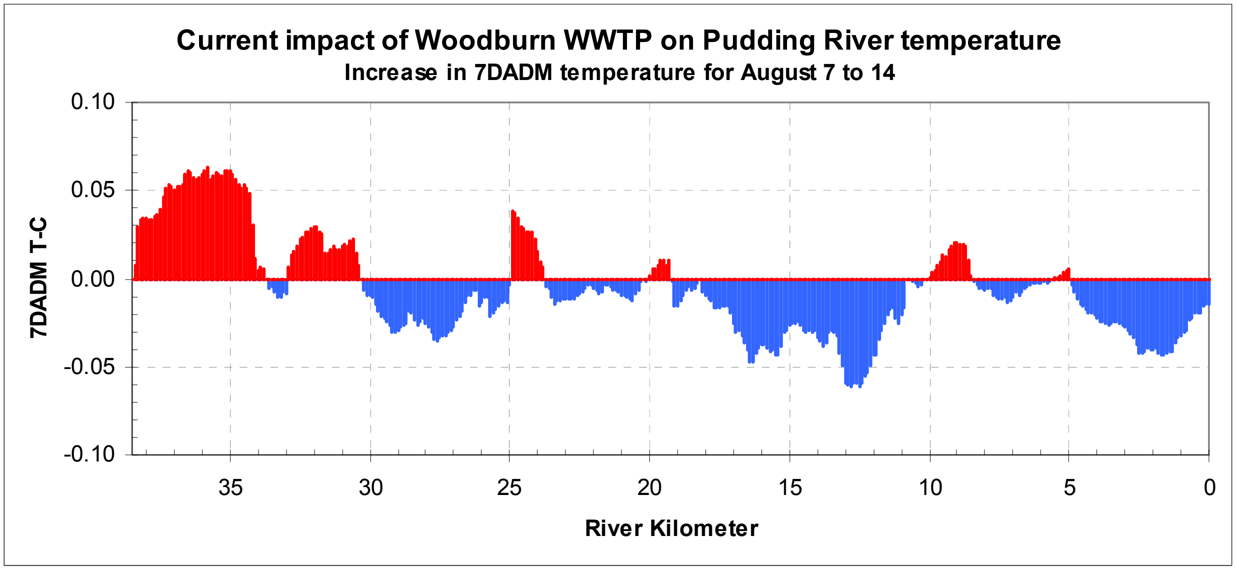

Figure A- 51: Current far-field impacts of Woodburn effluent on daily maximum river temperature.

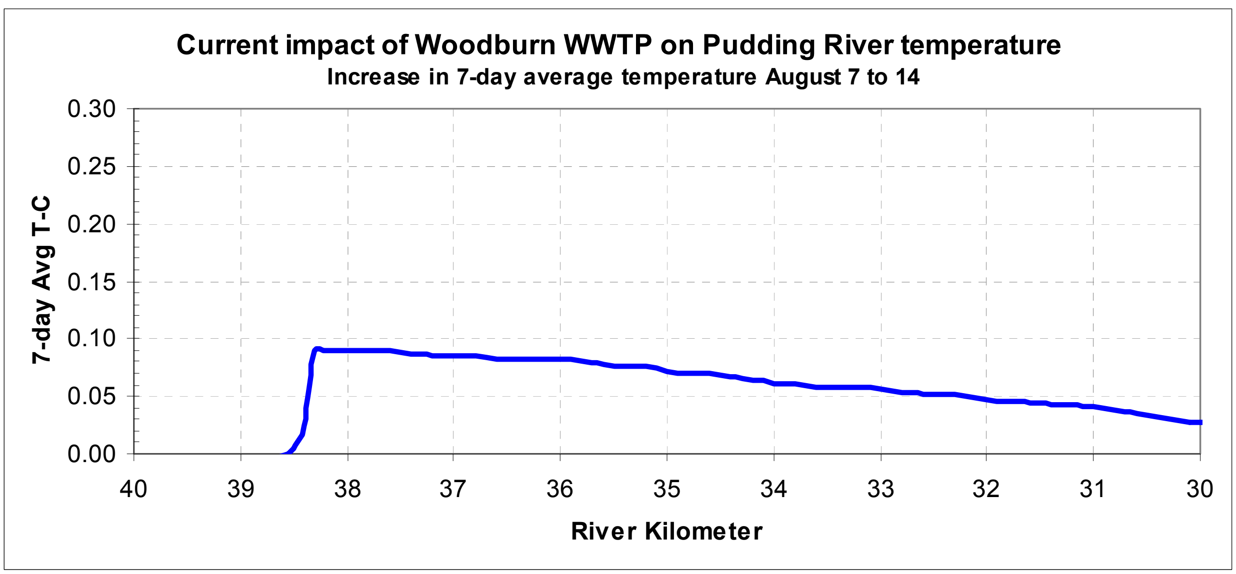

Figure A- 52: Current increase in average river temperature due to Woodburn WWTP.

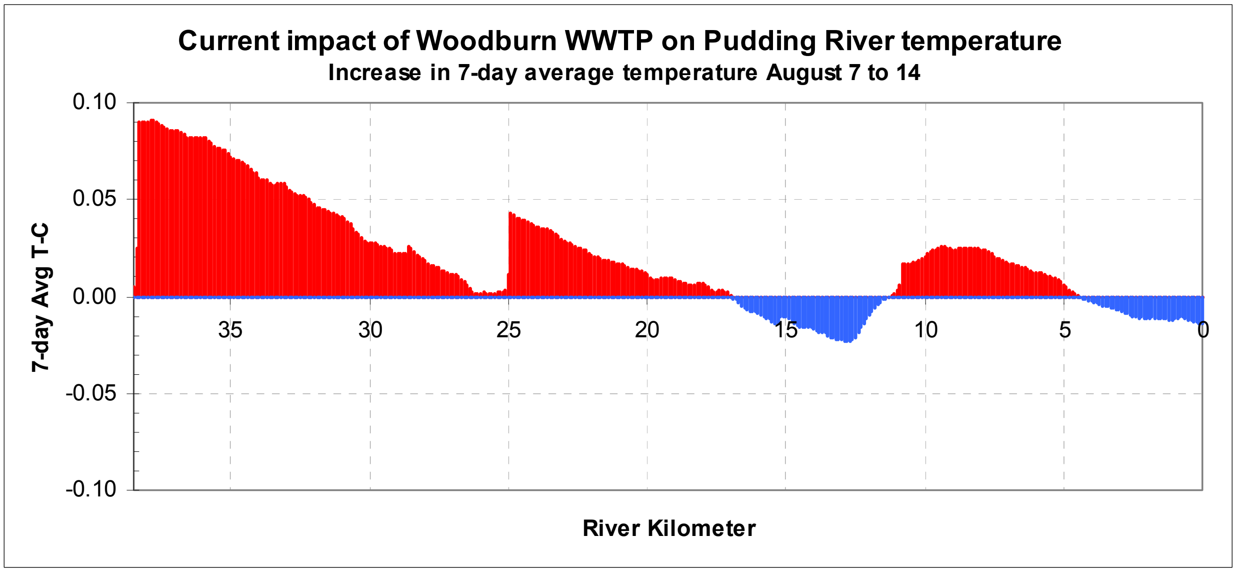

Figure A- 53: Current far-field impacts of Woodburn effluent on average river temperature.

AT 7Q10 FLOW AND NTP: STREAM TEMPERATURE EFFECTS FROM POINT SOURCE HEAT LOADS

While the current impact of the effluent on stream temperature is small, over time, as riparian vegetation conditions improve and stream temperatures decline, the impact of the effluent will increase.

If river flow rates equal 7Q10 low flow conditions and stream temperatures are reduced to natural thermal potential temperature (NTP) conditions, the Woodburn effluent would increase river temperatures 0.30°C for the two week period modeled (Table A- 15). NTP is "the thermal profile of a water body using best available methods of analysis and the best available information on the site-potential riparian vegetation, river geomorphology, river flows, and other measures to reflect natural conditions" (OAR 340-040-0002 (41)). The 0.30°C impact is calculated using Equation A4, below, and equates to an excess thermal load of 11.0 million kcal/day, as calculated via Equation A5 (ODEQ 2008). This impact exceeds the 0.2°C portion of the "human use allowance" allocated to point sources.

Table A- 15: Impact of Woodburn effluent on temperature for 7Q10 river flow and NTP temperature.

$Q_{R,}7Q10$	15 cfs (0.425 cms)	7Q10 low flow at Pudding R near Woodburn gage
$T_{R,NTP}$	20.7°C	Natural thermal potential river temperature at discharge location
Q_e	0.72 MGD (0.031 cms)	Maximum 7-day average effluent flow rate for August 1-14 , 2004 period modeled
T_e	24.78°C	Maximum 7DADM effluent temperature for August 1-14, 2004 period modeled
ΔT	0.30°C	Calculated Increase in river 7DADM temperature

Equation A4

$$\Delta T = \left(\frac{Q_e}{Q_e + Q_R} \right) (T_e - T_R)$$

where:

Q_R = river flow rate

Q_e = effluent flow rate

T_R = river temperature

T_e = effluent temperature

Equation A5

$$ETL = (\Delta T)(Q_R + Q_e)C_F$$

ETL = Excess Thermal Load, kcal/day

ΔT = allowable temperature increase, °C

Q_R = river flow rate upstream, m^3/s

Q_e = effluent flow rate, m^3/s

$C_F = 86.4 \times 10^6 \frac{kcal \cdot s}{°C \cdot m^3 \cdot day}$, conversion factor

Alternatively for flow as cfs:

Q_R, Q_e units: $\frac{ft^3}{sec}$

$C_F = 2{,}446{,}665 \frac{kcal \cdot sec}{°C \cdot ft^3 \cdot day}$

STREAM TEMPERATURE EFFECTS AT SYSTEM POTENTIAL VEGETATION

The TMDL provides an allocation of zero for anthropogenic solar radiation heat load. Anthropogenic solar radiation heat load is the heat load which enters the stream due to human impacts on vegetation, etc. The current anthropogenic solar radiation heat load is the heat load that currently enters a stream due to solar radiation minus the heat load which would enter the stream if riparian (streamside) vegetation were restored to natural levels.

To meet this allocation, effective shade targets are provided as surrogate measures. Effective shade is the percent of available solar radiation that is blocked by vegetation or topographic features such as hills or incised channels. The effective shade targets provided in the TMDL are the shade levels expected for a condition in which near-stream vegetation is restored to system potential levels. System potential vegetation was calculated using the same methodology as used for the nine of twelve Willamette River subbasins addressed in the 2006 Willamette TMDLs (ODEQ, 2006).

Modeling was performed to determine the shade and stream temperature improvements that would result from moving from current to system potential vegetation levels. The effective shade which would result from improving shade to system potential levels is shown in Figure A- 54. Shown are both model calculated current condition and system potential shade levels. The values shown are 1-kilometer averages of the much more variable 100 meter averages used in the model. As shown, restoring vegetation to system potential levels would result in higher levels of shade.

Restoring vegetation to natural potential levels would result in improved shade. The Pudding River Heat Source model indicates that improving near-stream vegetation to potential levels would reduce daily maximum temperatures 1.2^{o}C, on average, during the period modeled (Figure A- 55). Since the period modeled is a typical July/August condition, it is expected that such a reduction would apply for most of the summer.

Based on the 1.2^{o}C difference between current temperatures and temperatures with shade improved to system potential, the current anthropogenic solar radiation heat load, as Delta T, is 1.2^{o}C (Figure A- 56). In the vicinity of the Woodburn gage at RKm 38.0, where the 7Q10 low flow rate is 15 cfs, the impact is about 1.6^{o}C. Based on this impact and the 7Q10 river flow rate, the corresponding excess thermal load due to anthropogenic solar radiation (ETL) is 58.7 million kcal/day. This is about 5 times the 11.0 million kcal/day ETL contributed by the City of Woodburn effluent.

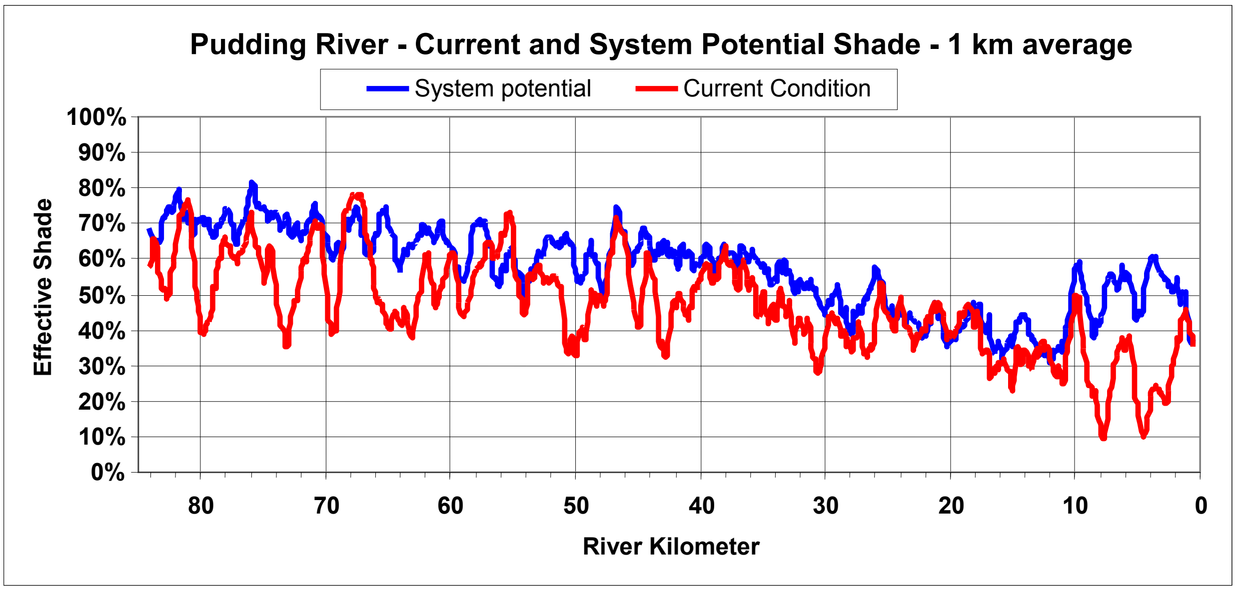

Figure A- 54: Current and system potential shade levels

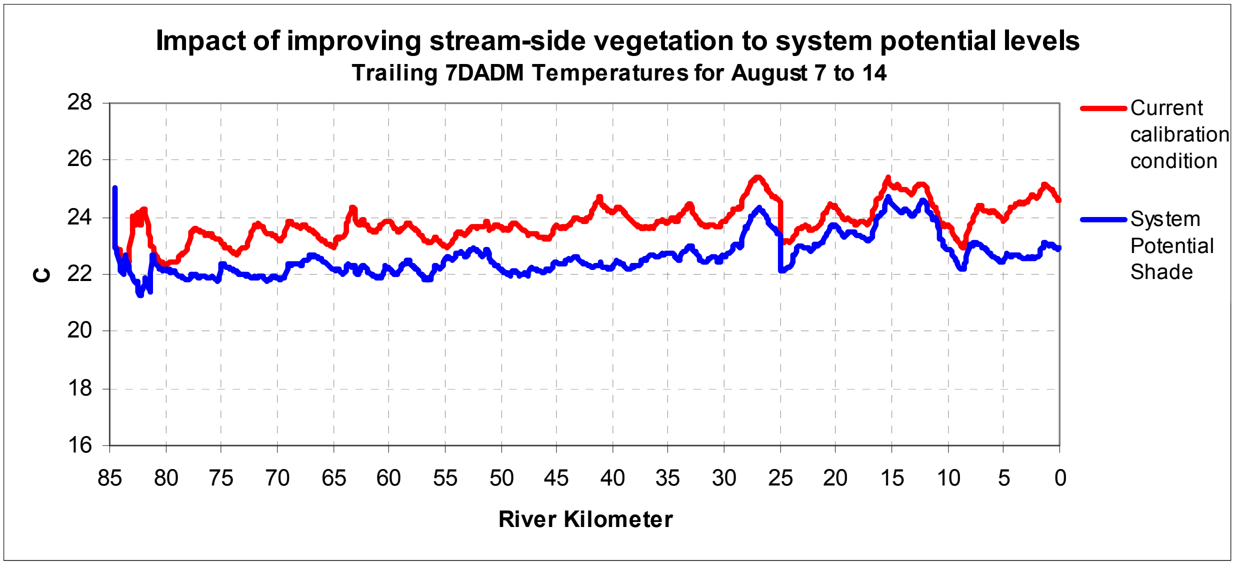

Figure A- 55: Impact on temperature of improving riparian vegetation to system potential levels

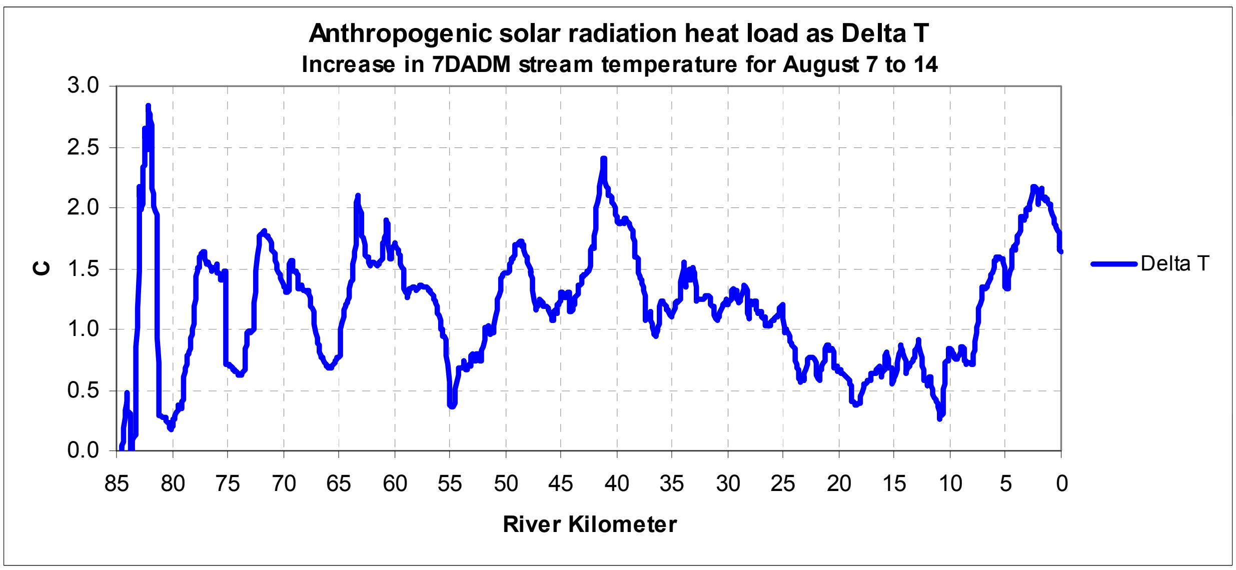

Figure A- 56: Impact on stream temperature of anthropogenic heat load.

STREAM TEMPERATURE EFFECTS AT SYSTEM POTENTIAL VEGETATION AND NO DISTURBANCE

System potential vegetation, as defined for purposes of determining effective shade targets for the TMDL, includes a provision for natural disturbance. An analysis was also performed to determine the effective shade levels and corresponding temperature improvements that would occur if near-stream vegetation were to be restored to mature levels with no disturbance. Resultant effective shade levels are shown in Figure A- 57.

The Pudding River Heat Source model indicates that improving near-stream vegetation to potential levels with no disturbance would reduce daily maximum temperatures an additional 1.0°C, on average, than the system potential with disturbance scenario, for a total reduction of 2.2°C from current condition temperatures (Figure A- 58). This suggests that improving vegetation on the mainstem Pudding River alone, without improving shade on tributaries, could reduce stream temperatures of up to 2.2°C.

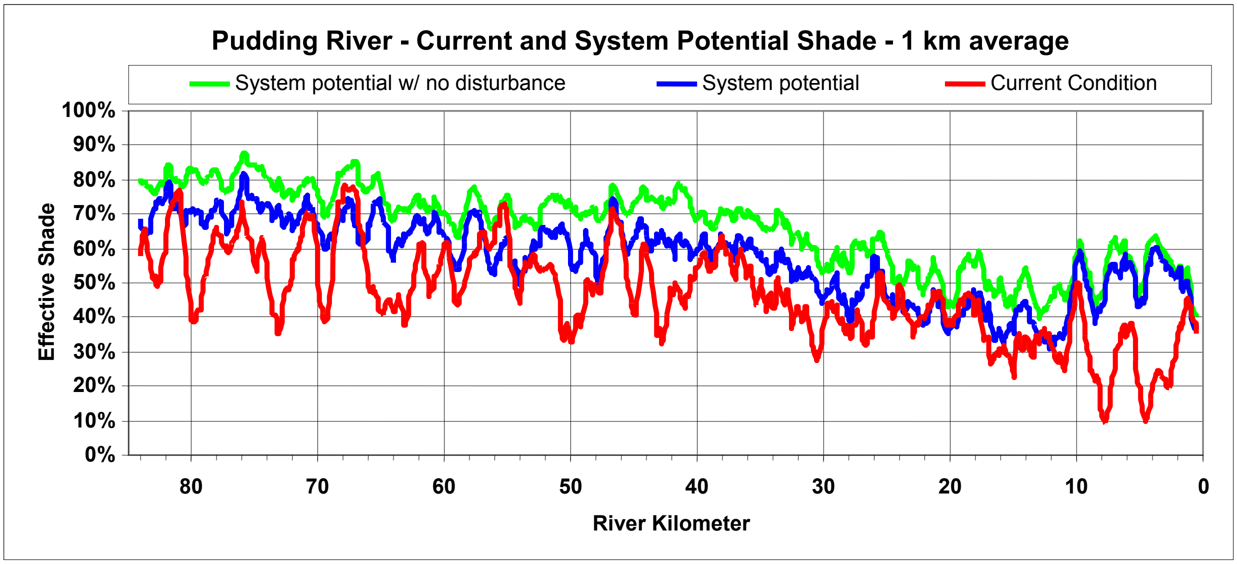

Figure A- 57: Current, system potential, and system potential without disturbance shade levels

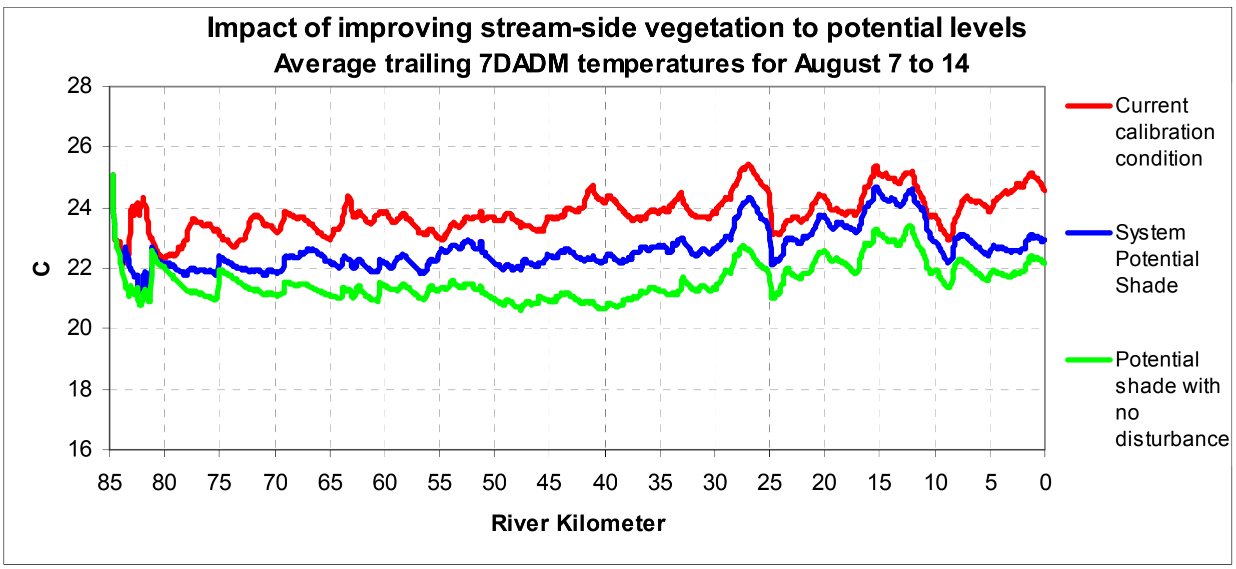

Figure A- 58. Impact of improving riparian vegetation to system potential levels with and without disturbance

STREAM TEMPERATURE EFFECTS FROM TRIBUTARY TEMPERATURES

Tributaries to the Pudding River were not modeled and, therefore, natural thermal potential tributary temperatures can not be calculated. Current temperatures at tributary mouths generally exceed applicable summer criteria of 18°C. The impact of reducing tributary temperature such that they meet the 18°C criteria at stream mouths will reduce temperatures throughout the Pudding River.

An example of estimated NTP is shown in Figure A- 59. As shown, the methodology that was used reduces both daily maximum temperatures and diel fluctuations, as would be expected if the stream were restored to natural conditions.

As shown by Figure A- 60 reducing tributaries temperatures enough to meet the 18°C temperature criteria at confluences with the Pudding River would result in Pudding River 7DADM temperatures that are 1.6°C less, on average, than current temperatures. In the vicinity of the Woodburn gage, the impact is 0.9°C. Assuming that NTP temperatures of tributaries do not exceed 18°C and that temperature increases above 18°C are due to anthropogenic heat loads, then the anthropogenic heat load provided by tributaries is 33.0 million kcal/day at the Woodburn gage.

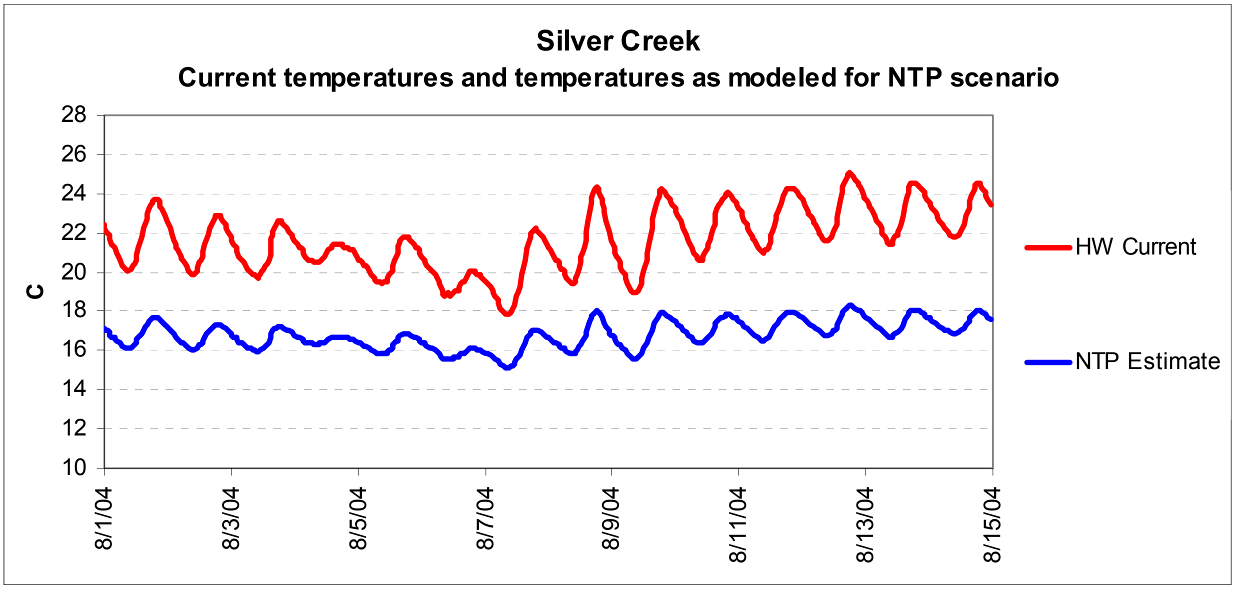

Figure A- 59: Theoretical tributary temperatures that meet the 18°C biological criterion.

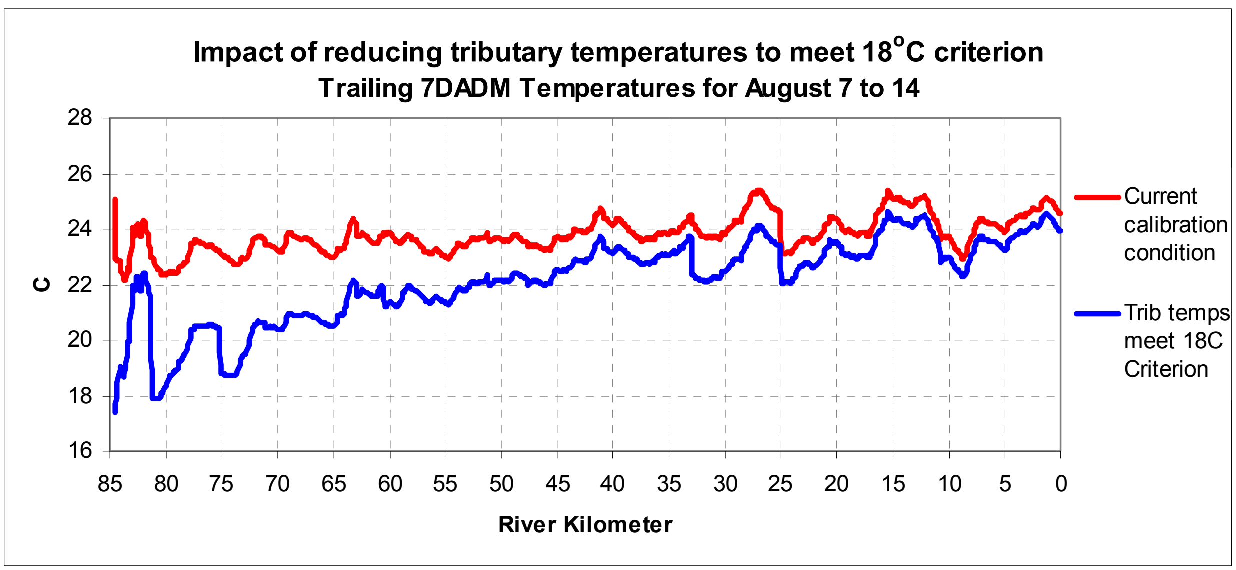

Figure A- 60: Impact of reducing tributary temperatures enough to meet 18°C biological criterion.

STREAM TEMPERATURE EFFECTS FROM CONSUMPTIVE USE

Modeling was performed to evaluate the impact of consumptive use on river temperature. The primary consumptive use in the Pudding River is irrigation, in which water diverted from streams either evaporates, transpires, percolates to deep groundwater, or otherwise is not returned to the stream. Any water diverted from a stream that returns to the stream via irrigation return flows, etc., is not part of the consumptive use.

Five consumptive use scenarios were considered. These range from the current low flow calibration condition (CCC) scenario, in which consumptive use (CU) from the Pudding River and tributaries is set to the estimated CU for the two weeks modeled (August 1-14, 2004), on up to a natural flow scenario in which CU is set to zero. Except for one day that it rained, consumptive use for the current flow condition was set to 90 to 110% of the typical August consumptive use, as determined from Oregon Water Resources Department data and model calibration on USGS gage data. For reduced consumptive use scenarios, consumptive use was reduced to maximums of 75%, 50%, 25%, and 0% of typical August consumptive use (Figure A- 61). The 0% of typical August consumptive use scenario is the natural flow scenario in which there is no CU from either the Pudding River or tributaries.

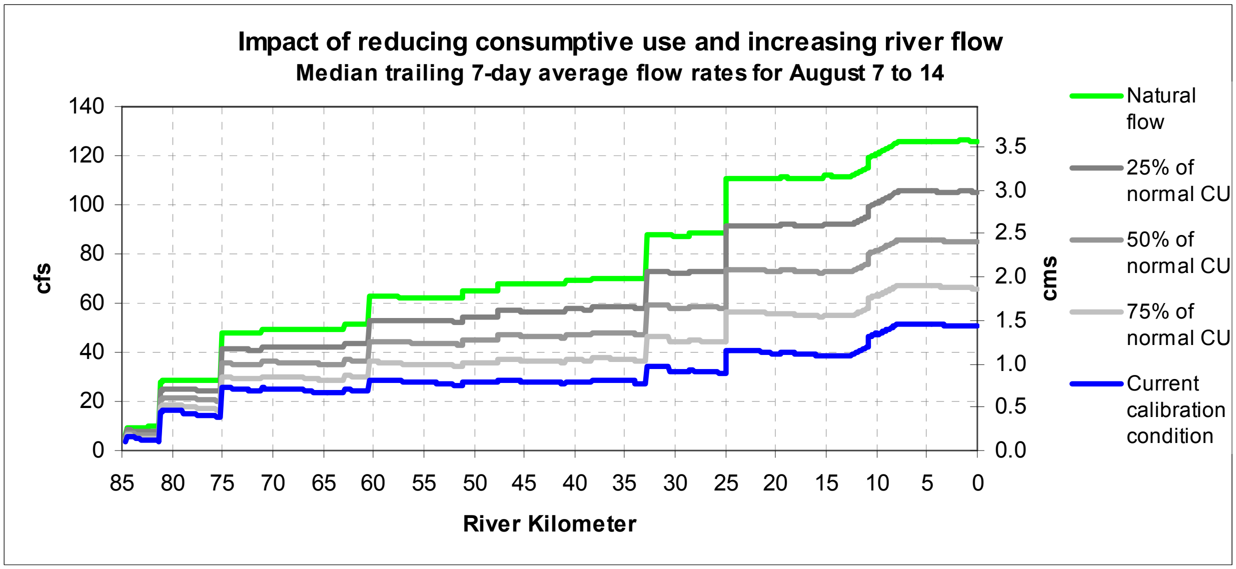

Figure A- 61: Flow rates for five consumptive use scenarios

Since tributaries weren't modeled, the impact of reducing CU on tributary temperatures could not be determined. Therefore, two sets of scenarios were modeled. For the first set, tributary temperatures were left at current condition levels. For the second set, tributary temperatures were reduced enough to meet the 18°C biological criterion, as described above. For both sets, eliminating consumptive use would result in an increase in average river flow for the period modeled from 28.8 cfs to 70.2 cfs at the Woodburn gage.

Tributary temperatures at CCC temperatures

The model indicated that reducing tributary and Pudding River consumptive use, without reducing tributary temperatures, would reduce river average daily maximum temperatures up to 1.1°C (Figure A-62and Table A- 16). It's likely that reducing consumptive use from tributaries would also result in reduced tributary temperatures.

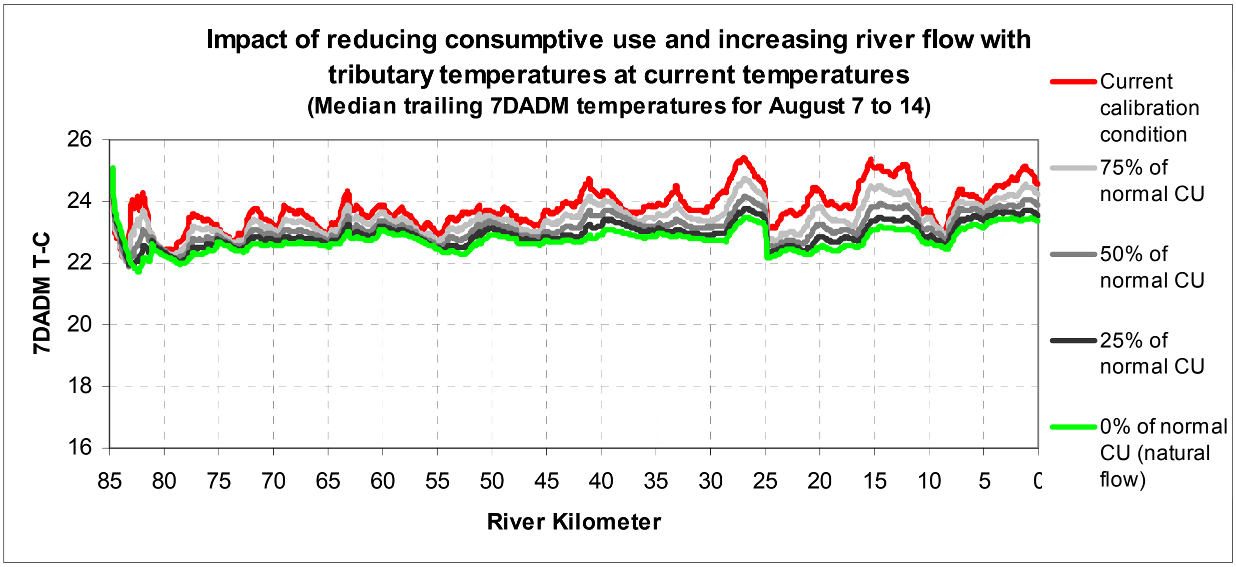

Figure A- 62. Impact on temperature of reducing consumptive use (with no change in tributary temperatures).

Table A- 16: River average impact of reducing consumptive use (with no change in tributary temperatures).

	Average 7-d Average Discharge at Woodburn	River Average 7DADM Temperature (°C)	Temperature Improvement (°C)
Current Calibration Condition	28.8 cfs (0.81 cms)	23.8	-
CU reduced to 75% of typical	37.6 cfs (1.07 cms)	23.4	-0.4
CU reduced to 50% of typical	48.0 cfs (1.36 cms)	23.2	-0.7
CU reduced to 25% of typical	58.6 cfs (1.66 cms)	22.9	-0.9
CU reduced to 0% of typical (natural flow scenario)	70.2 cfs (1.99 cms)	22.7	-1.1

Tributary temperatures at estimated NTP

The model indicated that reducing tributary and Pudding River consumptive use, while also reducing tributary temperatures enough to meet the 18°C criteria, would reduce river average daily maximum temperatures up to 3.5°C (Figure A- 63 and Table A- 17).

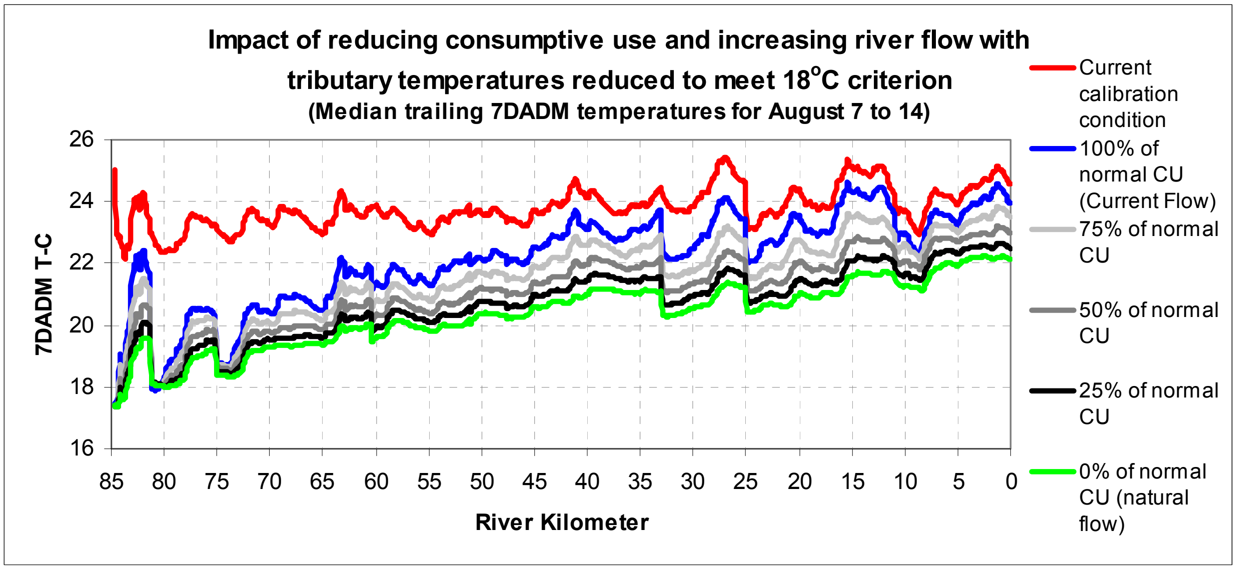

Figure A- 63. Impact on temperature of reducing CU (with tributary temperatures reduced to meet 18° criterion).

Table A- 17: River average impact of reducing CU (with tributary temperatures reduced to meet 18°C).

	Average 7-d Average Discharge at Woodburn	River Average 7DADM Temperature (°C)	Temperature Improvement (°C)
Current Calibration Condition	28.8 cfs (0.81 cms)	23.80	-
Current condition except tributary temperature = 18°C criteria	28.8 cfs (0.81 cms)	22.17	-1.63
CU reduced to 75% of typical	37.6 cfs (1.07 cms)	21.60	-2.20
CU reduced to 50% of typical	48.0 cfs (1.36 cms)	21.11	-2.69
CU reduced to 25% of typical	58.6 cfs (1.66 cms)	20.70	-3.10
CU reduced to 0% of typical (natural flow scenario)	70.2 cfs (1.99 cms)	20.35	-3.45

STREAM TEMPERATURE EFFECTS FROM COMBINED SHADE, FLOW, AND POINT SOURCES

System potential vegetation with disturbance

In order to derive natural thermal potential temperatures, shade was set to system potential levels (with natural disturbance), consumptive use was reduced to zero (the natural flow scenario), tributary temperatures were reduced to meet the 18°C criterion, and point source effluent discharges were eliminated. Therefore, NTP temperatures represent the combined impact of improving shade and flow to natural levels and eliminating point source discharges.

Model calculated natural thermal potential temperatures for the August 1 to 14, 2004 modeling period are shown in Figure A- 64. The river average NTP 7DADM temperature is 19.5°C, which is more than 4°C less than the current condition 7DADM river average temperature of 23.8°C. As shown in Figure A- 64 in the upper reaches NTP temperatures do not exceed the 18°C biologically-based numeric criterion and, therefore, 18°C is the applicable criterion. Further downstream, NTP temperatures exceed 18°C and, therefore, the NTP temperatures become the applicable criteria.

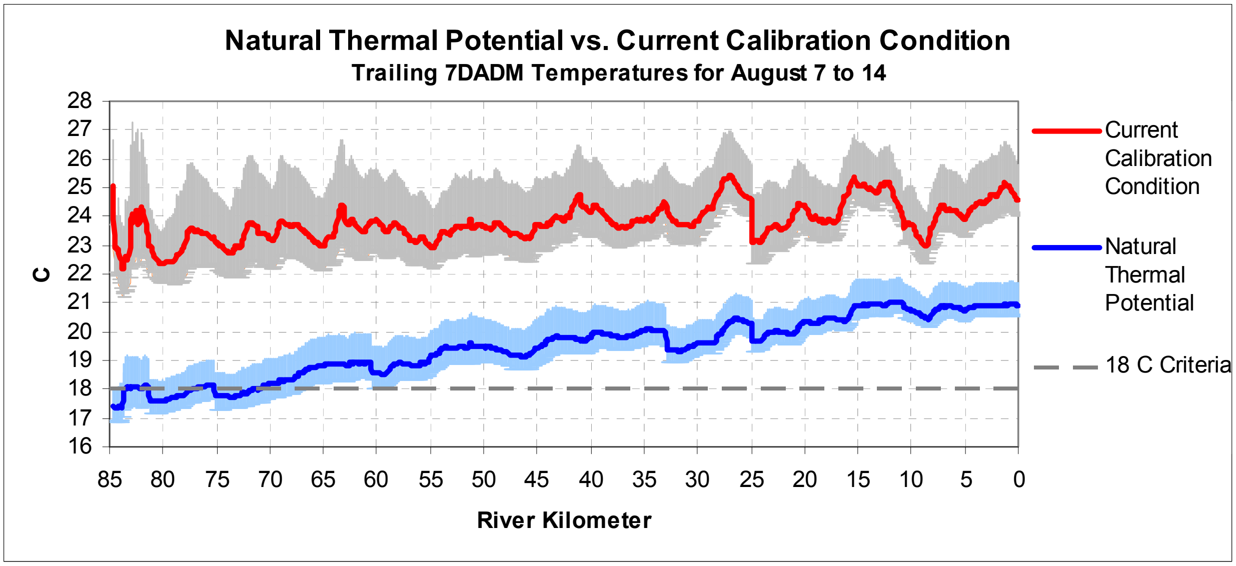

Figure A- 64: Natural thermal potential river temperatures

System potential vegetation at maximum levels (no disturbance)

An additional modeling simulation was performed in which all inputs are the same as the NTP scenario except for shade, which is set to the maximum shade scenario of system potential shade with no disturbance. Resultant average 7DADM temperatures for the August 1 to 14 modeling period are shown in Figure A- 65. The river average temperature for this scenario is 18.5^{o}C, which is more than 5^{o}C less than the current condition 7DADM river average temperature of 23.8^{o}C.

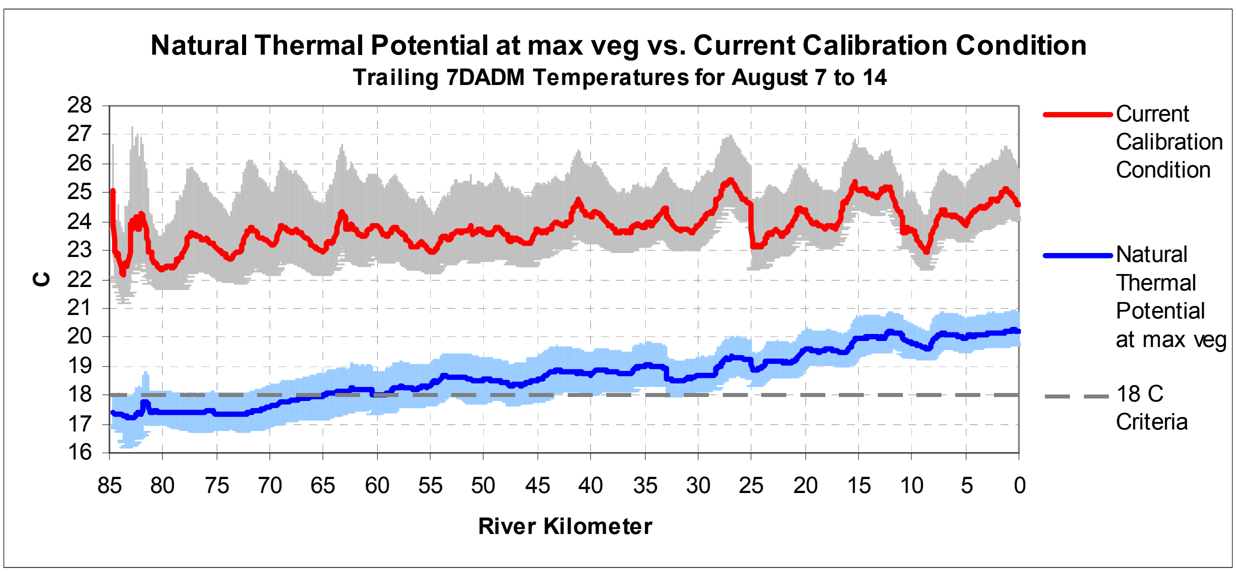

Figure A- 65: River temperatures for natural thermal potential scenario with vegetation at maximum levels.

SOLAR RADIATION AND EFFECTS ON EXCESS THERMAL LOADS

Solar radiation is a dominant source of stream heating. Comparing solar radiation energy loads for current vegetation conditions to the solar radiation energy loads for the system potential shade conditions provides an indication of anthropogenic solar radiation loads to the stream. This loading is a major source of excess thermal loads in streams.

Total daily solar heat from nonpoint sources and background: Molalla and Pudding Rivers

Solar heating is established as a primary pollutant in stream heating processes. The calculation of the overall heat load received by the stream system from solar radiation yields the nonpoint sources of solar heat for the total stream system as well as for each stream/river. The total daily solar heat loading is the cumulative solar heat energy received by a stream per day during the period of interest (i.e. July/August period). For the purposes of this analytical effort, the total solar heat loading is the sum of the products of the daily solar heat flux and surface area of exposure for each stream reach (i.e., for each stream data node every 100 feet).

$$H_{solar} = \sum\left(\Phi_{solar} \cdot A_y\right) = \sum\left(\Phi_{solar} \cdot W_{wetted} \cdot dx\right)$$

Background levels of solar heat estimate the portion of the total daily solar heat load that occurs when nonpoint sources of heat are minimized. The background condition is the system potential total daily solar heat load (i.e., where anthropogenic nonpoint sources are minimized) and is calculated by substituting the system potential daily solar flux and the potential wetted width into the equation above. In this fashion, the total daily solar load is calculated for both the current condition (H_{solar}) and the system potential condition ($H_{solar}^{Background}$). With the background portion of the total daily solar load accounted for, the remaining portion can be attributed to anthropogenic nonpoint sources. Therefore, the anthropogenic nonpoint source total daily solar load is the difference between the total daily solar load and the background total daily solar load. This relationship is represented by Equation A6. Derived total daily loads for background sources and anthropogenic nonpoint and point sources are presented in Table 18.

Equation A6

$$H_{solar}^{NPS} = H_{solar} - H_{solar}^{Background}$$

where,

A_y: Stream surface area unique to each stream segment (cm^2)

dx: Stream segment length and distance step in the methodology (cm)

Φ_{solar}: Solar heat flux unique to each stream segment (kcal cm^{-2} day^{-1})

H_{solar}: Total daily solar heat load delivered to the stream (kcal day^{-1})

H_{solar}^{NPS}: Portion of the total daily solar heat load delivered to the stream that originates from nonpoint sources of pollution (kcal day^{-1})

$H_{solar}^{Background}$: Portion of the total daily solar heat load delivered to the stream that originates from background sources of pollution that are not affected by human activities (kcal day^{-1})

W_{wetted}: Wetted width unique to each stream segment (cm)

Table A- 18: Total daily solar loading to Molalla and Pudding Rivers.

Watershed	Current Conditions Solar Loading (million Kcal/day)	Potential (Background) Solar Loading (million Kcal/day)	Anthropogenic Solar Loading (billion Kcal/day)	Portion from Anthropogenic Non-point sources
Molalla	6,983 (339 MW)	5,830 (283 MW)	1,154 (56 MW)	17%
Pudding	3,973 (192 MW)	3,285 (159 MW)	688 (33 MW)	17%

Total current condition, system potential, and anthropogenic solar radiation loads for various Pudding River reaches are shown in Table A- 19 in units of million kcals/day. The values provided are averages for the August 1 to 14, 2004 calibration period. The values were calculated by multiplying the wetted surface area of each river reach by the solar radiation calculated by the model at the surface of the stream (referred as SR6 radiation by Heat Source. As shown by the last line in Table A- 19, the cumulative solar radiation load received by the stream for the entire Pudding River is 3,973 million kcal/day for current vegetation and 3,285 million kcal/day for system potential vegetation. Therefore, 688 million kcal/day or 17% of the current solar radiation loading is anthropogenic.

Solar radiation loading as displayed in Table A- 18 and Table A- 19 is largely a function of stream surface area. Longer river reaches have larger loads than shorter river reaches because of greater surface area. Emphasis should be placed on the difference between natural background loads and current loads. The decrease in solar radiation to reach system potential reflects the daily reduction in kilocalories necessary to realize background heat loads.

Table A- 19: Solar radiation loading to the Pudding River on a per reach basis

Reach	**RKms**	**Current Condition**	**System Potential**	**Anthro-pogenic**	**Portion of current that is anthropogenic**
		Million kcal/day	**Million kcal/day**	**Million kcal/day**	
Headwaters to Abiqua Cr	**84.6 to 75.1**	166	119	47	28%
Abiqua Cr to Little Pudding R	**75.0 to 60.4**	435	317	118	27%
Little Pudding R to Zollner Cr	**60.3 to 47.6**	441	374	67	15%
Zollner Cr to Butte Cr	**47.5 to 32.9**	517	426	91	17%
Butte Cr to Rock Cr	**32.8 to 24.9**	415	353	62	15%
Rock Cr to Mill Cr	**24.8 to 10.8**	1,021	975	46	4%
Mill Cr to mouth	**10.7 to 0.0**	978	721	257	26%
Entire Pudding River	**84.6 to 0.0**	3,973	3,285	688	17%

Additional analyses: Excess Solar Radiation Loads as component of Excess Thermal Loads in the Pudding River

Cumulative solar radiation loads received by the Pudding River for current and system potential shade are shown in Figure A- 66. The difference between the two is the anthropogenic solar radiation load summarized in Table A- 19, above.

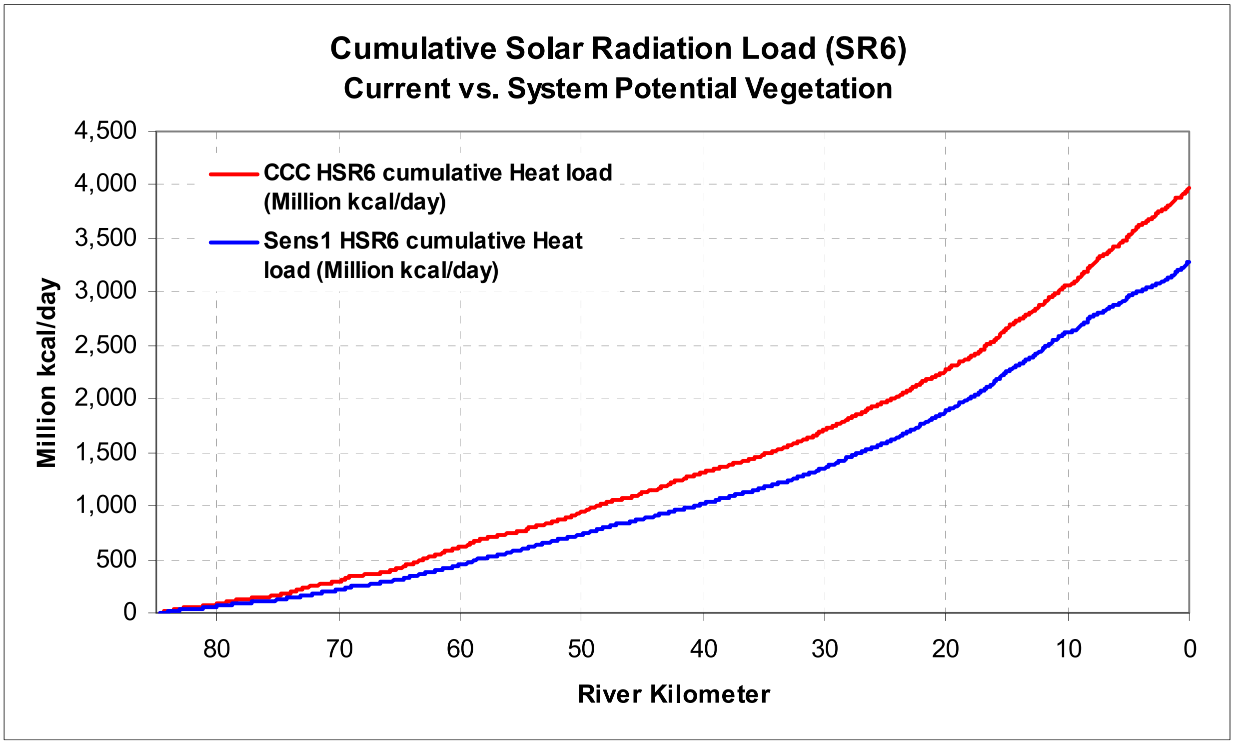

Figure A- 66. Cumulative solar radiation load for current and system potential shade conditions.

Solar radiation received by a stream causes it to warm, but not all of the heat load received by a stream is retained. Some of the heat received dissipates through longwave back radiation, conductive and convective processes, and evaporation. This is illustrated for the Pudding River by Figure A- 67 which shows the cumulative excess solar radiation load received by the river as well as the excess thermal load (ETL) retained by the river. The cumulative excess solar radiation load plotted is the anthropogenic solar radiation load, i.e., the solar radiation load received by the stream for current conditions minus the solar radiation load received by the stream for system potential shade conditions[3]. As shown by Figure A- 67, in the uppermost reach from RKm 84.6 to RKm 67, excess thermal loads in the river are similar to solar radiation loads received by the river. But downstream from RKm 67, ETLs in the stream are less than solar radiation loads received by the river due to loss of heat through mechanisms such as longwave radiation, conductive and convective processes, and evaporation.

[3] Heat Source modeling simulations used were CCC, which is the current calibration condition scenario, and Sens 1, which is a modeling scenario used to determine the sensitivity to system potential shade. Both scenarios modeled flow and meteorological conditions observed during the August 1 to 14, 2004 model calibration period. The only difference between CCC and Sens 1 is that for Sens 1 mainstem Pudding River vegetation was increased to system potential levels that represent natural shade levels. For both simulations tributary temperatures were set to current temperatures, so the simulations do not consider the potential impacts of system potential shade on tributary temperatures.

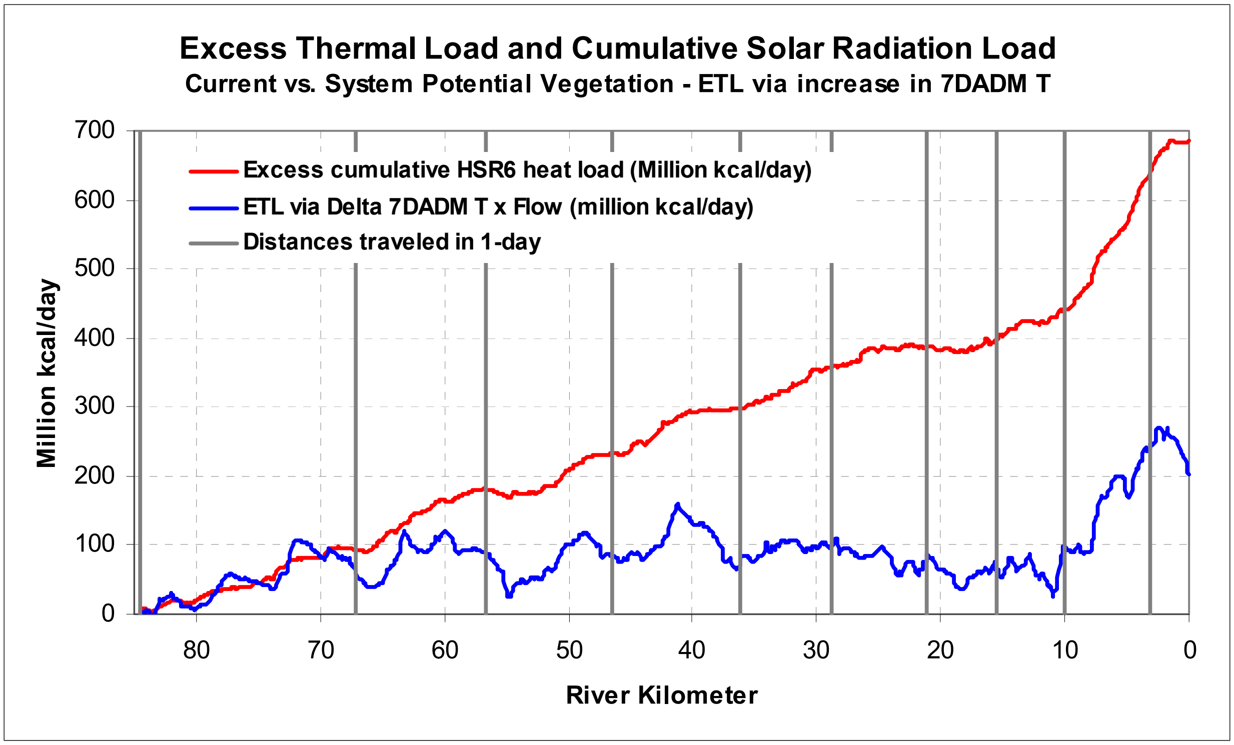

Figure A- 67. Cumulative solar radiation load vs. excess thermal load based on daily max temperatures.

The excess thermal load is the anthropogenic solar radiation load retained by the stream. ETLs are calculated by the following equation (Equation A7), where ΔT (Delta T) in the equation is the difference between model calculated current condition (CCC) temperatures and model calculated temperatures with shade improved to system potential levels (simulation: Sens 1) (Figure A- 68 and Figure A- 69):

$$ETL = (\Delta T)(Q_R)C_F \qquad \text{Equation A7}$$

where:

$ETL = \text{Excess thermal load}, \ \text{kcal}/\text{day}$

$\Delta T = \text{river temperature increase}, \ ^{o}C$

$Q_R = \text{river flow rate}, \ m^3/s$

$C_F = \text{conversion factor}$

$$C_F = 86.4 \times 10^6 \ \frac{\text{kcal} \cdot s}{^{o}C \cdot m^3 \cdot \text{day}}$$

Alternatively, for flow as cfs:

$Q_R \ \text{units}: \ ft^3/s$

$$C_F = 2{,}446{,}665 \ \frac{\text{kcal} \cdot s}{^{o}C \cdot ft^3 \cdot \text{day}}$$

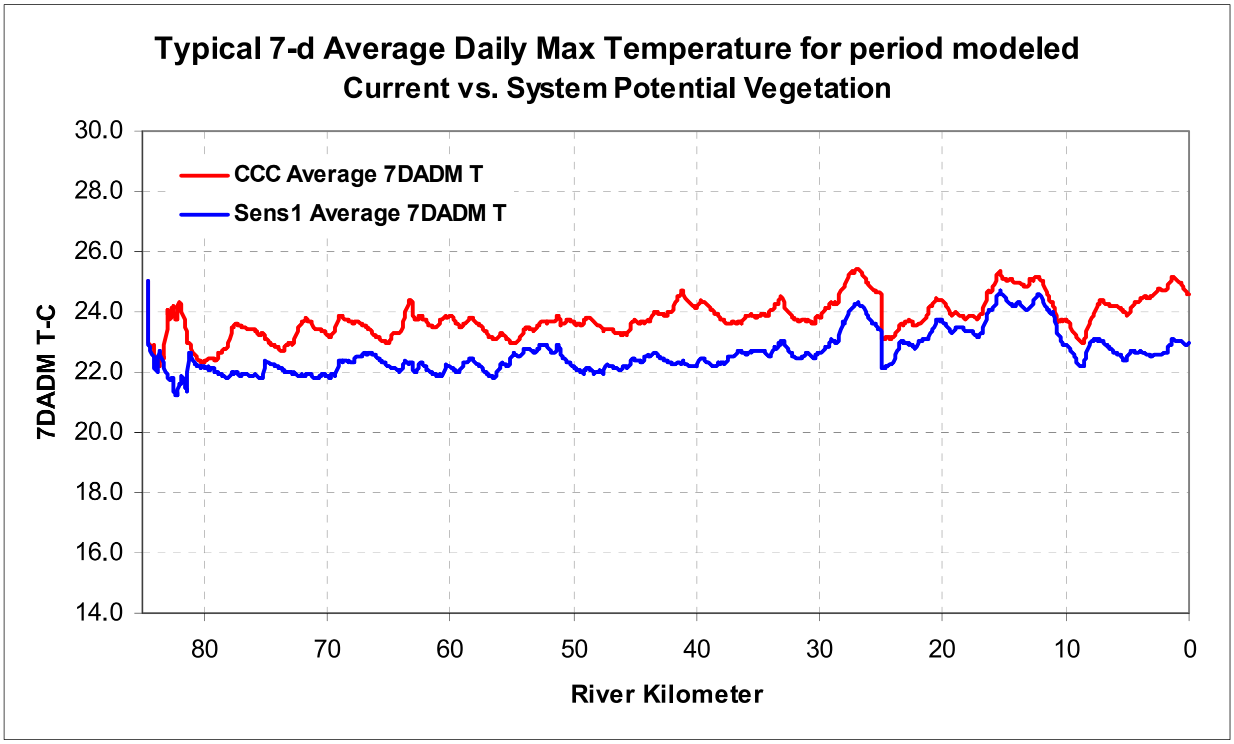

Figure A- 68. Model calculated 7DADM temperature for current and system potential vegetation.

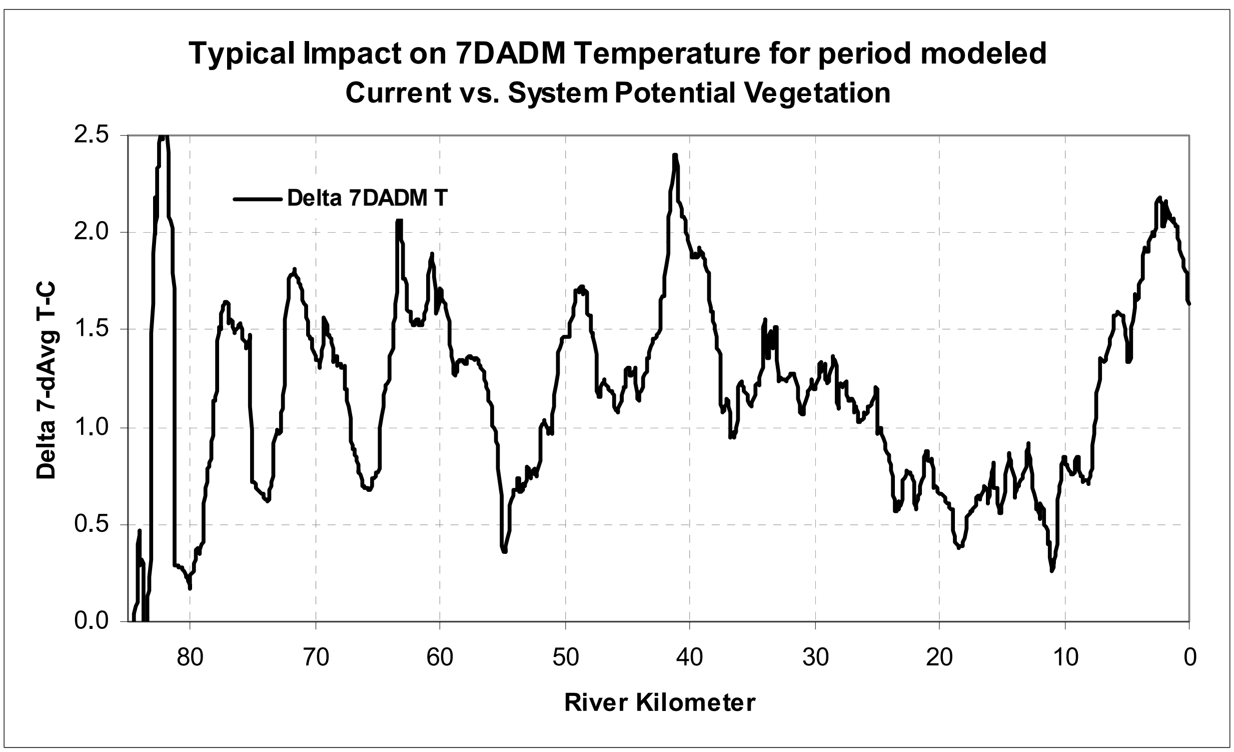

Figure A- 69. Effect of anthropogenic solar radiation on 7DADM stream temperature.

In Figure A- 70, vertical grey lines indicate distances river water travels in one day, based on average velocities for the August 1 to 14, 2004 calibration period. A particle released at the RKm 84.6 (Drift Creek) would travel to RKm 67.1 in one day, from RKm 67.1 to RKm 56.6 the next day, to RKm 46.5 the next day, etc. The total time-of-travel through the Pudding River from Drift Creek to mouth is slightly more than 10 days for the low flow period modeled. Figure A- 70 shows the cumulative time-of-travel as well as average river flow rate for the period modeled.

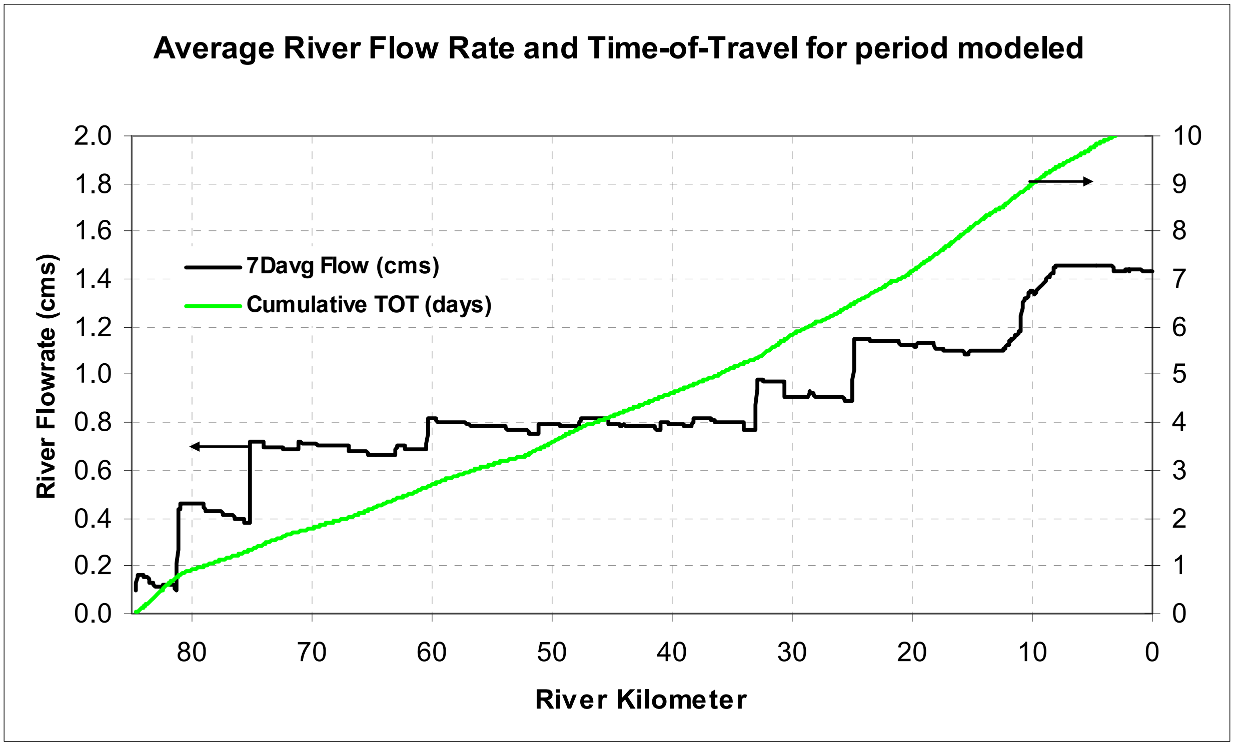

Figure A- 70. Average River flow rates and times-of-travel for August 1 to 14, 2004 calibration period

At several locations upstream of RKm 67, ETLs exceed the cumulative solar radiation loads received (see Figure A- 67). This is because solar radiation loads received are daily averages, whereas the ETLs are calculated using daily maximum stream temperatures. If daily average stream temperatures are used instead to calculate ETLs (Figure A- 71 and Figure A- 72), the calculated ETLs are less variable and never exceed cumulative received solar radiation loads (see Figure A- 73). ETLs calculated using such daily averages may provide a more accurate indication of excess load in the stream.

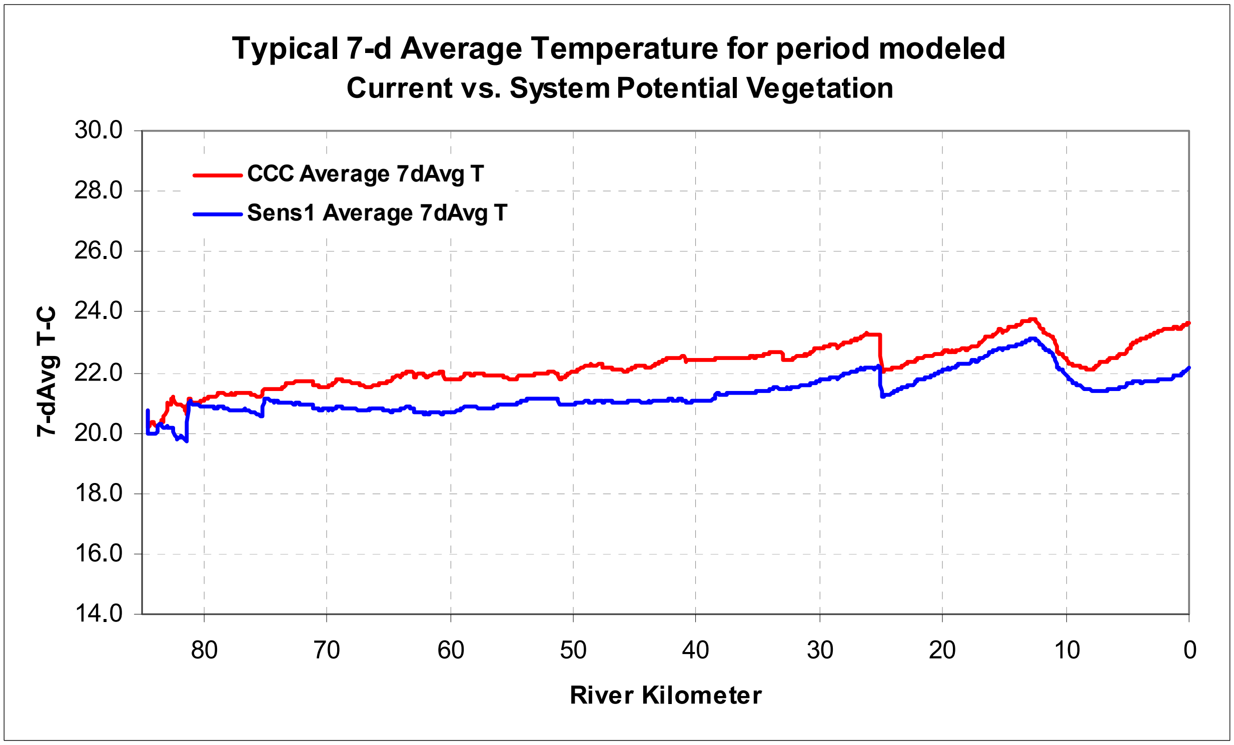

Figure A- 71. Model calculated 7-day average temperature for current and system potential vegetation.

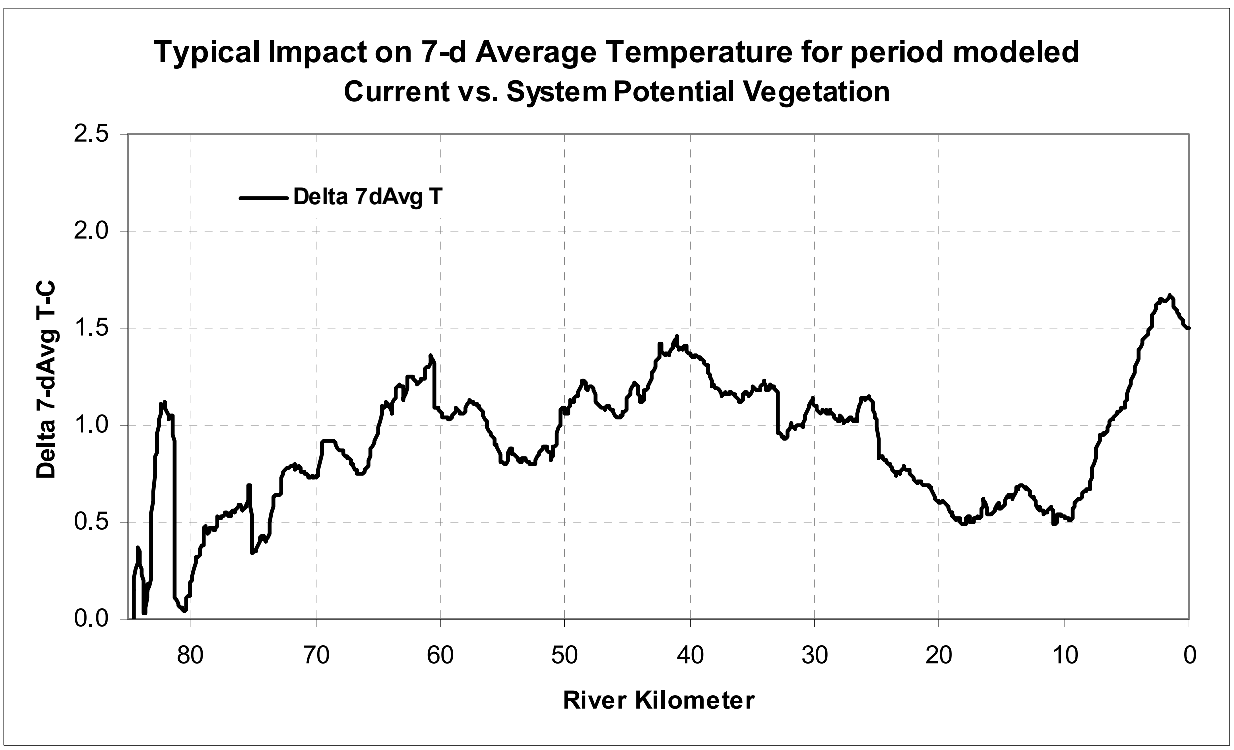

Figure A- 72. Effect of anthropogenic solar radiation on 7-day average stream temperature.

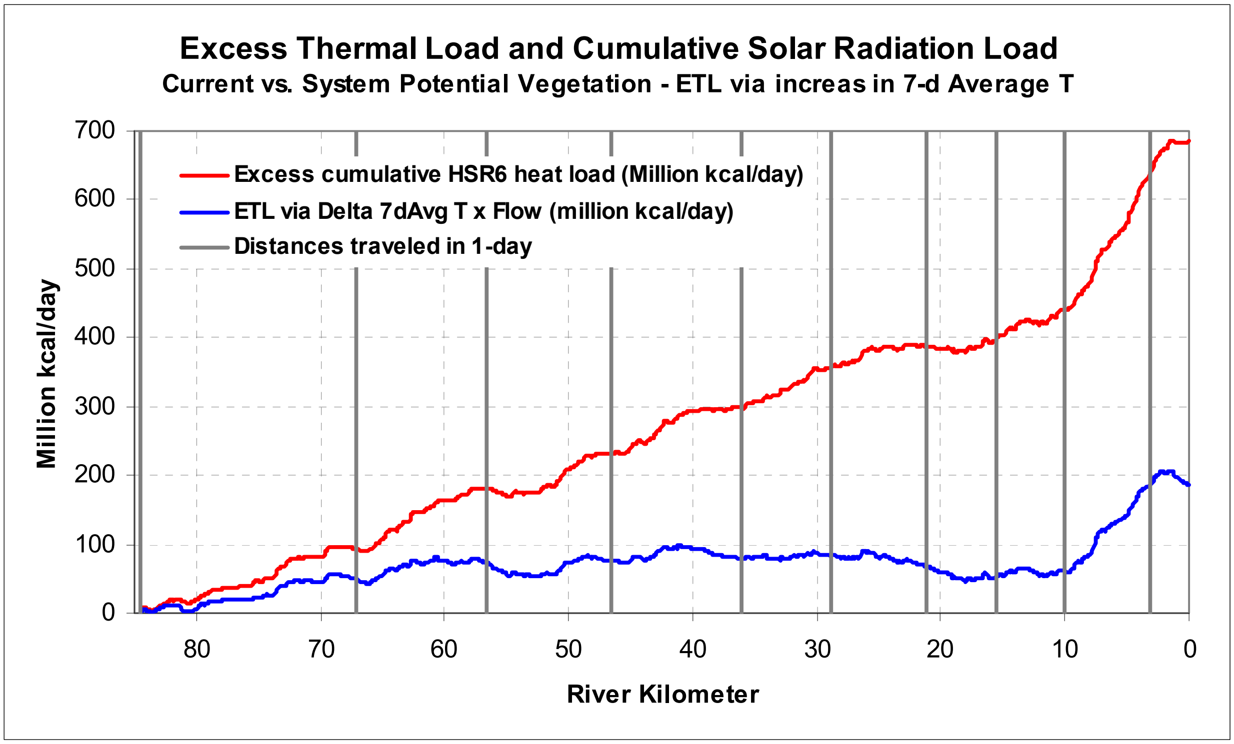

Figure A- 73. Cumulative solar radiation load and excess thermal load based on daily average temperatures.

As shown by Figure A- 73, the ETL remains relatively constant at less than 100 million kcal/day, even though the cumulative excess solar radiation load received by the stream steadily increases. This indicates that the stream has warmed to a level of dynamic equilibrium and that heat added during the day is gradually lost due to longwave radiation, evaporation, etc. This suggests that the stream is so warm that that fluxes out of the stream roughly equal solar radiation fluxes into the stream.

Below RKm 10, heat gains exceed losses and excess thermal loads more than double in one day. This suggests that this reach is relatively wide and that current shade levels are significantly less than system potential levels.

PROPORTIONS OF HEAT LOAD DUE TO VARIOUS SOURCES

Analyses were performed using the Pudding River model to determine the relative contributions to stream temperature increase beyond 18°C that are associated with four categories of stream heating: natural background heat loads, anthropogenic solar radiation heat loads, stream flow reductions to consumptive water use, and point source heat loads.

Even without anthropogenic impacts, natural heat loads increase stream temperature beyond the 18°C biologically-based numeric criteria. Anthropogenic solar radiation heat loads, which is the difference beyond solar radiation loads for current riparian vegetation conditions and solar radiation loads for a natural, system potential shade scenario, further increase stream temperatures. Consumptive water use due to diversions for irrigation and other uses reduces stream volumes and depths, which reduces the assimilative heat capacity of the stream, and reduces flow velocity, which increases the time of exposure to solar radiation loads. Thus, consumptive water use results in additional stream temperature increases. Finally, point source heat loads associated with wastewater discharges further increase stream temperatures. The cumulative impact is that stream temperatures are currently much warmer than natural thermal potential.

To evaluate the relative impacts of each category stream heating, each category was modeled independently. Note that the impacts of the four categories when added together exceed the cumulative impact with all four categories modeled concurrently. The impact of all four categories is the current calibration condition described previously and presented again in Figure A- 74. This is because the temperature increases caused by heat loads are greater when the stream is cool than when it is warm. For example, when the stream temperature is 18^{o}C, a 25^{o}C effluent can heat the stream quite a bit, but when the stream temperature is already nearly 25^{o}C due to anthropogenic heat loads and water diversions, the impact of the effluent is negligible.

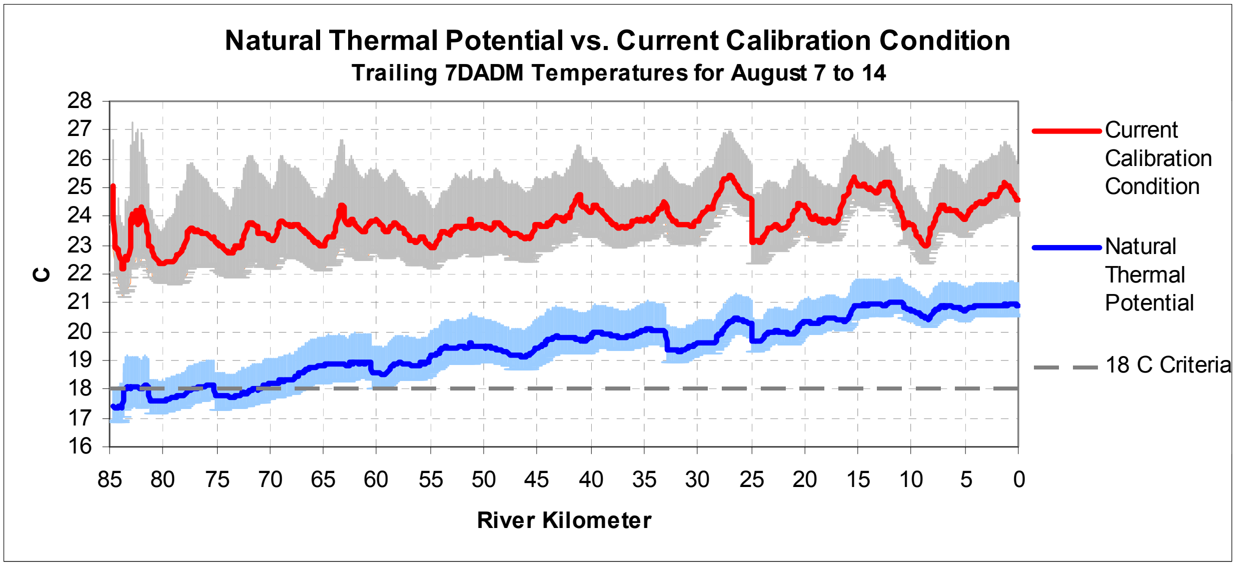

Figure A- 74: Model calculated natural thermal potential 7DADM Temperatures

Modeling of the four categories of stream heating was performed as follows:

1. Increase due to Natural Background

   To provide the increase in temperature associated with natural background heat loads, the 18^{o}C biological criterion is simply subtracted from the river temperatures calculated for the natural thermal potential (NTP) scenario.   When NTP temperatures are less than 18^{o}C, the difference is set to zero.

2. Increase due to anthropogenic solar radiation heat loads

   The anthropogenic solar radiation heat load is the heat load due to the additional solar radiation which enters the stream due to human impacts which reduce vegetative shading. It was determined by subtracting river temperatures calculated for the current calibration condition (CCC) scenario from temperatures calculated for simulation Sens 1. The only difference between Sens 1 and the CCC scenario is that for Sens 1 riparian vegetation is improved from current levels to system potential levels.

3. Increase due to consumptive water use (diversions)

   The impact of consumptive use on stream temperature was determined by subtracting river temperatures calculated for sensitivity simulation Sens 2 from temperatures calculated for simulation Sens 6B. Sens 2 is the same as the current calibration condition scenario, CCC, except that riparian vegetation is improved from current levels to system potential levels. Sens 6B is the same as Sens 2 except that, in addition to shade being improved to system potential levels, consumptive use is reduced to zero. Therefore, the stream flowrate for Sens 2 is a natural flow scenario.

4. Maximum potential increase due to point sources

   The impact of point sources was evaluated for the August 1 to 14, 2004 current calibration flow condition, but with vegetation improved to system potential levels. The impact due to point sources was calculated by subtracting temperatures calculated for simulation Sens 10 from temperatures calculated for simulation Sens 9. Simulation Sens 10 is the same as the current calibration condition (CCC) scenario, except that shade is improved to system potential levels, the temperatures of inflows to the Pudding R from tributaries are reduced to meet the 18°C 7DADM temperature criteria, and point sources are eliminated. Sens 9 is the same as Sens 10 except that point source flow rates are set to the maximum 7-day average summer flow rates (June through September) and effluent temperatures are set to the maximum 7DADM summer temperatures. Therefore, stream conditions for Sens 10 are the same as the natural thermal potential scenario except that river flow rates are maintained at August 1 to 14, 2004 calibration period flow rates. Therefore, since river flow rates and temperatures are low, while effluent flow rates and temperatures are at constant high values, the impact of point sources is quite a bit greater than that expected for current conditions.

CALCULATED INCREASES IN 7 DAY AVERAGE DAILY MAXIMUM STREAM TEMPERATURES

Two relatively large point sources, Silverton WWTP and Hubbard WWTP, discharge to tributaries to the Pudding River. The Silverton WWTP discharges to Silver Creek about 4 km from the mouth while Hubbard WWTP discharges to Mill Creek about 11 km from the mouth. The maximum potential impacts on the tributaries were calculating by setting stream flow rates to the August 1 to 14, 2004 calibration condition, stream temperatures to that which meet the 18°C criteria on a 7DADM basis, effluent flow rates to the maximum observed 7-day average rate for the summer (June through September), and effluent temperatures to the maximum observed 7DADM for the summer.

Since heat added by point sources gradually dissipates as the water flows downstream, the impact at stream mouths where they enter the Pudding River are less than those calculated for the discharge locations. Temperatures at stream mouths were estimated by applying similar heat dissipation rates estimated by the model for the Pudding River to the tributaries. For Silver Creek, 70% of the temperature increase calculated for Silverton at the point of discharge is applied to the stream mouth. For Mill Creek, since the discharge is further from the mouth, 30% of the temperature calculated for Hubbard at the point of discharge is applied to the stream mouth.

Resultant increases in 7-day average daily maximum (7DADM) Pudding River temperatures for the four categories of stream heating are shown in Figure A- 75. As shown, much of the stream temperature increase beyond 18°C is attributable to natural background. On average, 1.5°C of the increase beyond 18°C is due to natural background, and up to 2.9°C of the temperature increase at the stream mouth is due to natural background. Impacts due to anthropogenic solar radiation are 1.2°C, on average, and 1.9°C near the stream mouth. Impacts due to consumptive water use are 1.8°C, on average, and 2.0°C near the stream mouth. Maximum impacts of the Woodburn WWTP are 0.62°C at the point of discharge. Maximum impacts of the Silverton WWTP on the Pudding River are 0.43°C where Silver Creek enters the Pudding River and maximum impacts of the Hubbard WWTP are .08°C where Mill Creek enters the Pudding River. None of the point source impacts are cumulative.

Proportions of the 7-day average daily maximum temperature increase above 18°C that are attributable to each category are shown in Figure A- 76 On average, about 29% of the temperature increase beyond 18°C is attributable to natural background, 27% to anthropogenic solar radiation, 40% to consumptive use (diversions), and 4% to point sources. 12% of the temperature increase is due to the Woodburn WWTP effluent discharge at the point of discharge (RKm 38.3).

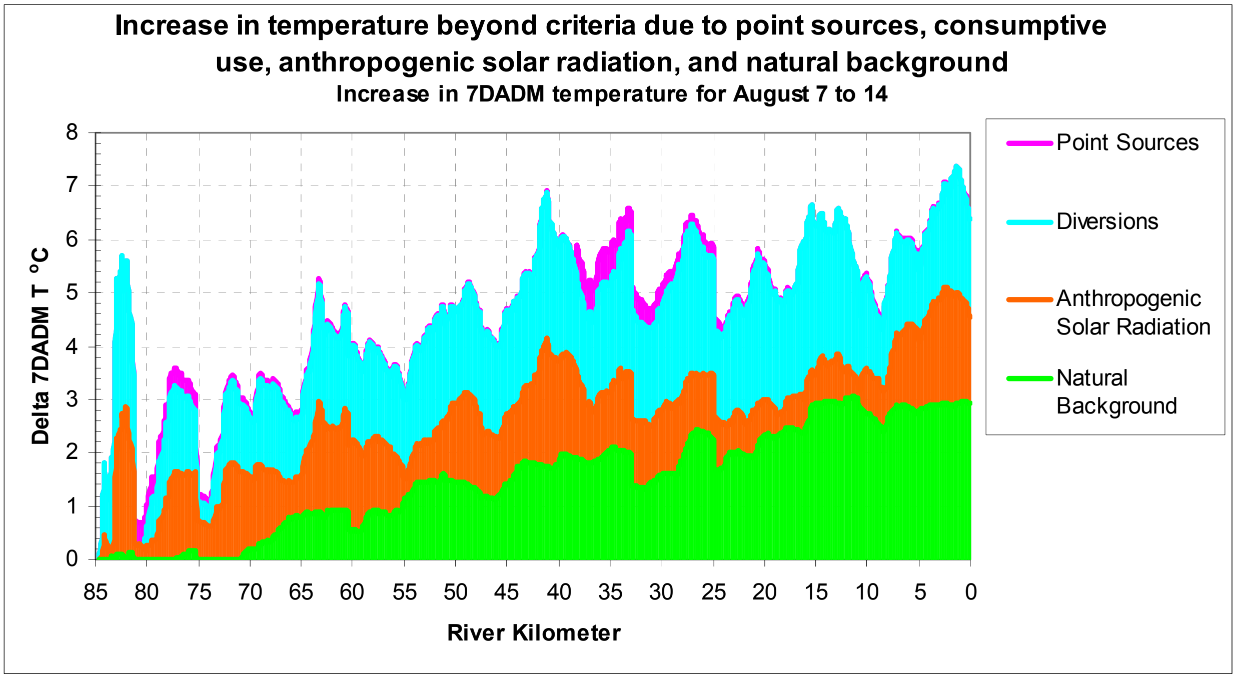

Figure A- 75. Increase in 7DADM river temperature above biological criterion due to various categories

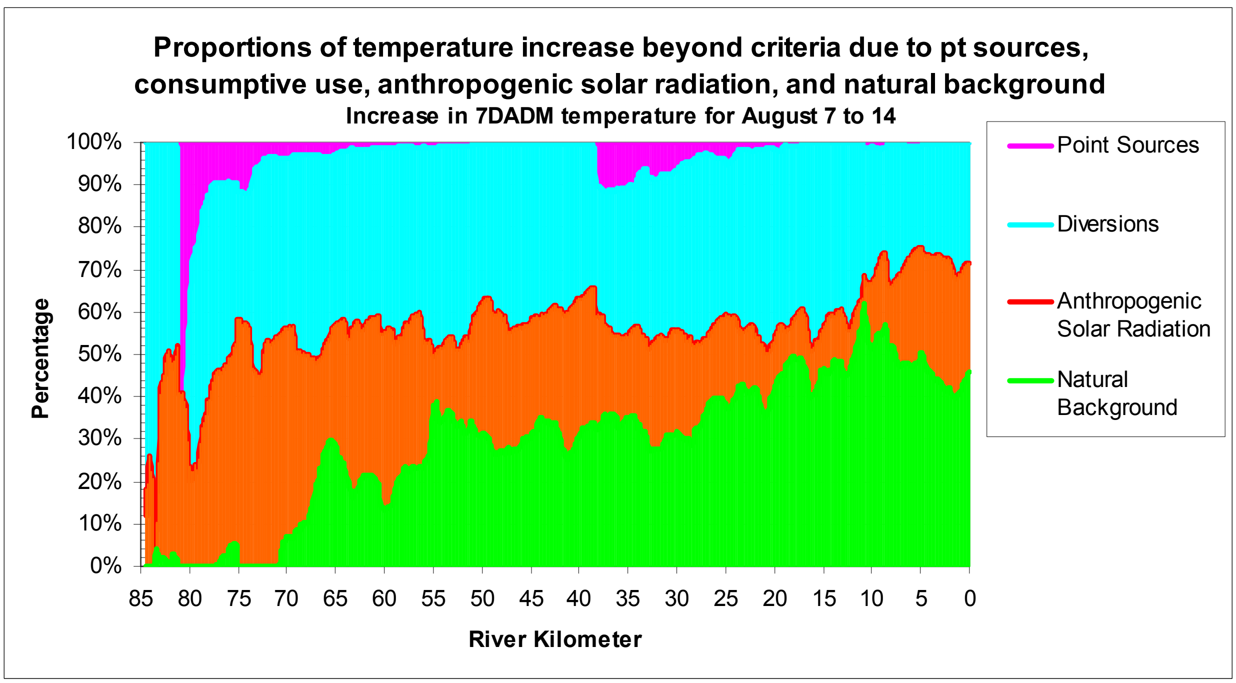

Figure A- 76. Proportions of 7DADM river temperature increase above biological criterion due to various categories

CALCULATED INCREASES IN DAILY AVERAGE STREAM TEMPERATURES

Impacts on daily average Pudding River temperatures are also of interest (although the temperature criteria is in terms of daily maximum temperatures). Resultant increases in 7-day average Pudding River temperatures for the four categories of stream heating are shown in Figure A- 77. On average, 1.4°C of the increase beyond 18°C is due to natural background, and up to 3.1°C of the temperature increase at the stream mouth is due to natural background. Impacts due to anthropogenic solar radiation are 1.9°C, on average, and 1.5°C near the stream mouth. Impacts due to consumptive water use are 2.0°C, on average, and 1.5°C near the stream mouth. Maximum impacts of the Woodburn WWTP are 0.74°C at the point of discharge. Maximum impacts of the Silverton WWTP on the Pudding River are 0.43°C where Silver Creek enters the Pudding River and maximum impacts of the Hubbard WWTP are 0.10°C where Mill Creek enters the Pudding River. None of the point source impacts are cumulative.

Proportions of the 7-day average temperature increase above 18°C that are attributable to each category are shown in Figure A- 78. On average, about 32% of the temperature increase beyond 18°C is attributable to natural background, 28% to anthropogenic solar radiation, 34% to consumptive use (diversions), and 6% to point sources. 14% of the temperature increase is due to the Woodburn WWTP effluent discharge at the point of discharge (RKm 38.3).

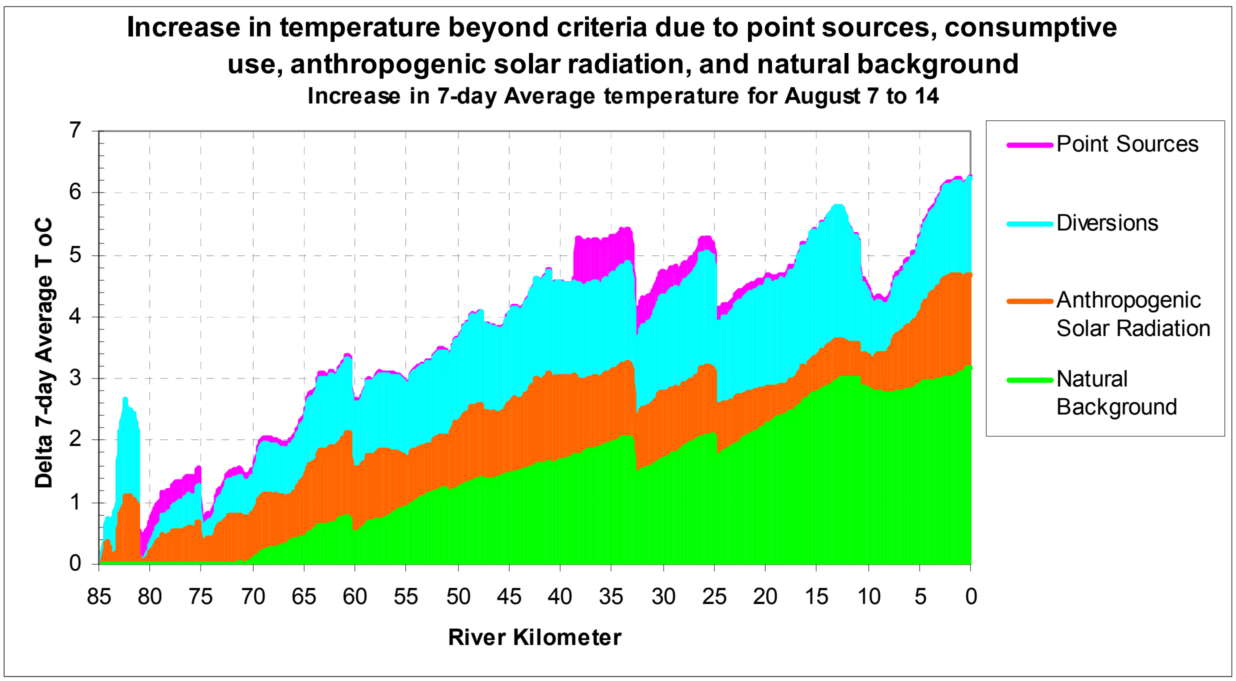

Figure A- 77. Increase in 7-day average river temperature above biological criterion due to various categories

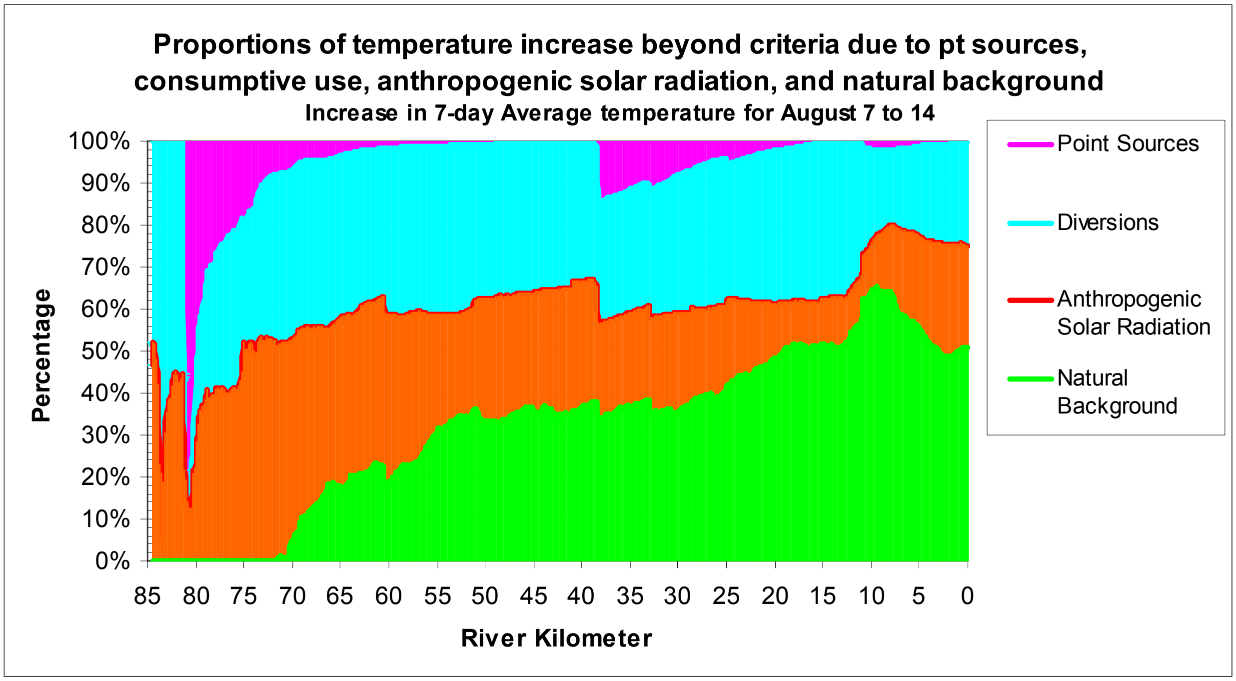

Figure A- 78. Proportions of 7-day average river temperature increase above biological criterion due to various categories

REFERENCES

Boyd, M.S. 1996. Heat Source: stream temperature prediction. M.S. Thesis. Oregon State University, Corvallis, Oregon

Boyd, M. and Kasper, B. 2002. TTools Users Manual, Oregon Department of Environmental Quality, Portland, Oregon

Boyd, M. and Kasper, B. 2003. Analytical Methods for dynamic open channel heat and mass transfer: Methodology for Heat Source model Version 7.0. Oregon Department of Environmental Quality, Portland, Oregon. Web site: http://www.deq.state.or.us/wq/TMDLs/tools.htm

Brown, L.C. and Barnwell, T.O. 1987. The enhanced stream water quality models QUAL2E and QUAL2E-UNCAS: Documentation and user manual. U.S. Environmental Protection Agency, Environmental Research Laboratory, Athens, Georgia.

ODEQ 2001. Tillamook Bay Watershed Total Maximum Daily Load (TMDL), State of Oregon Department of Environmental Quality, Portland, OR

ODEQ 2006. Willamette Basin Total Maximum Daily Load (TMDL), Technical Appendix C, Oregon Department of Environmental Quality, Portland, Oregon

ODEQ 2008. Methodologies for development of thermal wasteload allocations. Oregon Department of Environmental Quality, Portland, Oregon

OWRD 2002. Determining Surface Water Availability in Oregon. Open File Report SW 02-002. Oregon Water Resources Department, Salem, Oregon. Web site: http://www.oregon.gov/OWRD/SW/index.shtml